2011

Development And Validation Of A Flow Device To Study Platelet Function In Vitro And Elucidating The Role Of Thymosin β 4 In Various Physiological Processes

Harmanpreet Kaur
University of Windsor

DEVELOPMENT AND VALIDATION OF A FLOW DEVICE TO STUDY PLATELET FUNCTION IN VITRO AND ELUCIDATING THE ROLE OF THYMOSIN β 4 IN VARIOUS PHYSIOLOGICAL PROCESSES

By
Harmanpreet Kaur

A Dissertation

Submitted to the Faculty of Graduate Studies
through the Department of Chemistry and Biochemistry
in Partial Fulfillment of the Requirements for
the Degree of Doctor of Philosophy at the
University of Windsor

Windsor, Ontario, Canada
2011

Development and validation of a flow device to study platelet function in vitro and elucidating the role of thymosin beta 4 in various physiological processes

by

Harmanpreet Kaur

APPROVED BY:

S. Rafferty, External Examiner
Trent University

R. Carriveau, Departmental External
Department of Civil and Environmental Engineering

P. Vacratsis, Departmental Internal
Department of Chemistry & Biochemistry

S. Ananvoranich, Departmental Internal
Department of Chemistry & Biochemistry

B. Mutus, Advisor
Department of Chemistry & Biochemistry

Dr. M Ahmadi, Chair of Defense
Department of Electrical & Computer Engineering

October 2011

DECLARATION OF CO-AUTHORSHIP / PREVIOUS PUBLICATION

I. Declaration of Co-Authorship

I hereby declare that this thesis incorporates material that is the result of joint research, as follows:

This thesis incorporates the outcome of research efforts undertaken in the supervision of Dr. Bulent Mutus. In all cases experimental design, execution, data analysis, interpretation, and manuscript preparation were performed by the author.

I am aware of the University of Windsor Senate Policy on Authorship and I certify that I have properly acknowledged the contribution of other researchers to my thesis, and have obtained written permission from each of the co-authors to include the above materials in my thesis.

I certify that, with the above qualification, this thesis, and the research to which it refers, is the product of my own work.

II. Declaration of Previous Publication

This thesis includes 3 original papers that have been previously published/submitted for publication in peer reviewed journals, as follows:

Thesis Chapter	Publication Title and Full Citation	Publication Status
Chapter 2	Development of flow device to study effects of shear stress on endothelial cells and its applications	Accepted 2011
Chapter 4	Whole blood, flow-chamber studies in real-time indicate a biphasic role for thymosin β-4 in platelet adhesion.	Published 2010
Chapter 5	Thymosin β-4 alleviates endoplasmic reticulum stress in retinal pigment epithelial cells.	To be submitted

I certify that I have obtained permission from the copyright owner(s) to include the above published material(s) in my thesis. I certify that the above material describes work completed during my registration as graduate student at the University of Windsor. I declare that, to the best of my knowledge, my thesis does not infringe upon anyone‘s copyright nor violate any proprietary rights and that any ideas, techniques, quotations, or

any other material from the work of other people included in my thesis, published or otherwise, are fully acknowledged in accordance with the standard referencing practices. Furthermore, to the extent that I have included copyrighted material that surpasses the bounds of fair dealing within the meaning of the Canada Copyright Act, I certify that I have obtained a written permission from the copyright owner(s) to include such material(s) in my thesis. I declare that this is a true copy of my thesis, including any final revisions, as approved by my thesis committee and the Graduate Studies office, and that this thesis has not been submitted for a higher degree to any other University or Institution.

ABSTRACT

Parallel plate flow chambers, simulating *in vivo* fluid shear stress, provide a real time insight into the dynamic process of platelet aggregation and investigation of endothelial cell response to shear stress. This thesis describes the design and validation of – 1) A simple parallel plate flow chamber to study effects of shear stress on endothelial cells. This flow chamber is easy to use, inexpensive and fast to manufacture as compared to the flow devices reported previously. Moreover, it minimizes the number of cells and solution volumes to be used. It can be used as an effective *in vitro* system to study the effects of fluid shear stress on the structure and function of endothelial cells. 2) A four channel cylindrical flow device, constructed out of polydimethylsiloxane (PDMS) on microscope coverslips, to study platelet aggregation under *in vivo* like conditions. The novel aspect of this flow device is the surface chemistry we have devised for the facile patterning of immobilized proteins (fibrinogen and collagen) onto polydimethylsiloxane surfaces. The flow method introduced here was employed to determine the effect of thymosin β 4, a G-actin sequestering peptide, on the deposition of ADP-activated platelets onto fibrinogen cross-linked flow chambers. Platelets carry and release large amounts of thymosin β 4. Yet the role of thymosin β 4 on platelet thrombus formation has not been fully investigated. We demonstrate that thymosin β 4 has a dual role in platelet aggregation. Our results show that at low doses thymosin β 4 promotes platelet deposition and aggregation by yet unknown mechanism. However, platelet adhesion to fibrinogen is inhibited at high concentrations of thymosin β 4.

Exogenous thymosin β 4 has also been reported to promote wound healing, inflammation reduction and protection of human cornea epithelial cells against oxidative damage. Herein, we show that thymosin β 4 can also assuage endoplasmic reticulum stress in retinal pigment epithelium cells (RPE). Thymosin β 4 pre treatment before introducing endoplasmic reticulum stress decreases ROS, cholesterol levels and nuclear translocation of NFκB in RPE.

In conclusion, this body of work demonstrates the utility of flow devices to study platelet function and effects of shear stress in endothelial cells under *in vivo* like conditions. This work also reveals the role of thymosin β 4 in platelet function and alleviating ER stress in RPE, both of which might of considerable therapeutic relevance.

Dedicated to my parents and my husband for their tremendous love and support

ACKNOWLEDGEMENTS

It is with profound gratitude and appreciation that I acknowledge the able guidance of my revered supervisor, Dr. Bulent Mutus. I owe him a lot for his valuable guidance, concern, constructive criticism and thought provoking discussions at every step. I would also like to thank my committee members, Dr. Srinart Ananvoranich and Dr. Otis Vacratsis and for their insightful comments and encouragement.

I am highly obliged to our collaborator and my committee member, Dr. Rupp Carriveau for designing the flow chamber and for his guidance and valuable suggestions in these studies. I am also grateful to Dr. Gabriel Sosne for providing thymosin beta 4 for my work.

I would like to thank all the past and current members of Mutus lab over these years: Vasantha, Adam, Bei, Rebecca, Artur, Suzie, Rebecca, Christine, Ryan, Ruchi, Arun, Inga and Shane. My sincere thanks go to Marlene for her support and help. I must also acknowledge all the faculty and staff of the department for their help and assistance.

My deepest appreciation goes to my friend, Tanreet for always being there for me and supporting me all these years. Finally, I would like to thank my husband and my family for their unrelenting support, encouragement and understanding. Without their support, it would have been impossible for me to complete this work.

TABLE OF CONTENTS

LIST OF TABLES

CHAPTER 1

CHAPTER 3

LIST OF FIGURES

CHAPTER 1

General Introduction

CHAPTER 2

CHAPTER 3

CHAPTER 4

CHAPTER 5

LIST OF ABBREVIATIONS

Abbreviation	Definition
ACD	Acid Citrate Dextrose
ADP	Adenosine diphosphate
AMD	Age related macular degeneration
APTMES/AS	Aminopropyltrimethoxysilane
ATP	Adenosine triphosphate
BAEC	Bovine aortic endothelial cells
BCA	Bicinchoninic acid
bFGF	basic Fibroblast growth factor
BSA	Bovine serum albumin
Ca^{2+}	Calcium
CalDAG-GEFI	Diacylglycerol-regulated guanine nucleotide exchange factor I
CFD	Computational fluid dynamics
Coll	Collagen
DAF-DA	4,5-diaminofluorescein diacetate
DAG	Diacylglycerol
DHA	Docosahexaenoic acid
DNA	Deoxyribonucleic acid
DR	Diabetic retinopathy
DSS	Disuccinimidyl suberate
DTT	Dithiothreitol
ECM	Extracellular matrix
EDTA	Ethylenediaminetetraacetic acid
EITC	Eosin-isothiocyanate
eNOS	endothelial Nitric oxide synthase
ER	Endoplasmic reticulum
ERS	Endoplasmic reticulum stress
FAK	Focal adhesion kinase

Fas-L	Fas ligand
FcRγ	Fc receptor gamma
Fib	Fibrinogen
FITC	Fluorescein-isothiocyanate
GLUT	Glucose transporter isoform
GP	Glycoprotein
GPO	Gly– Pro–Hyp
H2DCFDA	2′,7′-dichlorodihydrofluorescein
HEPES	(4(2-hydroxyethyl)-1-piperazineethanesulfonic acid)
HUVEC	Human umbilical vein endothelial cells
ICAM-1	Intercellular adhesion molecule-1
Ig	Immunoglobin
IGF	Insulin like growth factor
IL-1	Interleukin-1
IP_3	Inositol 1, 4, 5 triphosphate
IPM	Interphotoreceptor matrix
IRBP	Interphotoreceptor retinoid binding protein
ITAM	Immunoreceptor tyrosine based activation motif
KC	Keratinocyte chemoattractant
LDL	Low density lipoproteins
LEDGF	Lens epithelium derived growth factor
LPS	Lipopolysaccharide
MCP-1	Monocyte chemoattractant protein-1
MIP 2	Macrophage inflammatory protein 2
NFκB	Nuclear factor kappa B
NHS	N-hydroxysulfosuccinimide
NO	Nitric oxide
NSMase 2	Neutral sphingomyelinase 2
PBS	Phosphate buffered saline
PDGF	Platelet derived growth factor
PDGF	Platelet derived growth factor

PDI	Protein disulfide isomerase
PDMS	Polydimethylsiloxane
PECAM-1	Platelet endothelial cell adhesion molecule 1
PEDF	Pigment epithelium derived factor
PF-4	Platelet factor-4
PFO-D4-GFP	Perfringolysin-domain 4-green fluorescent protein
PI3K	Phosphoinositide 3 kinase
PIP_2	Phosphatidyl inositol 4, 5 bisphosphate
PKC	Protein kinase C
PLCγ2	Phospholipase C gamma 2
PPFC	Parallel-plate flow chambers
PVDF	Polyvinylidene fluoride
ROS	Reactive oxygen species
RPE	Retinal pigment epithelium
SD	Standard deviation
SDS	Sodium dodecyl sulphate
SIPA	Shear induced platelet aggregation
SOD	Superoxide dismutase
SREBP	Sterol regulatory elements binding proteins
SSPE	Shear stress responsive elements
STIM1	Stromal interaction molecule 1
T2D	Type 2 diabetic
TNF α	Tumor necrosis factor α
Tβ4	Thymosin β 4
UPR	Unfolded protein response
UVB	Ultraviolet B
VCAM-1	Vascular cell adhesion molecule-1
VEGF	Vascular endothelial growth factor
vWF	von Willebrand factor

CHAPTER – 1

General Introduction

1. Platelets

Hemostasis is a co-ordinated event of various cellular and biochemical interactions, which involves the arrest of bleeding, formation of platelet aggregates and hence wound healing. Blood platelets play a very important role in every aspect of hemostasis. Platelets are small (2 to 4 µm in diameter), anuclear and disc-shaped and colourless cellular structures with a large number of secretory granules. These cells are derived from mature megakaryocytes via a process called thrombopoiesis. In the circulation of normal human beings, the number of platelets is in the range of 150,000 to 350,000 per µL. Their average life span is 6-10 days, after which they are destroyed by phagocytosis in the spleen.

Platelets have an important role in blood coagulation. Upon vascular injury, platelets are activated by subendothelial adhesive proteins like collagen and by a wide variety of soluble agonists including ADP, thrombaxane A2, thrombin and serotonin. These agonists induce signalling pathways by binding to their respective receptors on platelets, which leads to various signalling events such as platelet cytoskeletal changes and granule secretion. Upon activation by the agonists, platelets change their shape and adhere to newly exposed subendothelial tissues. The contents of the secretory granules (α granules and dense granules) are released at the site of vascular damage, which play an important role in haemostasis and thrombus formation (Zucker *et al* 1985). Platelet shape change and aggregation are of central importance for the formation of platelet thrombi and subsequently wound healing. Platelet plug formation at the site of injury occurs in three stages.

a) **Platelet adhesion –** Platelets detect vascular damage and adhere to the exposed subendothelium forming a monolayer of activated platelets.
b) **Platelet release reaction –** The platelets release active substances that are stored in their secretory granules. Serotonin, ADP, ATP and calcium are released by dense granules. Lysosomes release hydrolytic enzymes and α granules release platelet factor 4 (PF-4), beta thromboglobulin, platelet- derived growth factor (PDGF), fibrinogen, fibronectin, von Willebrand factor and albumin. The agonists released by the attached platelets activate and recruit more platelets.

c) **Platelet aggregation –** The recruited platelets aggregate with those already bound and form a platelet plug, which serves as a surface for fibrin deposition. The platelet plug formed is stabilized, eventually leading to wound healing.

1.1 Platelet receptors and signalling pathways

Platelet adhesion and aggregation on the exposed extracellular matrix (ECM) requires the coordinated interaction of different platelet surface receptors with adhesive macromolecules. Platelet receptors play a key role in regulating the cascade of events whereby circulating resting platelets make the rapid transition to an adhered, activated and aggregated thrombus. The mutation or absence of the receptors or binding proteins can affect the ability of the platelets to respond to vascular injury.

A wide variety of transmembrane receptors covers the platelet membrane, including many integrins ($\alpha_{IIb}\beta_3$, $\alpha_2\beta_1$), G-protein coupled seven transmembrane receptors (GPCR) (PAR-1 and PAR-4) thrombin receptors, $P2Y_1$ and $P2Y_{12}$ receptors and proteins belonging to the immunoglobulin superfamily (GP VI). Each of these receptors is capable of binding one or more ligand. Platelet receptors have a prominent role in the hemostatic function of platelets, allowing specific interactions and functional responses of vascular adhesive proteins and of soluble platelet agonists. Platelet receptors and their ligands are listed in Table 1.

TABLE 1 – Platelet membrane receptors and their ligands

Platelet Receptor	Ligands
GP IIb/IIIa, integrin $\alpha_{IIb}\beta_3$	Fibrinogen, vWF, Fibronectin
GP Ib-V-IX	vWF
GP Ia/IIa, $\alpha_2\beta_1$	Collagen
Protease activatable receptor (PAR)	Thrombin
α- adrenergic sites	Epinephrine
GP IV, GP VI	Collagen
$P2Y_1$ and $P2Y_{12}$	ADP

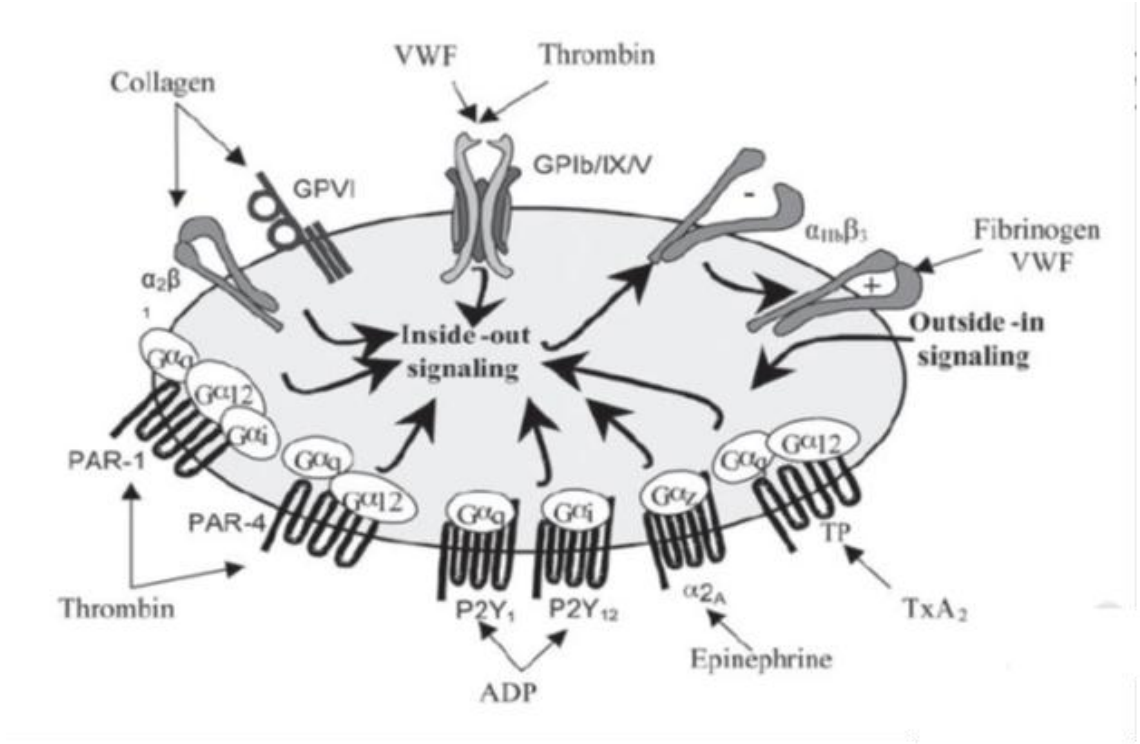

Figure 1 – Platelet receptors and ligand interactions (Image taken from Rivera *et al* 2009).

The platelet membrane receptors bind extracellular factors in response to platelet activation by different agonists, resulting in platelet adhesion and aggregation. PAR-1 and PAR-4 in the platelet membrane bind thrombin and mediate adhesion. Collagen can bind to either GP VI or integrin $\alpha_2\beta_1$. Von Willebrand Factor (vWF), epinephrine and thromboxane A_2 (TxA_2) bind to GP Ib/IX/V, α_{2A} and thromboxane receptor (TP) respectively. The binding of these agonists transmits intracellular signals leading to elevation of cytosolic Ca^{2+}, cytoskeletal changes, secretion of agonists such as ADP (that activates G protein-coupled $P2Y_1$ and $P2Y_{12}$ receptors), and activation of the integrin $\alpha_{IIb}\beta_3$ that binds vWF or fibrinogen and mediates platelet aggregation

a) GP VI – It is a 62kDa platelet–specific type 1 transmembrane glycoprotein of the immunoglobin superfamily. It is an important collagen receptor of high potency in terms of initiating platelet activation, aggregation and thrombus formation (Nieswandt *et al* 2003). It is one of the most important members of immunoglobin (Ig) suprefamily on platelets. It binds ligands including collagen, collagen related peptide (CRP) and the snake venom protein, convulxin.

Fc receptor gamma (FcRγ) is required for GP VI expression and is associated with the GP VI via a salt bridge in the transmembrane domains of GP VI (arginine) and FcRγ (aspartic acid) (Farndale *et al* 2004). The signalling pathway involves the FcRγ- chain and the Src kinases (likely Fyn/Lyn), the adapter protein; linker of activated T cells (LAT), and leads to the activation of phospholipase C gamma 2 (PLCγ2). GP VI initiates binding to fibrillar collagen under flow conditions, which then activates integrin $\alpha_2\beta_1$ which binds collagen more tightly. GP VI deficiencies cause only a mild bleeding tendency, probably because integrin $\alpha_2\beta_1$ is able to minimally initiate collagen binding.

b) GP Ib-IX-V – GP Ib-IX-V consists of four transmembrane glycoproteins, which are all members of the leucine rich protein family (Berndt *et al* 1995). It is a complex of glycoproteins constituting GP Ibα and GP Ibβ linked by a disulfide bond, and non covalently linked to GP IX and GP V. This receptor is constitutively expressed on the platelet plasma membrane. GPIbα is the major ligand-binding subunit, with a globular N-terminal ligand-binding domain elevated from the cell surface by a sialomucin core (Andrews *et al* 2003). It also plays a substantial role in platelet interaction with activated endothelial cells and with leukocytes, through the binding of P-selectin and Mac-1 ($\alpha_M\beta_2$), respectively. There are around 25,000 copies of the GP Ib-IX complex per platelet and there are approximately half as many copies of GP V per platelet, which suggests that GP V forms a 1:2 complex with GP Ib-IX on the platelet surface (Modderman *et al* 1992).

Under high shear, GP Ib-IX-V complex interacts with vWF, an extracellular multimeric adhesive glycoprotein associated with subendothelial matrix, and mediates the initial adhesion of platelets to the subendothelium. vWF undergoes a conformational

change when it is bound to matrix or under high shear conditions, which permits its binding to GP Ib-IX-V complex.

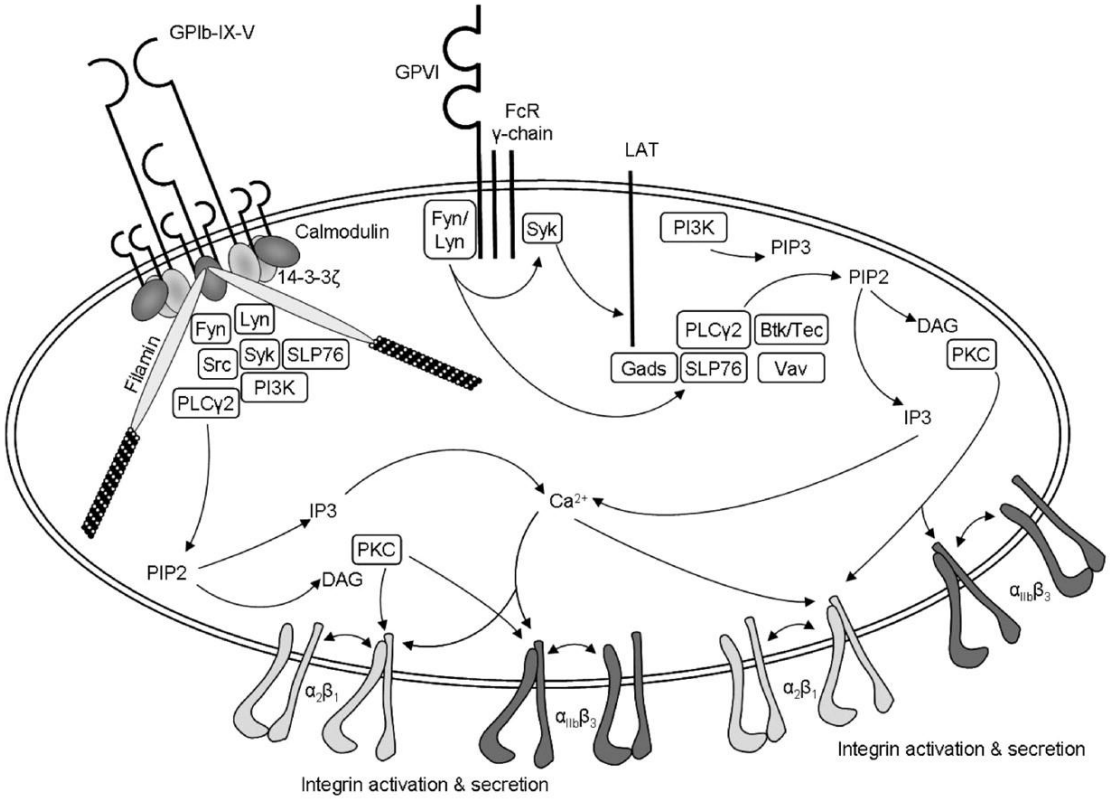

Figure 2 – Platelet signalling through GP VI and GP Ib/IX/V (Image taken from Rivera *et al* 2009).

GP VI has a short cytoplasmic tail which binds Fyn and Lyn Src kinases. FcRγ complexes with GP VI, has an immunoreceptor tyrosine based activation motif (ITAM) which acts as the signal transducing subunit of the receptor. Collagen binding to the GP VI phosphorylates ITAM by Src kinases which activate Syk and downstream signalling pathways. These downstream pathways consist of formation of a signalosome, composed of various adapter and effector proteins (LAT, SLP-76, Gads), and ultimately activates PLCγ2. PLC catalyzes the hydrolysis of phosphatidyl inositol 4, 5 bisphosphate (PIP_2), thus leading to release of inositol 1, 4, 5 triphosphate (IP_3) and diacylglycerol (DAG) and hence integrin activation. The cytoplasmic tail of GP Ibα is associated with filamin and calmodulin, which links it to the relevant signalling proteins including Src related tyrosine kinase, focal adhesion kinase (FAK), GTPase activating protein and PI3K. When vWF binds GP 1b/IX/V, activation signals such as cytoplasmic Ca^{2+} release, ADP release and $\alpha_{IIb}\beta_3$ activation are elicited. The actual mechanisms as to how these signals are transmitted are not yet clear.

c) Integrins – Integrins are a ubiquitously expressed family of transmembrane receptors which consist of an α and β subunit. Integrins are present on platelet membrane in a low affinity state until platelets are activated by agonists. Platelet activation transforms integrins into a high affinity form and they can bind their ligands. Integrin $\alpha_{IIb}\beta_3$ receptor is a dominant receptor, which is present in large copy numbers (40,000 – 80,000 per platelet) on the platelet surface. It acts as a principle receptor which mediates platelet aggregation through binding of plasma fibrinogen (Gruner *et al* 2003). Its absence or deficiency causes the most common bleeding disorder Glanzmann thrombasthenia.

The second most important integrin receptor on platelet surface is $\alpha_2\beta_1$. It is the major collagen adhesion receptor and is present at about 2000 – 4000 copies per platelet. The $\alpha_2\beta_1$ integrin, commonly referred to as GP Ia/IIa, also plays a role in the adhesion of platelets to collagen and subsequent optimal activation (Sarratt *et al* 2005).

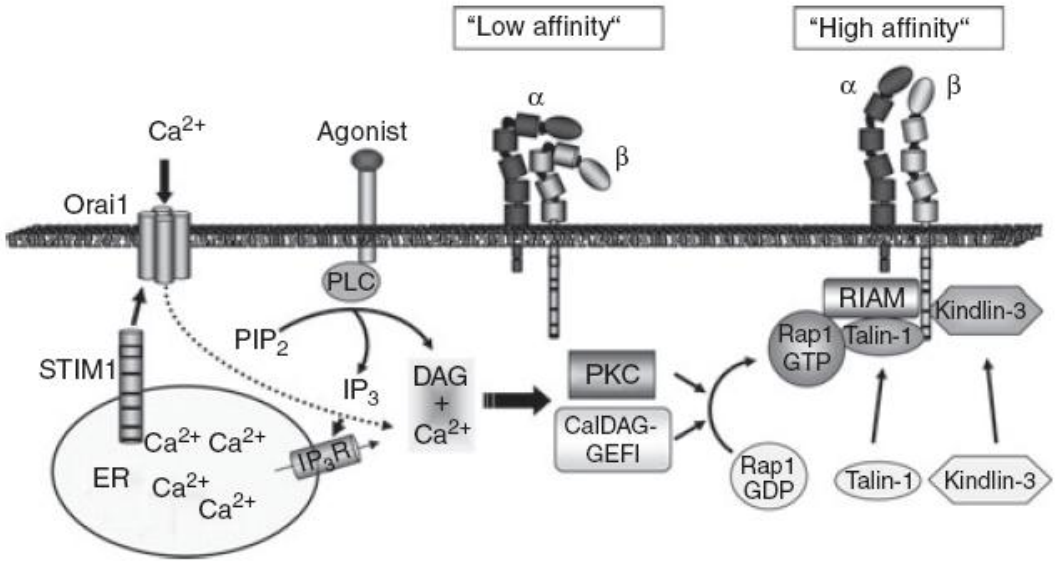

Figure 3 – Integrin activation (Image taken from Nieswandt *et al* 2009).

Phospholipase C (PLC) is activated after stimulation by the agonists. PLC catalyzes the hydrolysis of phosphatidyl inositol 4,5 bisphosphate (PIP_2) into inositol 1,4,5 triphosphate (IP_3) and diacylglycerol (DAG). IP_3 binds and activates IP_3 receptors on the endoplasmic reticulum (ER) membrane resulting in the release of calcium from the ER. Ca^{2+} concentration inside the cell is further increased by the opening of plasma membrane Ca^{2+} channel Orail by stromal interaction molecule 1 (STIM1). DAG and Ca^{2+} activate protein kinase C (PKC) and diacylglycerol-regulated guanine nucleotide exchange factor I (CalDAG-GEFI), which further activates and translocates Rap1 to the plasma membrane. RAP1 effector molecule RIAM interacts with Rap1-GTP and talin-1. This interaction exposes the integrin binding site of talin-1. The salt bridge between the transmembrane regions of α and β integrin subunits is disrupted by the binding of talin-1, which results in a conformational change in the extracellular domains and hence ligand binding. This step also requires binding of kindlin-3 to the NPXY motif of the integrin β tail.

d) ADP receptors – ADP plays a central role in regulating platelet function. It induces platelet aggregation via the activation of 2 major ADP receptors, $P2Y_1$ and $P2Y_{12}$. ADP binds the G_q-protein-linked $P2Y_1$ receptor on platelets, which causes a change in cell shape, mobilization of calcium, and initiation of reversible aggregation. It also binds the G_i-linked $P2Y_{12}$ receptor to amplify aggregation via adenylyl-cyclase-mediated cyclic AMP production (Communi *et al* 2000). This receptor is also a main target for many anti-thrombotic drugs. Coactivation of G_q-coupled $P2Y_1$ and G_i-coupled $P2Y_{12}$ receptors is essential for ADP-induced platelet aggregation (Jin *et al* 1998).

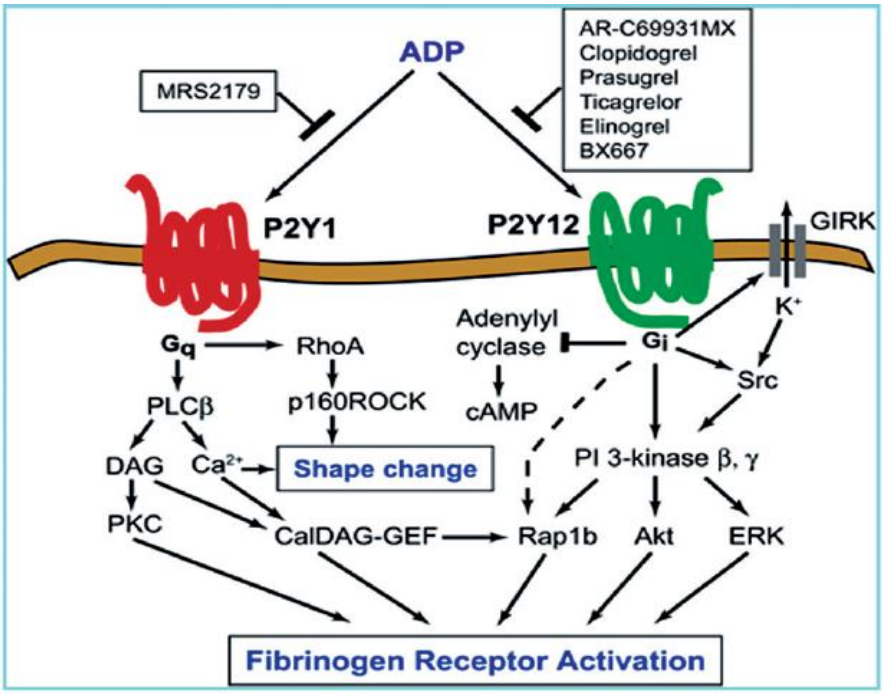

Figure 4 – ADP receptors and downstream signalling (Image taken from Kim *et al* 2011).

ADP activates platelets through G_q coupled $P2Y_1$ receptor and G_i-coupled $P2Y_{12}$ receptor and causes a number of downstream intracellular signalling events that contribute to fibrinogen receptor activation and platelet aggregation. G protein gated inwardly rectifying potassium channels, PI3K, Akt, ERK, Rap 1b and Src family kinases are all activated through the $P2Y_{12}$ receptor. Both Rap1b and Akt are signalling mediators that contribute to platelet aggregation and are activated in a PI3K-dependent manner. RhoA protein is activated by $P2Y_1$, which causes cytoskeletal and shape changes in activated platelets. These receptors are also the target of many anti-thrombotic drugs including clopidogrel, prasugrel and elinogrel. MRS2179 is $P2Y_1$ antagonist.

1.2 Major proteins involved in thrombosis

Blood coagulation cascade involves numerous different proteins eg fibrinogen, collagen, tissue factor, factor VII, factor VIII, vWF etc. The properties and functions of 3 major proteins related to the work in this thesis are described below.

a) Fibrinogen – Fibrinogen is a large (340 kDa), complex glycoprotein which is primarily synthesized by hepatocytes. It consists of three pairs of polypeptide chains, Aα, Bβ and γ, linked by 29 disulfide bonds. These polypeptide chains are encoded by different genes located on chromosome 4. It is normally present in blood plasma at a concentration of about 2.5g/L with a half life of around 100 h. The primary platelet receptor for fibrinogen binding is integrin $\alpha_{IIb}\beta_3$ (Weisel 2005). Fibrinogen is essential for hemostasis and plays an important role in wound healing, inflammation and other biological functions.

Fibrinogen is not only necessary for platelet aggregation, which is an initial step in hemostasis but also in the formation of insoluble fibrin clots in the final stages of the blood coagulation cascade. Fibrinogen binds to integrin receptor $\alpha_{IIb}\beta_3$ on the activated platelets and act as a bridge to link platelets causing platelet aggregation and hence thrombus formation. Human fibrinogen contains three integrin binding sites: two arginine-glycine-aspartic acid (RGD) sequences within the Aα chain and a non RGD sequence in the γ chain (Weisel 2005).

Fibrinogen also plays a role during inflammation and immune response and mediates the adhesion and transendothelial migration of leukocytes. The synthesis of fibrinogen is increased during inflammation. Two leukocyte integrins, $\alpha_M\beta_2$ (CD11b/CD18, Mac-1) and $\alpha_X\beta_2$ (CD11c/CD18) are the main fibrinogen receptors expressed on neutrophils, monocytes, and macrophages. Fibrinogen interacts with CD11b/CD18 and intercellular adhesion molecule-1 (ICAM-1) on endothelial cells and acts as a bridging molecule to enhance leukocyte adhesion to endothelial cells (Languino *et al* 1993; Simmons *et al* 1988).

b) Collagen – Collagen is the most abundant protein in the human body and a major protein of the extracellular matrix. Collagen plays a major role in the hemostatic cascade. Platelet adhesion and aggregation on collagen is an integrated process that involves

various platelet receptors, including GP VI and integrin $\alpha_2\beta_1$. The human genome has genes for more than 20 forms of collagen. Approximately 9 forms of collagen are expressed in the vascular wall (Type I, III, IV, V, VI, VIII, XII, XIV), of which types I and III are the major constituents of the extracellular matrix. Repetitive Gly–X–Y sequences are the characteristic feature of the primary structure of triple-helical regions of collagen. Gly– Pro–Hyp (GPO) is the most prevalent sequence, which forms about 10% of the primary structure of collagen types I and III (Baum *et al* 1999). For the close packing of the chains, every third residue must be glycine.

GP Ia/IIa ($\alpha_2\beta_1$) and GPVI are the two major collagen binding receptors present on platelet membrane. Under normal conditions, collagen is not exposed to flowing blood. After vascular injury, collagen becomes exposed to the flowing blood; the platelets adhere to the matrix and form an aggregate. Under high shear rates, platelet adhesion to collagen requires vWF (Sixma *et al* 1997).

c) von Willebrand Factor (vWF) – vWF is a multimeric adhesive glycoprotein present in the plasma, the subendothelial matrix and on the surface of activated endothelial cells. vWF is stored in storage granules (Weibel-Palade) of endothelial cells and α granules of platelets and is released upon activation of both types of cells. vWF has binding sites for platelet GP Iba and GP IIb-IIIa, and for various subendothelial constituents, including collagen types I, III**,** and VI. For the initial tethering of flowing platelets at the very high shear rates found in small arteries and arterioles, the interaction between glycoprotein Ib-V-IX (GPIb-V-IX) and von vWF immobilized on collagen is very critical (Moroi *et al* 1999).

1.3 Methods to study platelet function

1. **Light transmission aggregometery**

Aggregometry has been used as a standard approach to study platelet aggregation in research. The use of light transmission through platelet suspensions to determine aggregation was introduced in the early 1960s (Born *et al* 1962). Shape change and aggregation can be studied with a platelet aggregometer, which records the transmission

of light through a stirred platelet suspension. The agonist (ADP, thrombin, collagen) is added to the platelet suspension and the dynamic measure of platelet aggregation is recorded over time at 600nm. This platelet aggregation test can be done by using platelet rich plasma (PRP) maintained at 37^{o} C. When the agonist is added, the platelets aggregate and absorb less light and so the transmission increases. The change in optical density can be plotted to view the aggregation curve. Lumiaggregometry is a modification of light transmission aggregometry which measures platelet secretion along with platelet aggregation.

2. Cone and plate viscometers

Fluid mechanical forces can exert profound effects on blood cell function. Over the past years, shear forces generated by blood flow have been recognized to have a significant impact on platelet adhesion and thrombus formation. Cone and plate viscometers have been used for the continuous measure of platelet agglutination generated by shear forces (Fukuyama *et al* 1989). The role of shear forces in inducing platelet activation has been measured by subjecting platelets in suspension to a range of shear rates in a viscometer (Goto *et al* 1998, 2002; Ikeda *et al* 1991).

As shown in Fig. 5, the cone is of a very shallow angle and is in bare contact with the plate. The platelet suspension is placed between the cone and plate and rotation of the cone at a calculated rate induces shear in the suspension. The rate of shear as well as the shear patterns can be controlled by the angle of the cone (α), the speed of rotation (ω), the viscosity of the medium (μ) and the distance between the cone (h(r)) and the plate. The platelets can be exposed to different range of shear stress and the sample volume required is around 500μL – 2mL.

A major advantage of a cone and plate viscometer is the constant shear rate throughout the entire sample. It requires very low volumes of blood/platelet suspensions and can be used to study both laminar and turbulent flows. It allows measurement of relatively high shear rates, requires small sample volumes and is easy to clean. The main disadvantage of the cone and plate viscometer is that it has geometric disparity from the vessels in the cardiovascular system. Also, it cannot be used to study platelet function in real time.

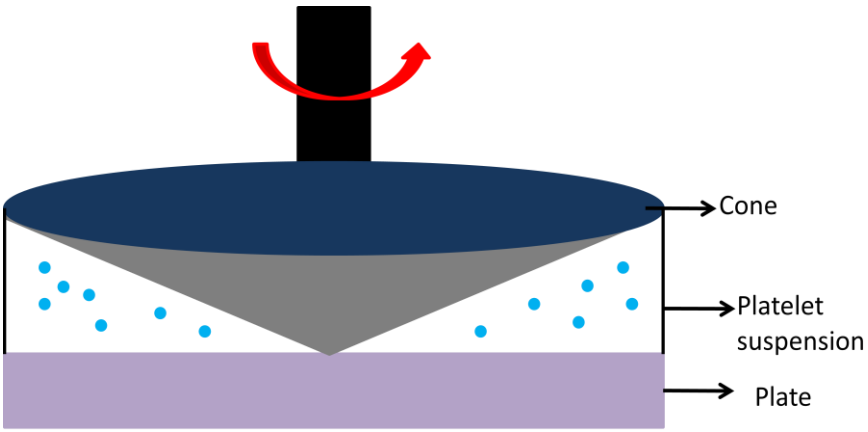

Figure 5 – Cone and plate viscometer.

3. **Perfusion chambers**

Wall shear has been identified as an important parameter governing the growth of platelet thrombi. The platelets experience shear stresses in the range of 1 – 60 dyne/cm^2 in the venous and arterial circulation. The perfusion chambers are used to study the influence of laminar blood flow at various shear rates on thrombus formation.

A perfusion device consists of a perfusion chamber with a glass coverslip, a pump, vials containing blood/platelet samples and tubing to connect the chamber and the pump. The matrix proteins (collagen, fibrinogen) are coated on the glass coverslips. The main advantage of these perfusion chambers is that they allow studies at various pathophysiological shear rates and also, coating the chamber surfaces with matrix proteins is a very simple procedure. These perfusion chambers also allow us to study the dynamics of platelet aggregation in real time. The limitation of these chambers is that blood flow is pulsatile and blood vessels can dilate, whereas in these flow chambers the blood flow is constant and walls are rigid.

Parallel plate flow chambers are the most commonly used perfusion chambers to mimic flow conditions occurring *in vivo* and study platelet function *in vitro*. The role of various platelet membrane receptors, adhesive proteins at the vessel wall, plasma proteins, thrombin formation and shear rate on platelet adhesion and aggregate formation can be investigated using these perfusion chambers. Various studies have used these

parallel plate flow chambers to determine the interaction of platelets with adhesive surfaces (collagen, fibrinogen, vWF) at various shear rates (Savage *et al* 1996; Loncar *et al* 2006). Tubular flow chambers which retain the cylindrical shape of the vasculature have been used to study the growth and stability of platelet aggregates and also to study the flow mechanisms for depositing platelets on various surfaces (Badimon *et al* 1987). Flow chambers with built in eccentric cosine shaped stenoses in the blood flow channel have been used to study the effects of fluid dynamic factors on thrombus formation at arterial stenotic lesions (Barstad *et al* 1994). Apart from the conventional flow chambers, microfluidic devices are also used, which reduce the blood volumes required for platelet studies (Gutierrez *et al* 2008).

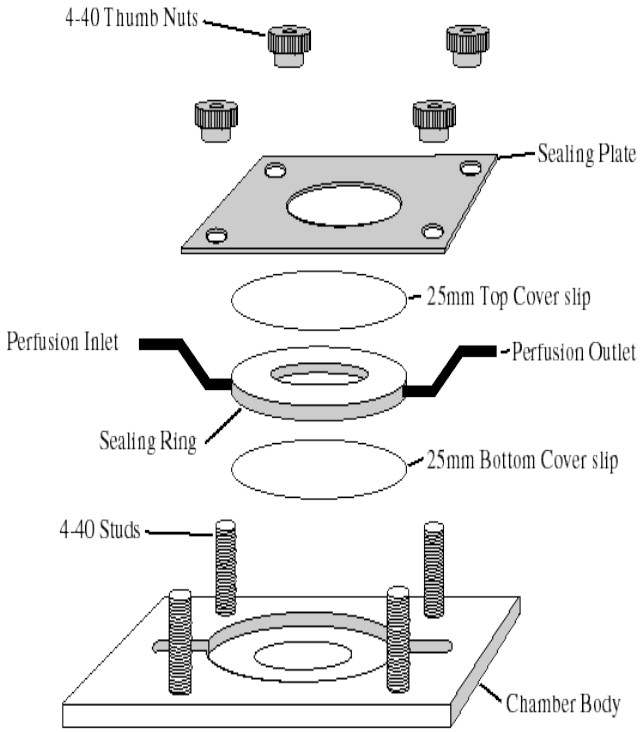

Figure 6 – Perfusion Chamber (Image taken from www.dagan.com)

2. Shear Stress

In normal physiological conditions, various mechanical forces act on blood vessels and the endothelial cells lining them. Two types of superficial stresses develop at the vessel walls due to blood flow – circumferential stress due to variation of pulse pressure inside blood vessels and shear stress due to blood flow. These forces consist of pressure acting perpendicular to the vessel wall, cyclic strain, and shear stress acting parallel to the wall, creating a frictional shear force on the surface of the endothelium. Shear stress is measured in dynes/cm^2. For Newtonian fluids flowing upon a planar surface, shear stress is calculated as

$$\tau = \mu \quad du/dy$$

where τ is shear stress, μ is kinetic viscosity, u is fluid velocity, y is distance from the surface and du/dy is the velocity gradient (Shames *et al* 2003).

The arteries and veins are exposed to different levels of shear stress, which may produce alterations in the structure, exposure, or clustering of externally oriented molecules in cell membranes. Normal time-average levels of fluid shear stress in the venous circulation are approximately 1 – 6 dyne/cm^2, and in the arterial circulation approximately 5 – 60 dyne/cm^2. In contrast, higher shear stress values can be observed in arteries with strong curvatures such as aortic arches, arterioles and vasculature partially obstructed by atherosclerosis (McDonald *et al* 1974).

2.1 Role of shear stress in platelet adhesion and aggregation

Shear stress has an important role in maintaining vascular homeostasis. Various studies have focused on the physiological effects of shear stress. Blood rheology is one of the key factors regulating the dynamics of thrombus development. The mechanisms of platelet deposition and thrombus growth are to a large extent determined by the alterations in the local hemodynamic environment (Mustard *et al* 1966). In healthy arteries, blood flow is laminar and platelets are exposed to uniform hemodynamic forces during hemostatic plug formation. At the site of vascular injury, shear forces generated by the flowing blood play an important role in platelet adhesion mechanisms. These mechanical forces not only transport platelets to the vessel wall but also dictate the role of various receptors in

mediating platelet adhesion. Activation of platelets by pathologically high shear stress can lead to arterial thrombotic disease.

High fluid shear may trigger platelet aggregation (Kroll *et al* 1996; Andrews *et al* 1997). This condition is known as shear induced platelet aggregation (SIPA) and is known to play an important role in the pathogenesis of various diseases including atherosclerosis and acute myocardial infarction. Rapid and dramatic changes in blood flow may activate passing blood platelets. Various studies on effects of shear rates have shown that increasing shear stress leads to increased deposition of platelets onto thrombogenic surfaces and increased rates of thrombus growth (Turitto *et al* 1979; Ikeda *et al* 1991; Tsuji *et al* 1999; Ruggeri *et al* 2006). A recent study has demonstrated that at pathological shear rates (> 10,000s^{-1}), large rolling aggregates can develop independently of integrin $\alpha_{IIb}\beta_3$ and platelet activation (Ruggeri *et al* 2006).

Platelet aggregation is a consequence of the bridging of platelet surface integrin $\alpha_{IIb}\beta_3$, by fibrinogen. Although the receptor complexes in resting or unactivated platelets do not bind the bridging ligand, high shear forces are thought to induce conformational changes in the GpIb/IX/V complex or vWF, and consequent platelet aggregation via the bridging molecule vWF (Ikeda *et al* 1991; Kroll *et al* 1996). vWF binding to $\alpha_{IIb}\beta_3$is minimal, but when high shear stresses are applied to platelets, vWF binds to $\alpha_{IIb}\beta_3$ as well as to the GP Ib/IX/V complex, and this binding contributes substantially to direct shear-induced platelet aggregate formation (Goto *et al* 1995).

In small arteries and arterioles where shear rate is very high, initial platelet adhesion depends on the binding of GP Ibα to immobilized vWF. This interaction is crucial for the initial tethering of flowing platelets. This complex continues to recruit platelets, thereby increasing the shear rate due to growing thrombi, however this binding is not sufficient to make stable platelet aggregates and the platelets continue to be translocated in the direction of blood flow. It can keep platelets in contact with the surface and with each other only for a short time. High shear stress induces binding of platelet GP-IX-V to plasma von Willebrand factor (vWF) which initiates platelet aggregation (Savage *et al* 1998). This molecular mechanism initiates various signalling pathways which lead to increased intracellular calcium and $\alpha_{IIb}\beta_3$ integin receptor activation. This leads to thrombus formation which can block blood supply to the heart and brain causing

heart attack and stroke (Kroll *et al* 1996; Gawaz *et al* 2004). Activated platelets also interact with leukocytes circulating in the blood flow and mediate platelet-leukocyte-endothelial cell adhesion. In atherothrombosis, platelets promote the interaction of inflammatory leukocytes with the vessel wall, which initiates formation of atherosclerotic plaques (Gawaz *et al* 2004; Massberg *et al* 2002).

2.2 Endothelial cell responses to shear stress

Endothelial cells constitute the inner lining of blood vessels and constantly experience fluid shear stress, the tangential component of hemodynamic stresses. When shear stress is applied on the luminal surface of endothelial cells, the mechanical-chemical signaling can be transmitted throughout the cell and to cell– extracellular matrix (ECM) adhesions on the luminal surface of endothelial cells. Endothelial cell surfaces are equipped with various mechanoreceptors which convert physical stresses into biochemical signals. Endothelial cells sense shear stress and respond by modifying gene expression, intracellular signalling, protein expression and other cell functions. Under normal conditions, the blood flow is unidirectional and laminar, whereas low and disturbed blood flow promotes development of atherosclerotic plaques (Davies *et al* 1995).

Numerous studies have been done *in vitro* and *in vivo* to demonstrate the effects of shear stress on the morphology and cellular behaviour of endothelial cells. Sustained shear stress results in reorientation of the actin cytoskeleton, microtubules, and intermediate filaments in the direction of flow (Malek *et al* 1996; Girard *et al* 1995). Some of the early responses of endothelial cells to shear stress such as the activation of Ca^{2+} and K^{+} transmembrane channels (Yoshikawa *et al* 1997) and platelet endothelial cell adhesion molecule 1 (PECAM-1) phosphorylation (Osawa *et al* 1997) can be detected within a few seconds after the onset of flow. Shear stress also leads to the activation and phosphorylation of various signalling molecules e.g. MAP kinases (Tseng *et al* 1995), focal adhesion kinase, jun C terminal kinase (Li *et al* 1997) and protein kinase C (Traub *et al* 1997). Laminar shear stress also enhances endothelial cell migration in wound healing (Li *et al* 2002; Hsu *et al* 2001; Albuquerque *et al* 2000). Physiological shear stress decreases the rate of apoptosis from growth factor depletion, tumor necrosis factor α or hydrogen peroxide exposure (Levesque *et al* 1990; Chiu *et al* 1998) via activation of

Akt and attenuated caspase mediated killing (Dimmeler *et al* 1996).

Prolonged shear stress causes distinct structural and morphological changes in endothelial cells and also affects the overall vascular tone through the regulation of various vasoconstrictors and vasodilators. Shear stress is essential to maintain endothelial integrity and cardiovascular health. It has been shown that fluid shear stress plays an important role in blood vessel formation and maintenance although the mechanisms are not fully understood yet.

2.3 Shear stress sensors

The ability of endothelial cells to respond to shear stress indicates that they can sense shear stress as a signal. Various studies have been done to understand the mechanisms of signal mechanotransduction in shear stress. Shear stress is detected by various receptors, tranducers and sensor proteins on the cell surface and multiple pathways are involved in the shear stress signal transduction including G proteins, tyrosine kinase receptors, caveolae and ion channels.

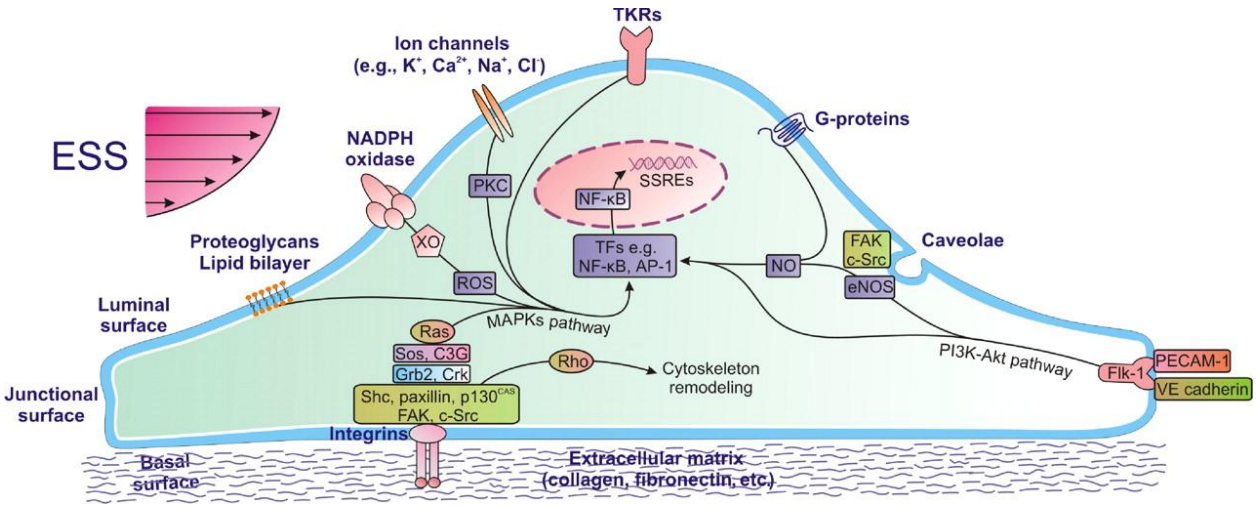

Figure 7 – Mechanotransduction of endothelial shear stress (Image taken from Chatzizisis *et al* 2007).

Shear stress is sensed by various mechanoreceptors including integrins, caveolae, ion channels, G coupled proteins, tyrosine kinase receptors and proteoglycans. Integrins are activated when shear stress signals are transmitted through the cytoskeleton to the basal endothelial surface. Various other proteins and protein complexes including adaptor proteins (Grb2, Crk), non receptor tyrosine kinases (FAK, c-Src, Shc, paxillin, p 130^{CAS}) and guanine nucleotide exchange factors (Sos and C3G), are phosphorylated and activated by the integrins. This activates the Ras family GTPase, which triggers downstream cascades of serine kinases, ultimately activating mitogen activated protein kinases (MAPKs). Shear stress signals transmitted through the cytoskeleton to the junctional or luminal endothelial surface activates protein kinase C (PKC), Rho family small GTPases which mediate cytoskeletal remodelling and phosphoinositide 3 kinase (PI3K) - Akt cascade. All of these signalling pathways lead to phosphorylation of various transcription factors, which bind to shear stress responsive elements (SSPE) at promoters of mechanosensitive genes, thereby inducing or suppressing their expression

2.4 Shear stress, endothelial dysfunction and atherosclerosis

Atherosclerosis is a chronic and inflammatory disease of conduit arteries and is the leading cause of death in developed countries. It is associated with several other well defined risk factors including hypertension, hyperlipidemia and diabetes mellitus. The atherosclerotic lesions form at specific regions of the arterial tree, such as in the vicinity of branch points, the outer wall of bifurcations, and the inner wall of curvatures, where disturbed flow occurs. It has been widely shown that atherosclerosis preferentially develops in vascular regions with low shear (Malek *et al* 1999; Nerem *et al* 1993). On the other hand, the vessel regions which are exposed to laminar, steady and high shear flow remains disease free.

Sterol regulatory element binding proteins (SREBPs) are also activated by low shear stress. These endoplasmic reticulum-bound transcription factors upregulate the expression of genes encoding the LDL receptor, cholesterol synthase, and fatty acid synthase (Liu *et al* 2002). SREBPs also increase the permeability of the endothelial surface to LDL (Traub *et al* 1998) and production of reactive oxygen species (ROS). The circulatory inflammatory cells (monocytes, T lymphocytes and mast cells) are recruited into the tunica intima, the innermost layer of the arteries, to scavenge oxidized LDL. NFκB is activated which upregulates genes encoding vascular cell adhesion molecule-1 (VCAM-1), intercellular adhesion molecule-1 (ICAM-1), monocyte chemoattractant protein (MCP)-1; and pro-inflammatory cytokines, such as tumor necrosis factor α (TNF α) and interleukin (IL)-1. These adhesion molecules mediate rolling and adhesion of leukocytes on endothelial cells. MCP-1 promotes recruitment of leukocytes into the intima. After leukocyte infiltration into endothelial cells, they differentiate into macrophages, which sustain inflammation and hence promote atherosclerosis.

Shear stress is also associated with endothelial proliferation. Endothelial cell proliferation increases by 18 times within 48 hours of shear stress reduction (Mondy *et al* 1997). Decrease in shear stress also causes vascular smooth muscle cell proliferation, differentiation and migration into the intima, endothelial cell loss and decrease in actin stress fibres (Walpola *et al* 1993, 1995).

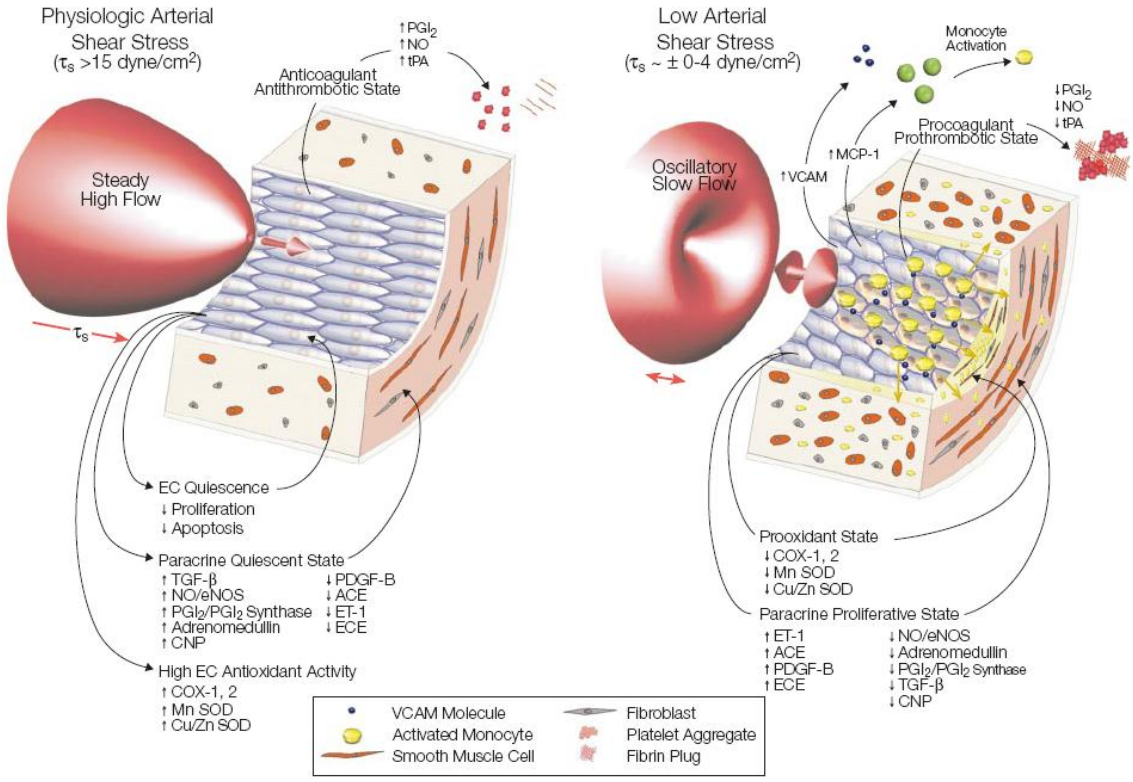

Figure 8 – Effects of disturbed shear rates on endothelial cell function (Image taken from Malek *et al* 1999).

Hemodynamic shear stress is very important for maintaining endothelial integrity and function. Arterial-level shear stress (>15 dyne/cm^2) induces endothelial quiescence by decreasing proliferation and apoptosis. It also upregulates the expression of atheroprotective genes including eNOS. However, low shear stress (<4 dyne/cm^2), which is prevalent at atherosclerosis-prone sites, stimulates an atherogenic phenotype by decreasing antioxidants production and atheroprotective genes. Increased expression of VCAM and MCP-1 activates the monocytes, enhancing the progression of atherogenesis.

2.5 Parallel plate flow chambers

To study the dynamic response of vascular endothelial cells to controlled levels of fluid shear stress, various types of *in vitro* systems that allow cultured endothelial cells to be exposed to well-defined flow conditions have been developed. These systems include a cone-plate apparatus (Dewey *et al* 1981), orbital shakers (Dardik *et al* 2005), capillary flow tubes (Olesen *et al* 1988; Jacobs *et al* 1995), and parallel-plate flow chambers (PPFC) (Ruel *et al* 1995; Chiu *et al* 1998).

Among *in vitro* systems employed to study the effects of flow conditions on endothelial cells, PPFC have been the most commonly used for flow stimulation of endothelial cells (Brown *et al* 2000). PPFC are generally used to mimic shear flow on cultured endothelial cells. A typical PPFC consists of a silicon gasket, a polycarbonate distributor, which has inlet and outlet ports, and a glass coverslip on which endothelial cells are grown. The endothelial monolayer is subjected to fluid flow by creating a pressure gradient along the chamber. The design of PPFCs is very simple and they are very easy to operate. The main advantage of PPFC is that it can be used to produce shear rates ranging from 0.01 – 60 dyne/cm^2 and studies can be visualized in real time.

Studies using the PPFC have provided insight into the effects of shear on endothelial cell alignment and elongation, aided investigators in fine tuning the application and adjustment of shear and helped lay the groundwork for future devices. For example, endothelial cells have been subjected to steady and pulsatile shear stress to measure and correlate their production of prostacyclin (Hanada *et al* 2000; Grabowski *et al* 1985), determine their orientation with respect to flow direction and reveal that higher shear stress results in a higher degree of cell elongation (Levesque *et al* 1985). Mechanotransduction in endothelial cells has been studied using many *in vitro* and *in vivo* approaches.

PPFCs have been used to study the effects of shear stress on the apoptosis of HUVECs induced by lipopolysaccharide (LPS) (Zeng *et al* 2005) and expression of proto-oncogenes, c-fos and c-myc in HUVECs (Li *et al* 2002). The effects of fluid shear stress on MCP-1 induction in endothelial cells have also been investigated using PPFCs (Yu *et al* 2002). PPFCs have also been used to study the mechanisms underlying proliferation, adhesion and metastasis of cancer cells (Zhang *et al* 2003).

3. Thymosin β 4

Thymosins are a group of peptides which were first isolated from calf thymus. These are divided into 3 different groups based on their isoelectric point: α thymosin (pI < 5), β thymosin (5 < pI < 7) and γ thymosin (pI > 7). β thymosins are a family of structurally related proteins, which have highly conserved amino acid sequences among different species. Thymosin β 10 and thymosin β 15 are expressed in breast, thyroid and prostate metastatic tumors and are thought to be the prognostic markers of these cancers (Bao *et al* 1996; Santelli *et al* 1999). There are 16 members of the β thymosin family and thymosin β 4 (Tβ4) is the most studied of all the members of the family.

Tβ4 is a highly conserved peptide, which was first isolated from thymus tissue in 1981 (Low *et al* 1981; Yu *et al* 1994). It has 43 amino acids with a molecular weight of 4.9 kDa. It is found in concentrations of 10 nM – 600 μM in different tissues and cell types (Hannappel *et al* 1985, 1987). The concentration of free Tβ4 in blood is about 10–200 nM (plasma and serum). It is regarded as a major intracellular G actin sequestering peptide in mammalian cells. It forms a 1:1 complex with G actin and inhibits its salt induced polymerization to F actin (Hannappel *et al* 1993; Huff *et al* 2001). Tβ4 is also present inside the cell and extracellular fluid.

3.1 Structure and properties

Tβ4 has a dynamic and flexible conformation. Three dimensional structure determinations by NMR-techniques have demonstrated that Tβ4 is unstructured in aqueous solutions. However, when fluorinated alcohols are added to the aqueous solution a defined 3D-structure can be obtained (Zarbock *et al* 1990). The data obtained under these conditions indicated that Tβ4 is a rather extended molecule of almost 5 nm in length. Both the N- and C-terminal conserved sequence stretches ranging from residues 5 to 15 and 30 to 40, respectively, form short α-helices linked by a flexible loop.

Proteins which lack a definite secondary structure in aqueous solutions attain a defined tertiary structure on binding their target proteins and undergo a number of structural intermediate states after forming the initial collision complex (Sugase *et al* 2007). Due to their ability to attain different conformations, such proteins can also interact with a number of different proteins. β thymosins might also behave in a similar

way. In other words, their binding to actin may induce a stable three-dimensional structure with defined secondary structural elements. The ability to adopt different conformations might explain the promiscuous protein interactions and multiple extracellular functions of β thymosins.

3.2 Biological functions

Various studies have shown diverse biological roles of Tβ4. It promotes wound repair, angiogenesis, cell migration, tissue protection, regeneration in the skin, eyes and heart, and prevents apoptosis and inflammation.

3.2.1 Tβ4 promotes cell migration and adhesion

The regulation of polymerization and depolymerization of actin subunits is a key mechanism by which Tβ4 enables cells to migrate (Malinda *et al* 1997; Grant *et al* 1995). It also upregulates the gene expression of laminin -5, a subepithelial basement membrane protein believed to be one of the best ligands for keratinocyte adhesion and migration, and influences cell migration (Sosne *et al* 2004). Tβ4 also activates Akt, which plays a very potent role in cell growth, survival and motility (Bock-Marquette *et al* 2004). During the morphological differentiation of endothelial cells into capillary-like tubes, there is a five fold increase in Tβ4 mRNA level. When the endothelial cells are transfected with Tβ4, there is an increased rate of attachment and spreading on matrix components and an accelerated rate of tube formation on Matrigel (Grant *et al* 1995). Tβ4 also stimulates the migration of HUVECs (Malinda *et al* 1997) and induces matrix metalloproteinase 2 *in vitro* and *in vivo* (Malinda *et al* 1999). Another study indicated that local production of Tβ4 is increased during muscle injury and it promotes myoblast migration, hence facilitating skeletal muscle regeneration (Tokura *et al* 2011).

3.2.2 Tβ4 prevents apoptosis and promotes cell survival, angiogenesis and cell differentiation

Tβ4 has been shown to reduce apoptosis and promote induction of anti apoptotic genes. A previous study on the pro-apoptotic effects of ethanol on corneal epithelial cells has

shown that Tβ4 decreases cytochrome c release from the mitochondria and caspase activation. It also increases the expression of anti-apoptotic protein, bcl-2 (Sosne *et al* 2004). In cardiomyocytes, it activates the phosphoinositide/Akt cell survival signalling pathway and inhibits endothelial apoptosis (Hinkel *et al* 2008).

Tβ4 is known to be an important angiogenic molecule that promotes angiogenesis by differentiation and directional migration of endothelial cells (Malinda *et al* 1997; Grant *et al* 1999). It promotes coronary vessel development and collateral growth during embryonic development and also stimulates epicardial vascular progenitors which can later differentiate into endothelial and smooth muscle cells (Smart *et al* 2007). Tβ4 has been shown to induce dermal repair and hair growth by promoting stem cell migration and differentiation into keratinocytes and hair follicles (Philip *et al* 2004).

3.2.3 Role of Tβ4 in thrombosis

The concentration of Tβ4 is very high in white blood cells and in plasma is very low, however during blood clotting, Tβ4 concentration in the serum increases substantially. In 1987, it was shown that Tβ4 is present in human blood platelets in very high concentrations (Hannappel *et al* 1987). In resting platelets, the Tβ4 concentration is ~ 560μM, of which ~ 280μM is in complex with G actin and ~280μM is free (Nachmias *et al* 1993).

During blood coagulation or ADP induced aggregation of platelets Tβ4 is liberated from platelets and partially cross-linked to fibrin by a transglutaminase, factor XIIIa (Huff *et al* 2002). Tβ4 crosslinking to the fibrin occurs in a time and Ca^{2+} dependent manner. Factor XIIIa incorporates Tβ4 preferentially into the fibrin αC-domains, a domain often used to attach biologically active peptides to fibrin (Makogonenko *et al* 2004). The covalent cross-linking of Tβ4 to the fibrin clot might represent a mechanism to guarantee a high local concentration of the peptide at the site of injury probably supporting subsequent wound healing. This could be a potential molecular mechanism to bring Tβ4 near the site of vascular injury and leads to clotting and wound repair by Tβ4.

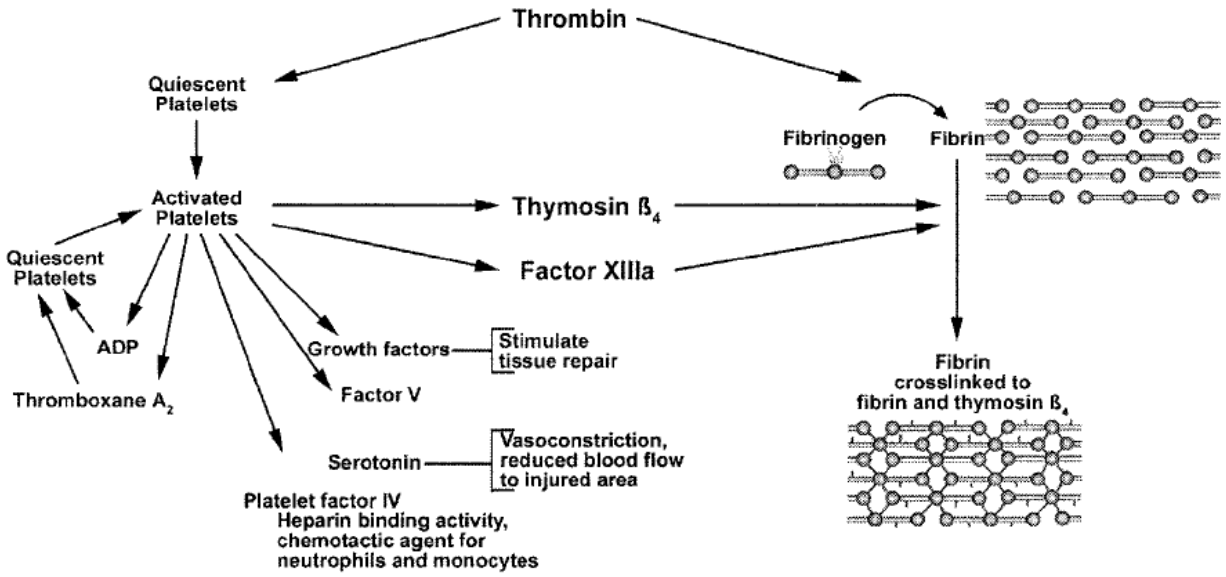

Figure 9 – Tβ4 and blood coagulation (Image taken from Huff *et al* 2002).

When the platelets are stimulated with ADP, various cytoskeletal changes take place. The platelets change shape and there is secretion of ADP, Factor V, Tβ4, serotonin, thromboxane A_2 and growth factors. The platelets aggregate and form a platelet plug, which must be stabilized by a fibrin clot to ensure wound closure. The fibrin monomers attach to the platelet plug and are further cross linked by factor XIII to form an insoluble clot. Tβ4 released from the platelets is also fixed to the fibrin clot by factor XIII

3.2.4 Role of Tβ4 in inflammation and corneal wound healing and repair

Previous studies have shown that Tβ4 decreases inflammation and promotes corneal wound healing. It decreases matrix metalloproteinases and proinflammatory cytokines and chemokines. In mouse models, topical application of Tβ4 after alkali injury downregulates the expression of the potent chemoattractants, macrophage inflamatory protein 2 (MIP 2) and keratinocyte chemoattractant (KC) in the cornea (Sosne *et al* 2002). It also accelerates epithelial cell migration and re-epithelialization after alkaline and alcohol injuries and scrape wounding in a dose-dependent manner in rat corneal wound models (Sosne *et al* 2002, 2005). Tβ4 has been shown to protect corneal endothelial cells from apoptosis and oxidative stress induced by low dose ultraviolet B (UVB) exposure (Ho *et al* 2010). It protects human corneal epithelial cells against Fas ligand (Fas-L) and H_2O_2 induced damage. Internalization of Tβ4 is critical for its cytoprotective effect (Ho *et al* 2007).

Tβ4 is hypothesized to be an anti-inflammatory agent. It interferes with the NFκB signalling pathway, which is activated by the potent pro-inflammatory cytokine TNFα. Tβ4 pre treatment reduces nuclear NFκB protein levels, NFκB activity, and p65 subunit phosphorylation, and nuclear translocation in corneal epithelial cells stimulated with TNF α (Sosne *et al* 2007). No receptors have been identified for Tβ4 thus far. Future investigation of putative Tβ4 receptors would provide critical information for understanding how extracellular Tβ4 exerts its biological activities in cells.

4. Retinal Pigment Epithelium

Retinal pigment epithelium (RPE) is a monolayer of pigmented cuboidal cells present between the retinal photoreceptors and choriocapillaris. It is separated from the choriocapillaris, which supplies blood flow to the RPE, and the outer one-third of the retina (including the photoreceptors), by Bruch's membrane. The human RPE incorporates approximately 3.5 million epithelial cells arranged in a regular hexagonal pattern. RPE are bound together by junctional complexes with prominent tight junctions. These junctions divide the cells in an apical half that faces the retina and a basal half that faces the choroid (Hudspeth *et al* 1973). The only anatomical contact between the photoreceptors and RPE is the interphotoreceptor matrix. Under pathological conditions such as retinal detachment, fluid accumulates in the subretinal space and photoreceptors are separated from the RPE. This causes a loss of photoreceptor function.

The embryonic development and differentiation of RPE and photoreceptors is interrelated. Both photoreceptors and choriocapillaries depend on the RPE for their survival. RPE is crucial for the development of the retina. It secrets various growth factors required for photoreceptor differentiation and survival. It has been shown in an animal model of retinal dystrophy, that RPE secretes basic fibroblast growth factor (bFGF), which promotes the survival of photoreceptors (Faktorovich *et al* 1990). Neuronal retina and photoreceptors are affected the most by RPE loss.

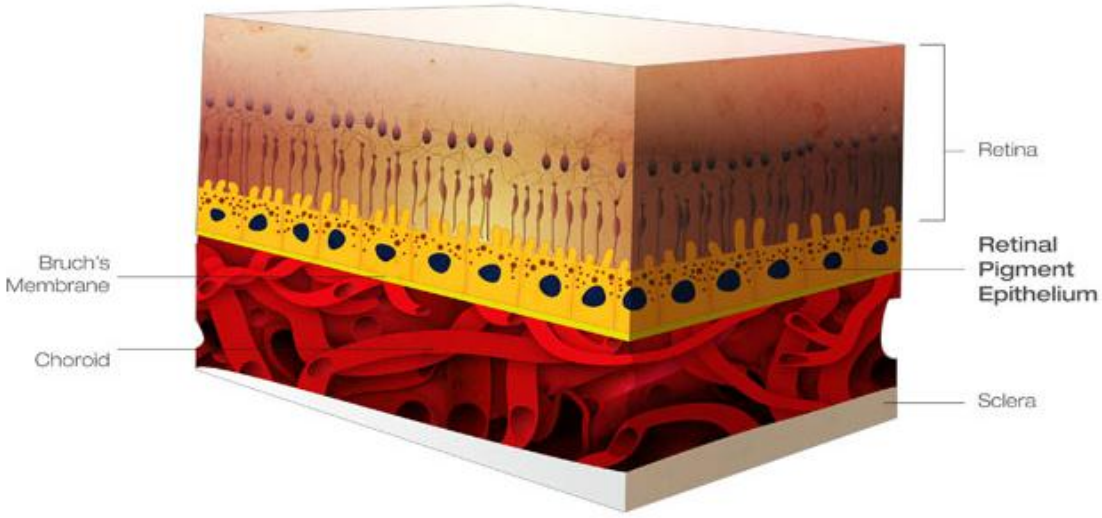

Figure 10 – Retinal pigment epithelium. (Image taken from www.dev.ellex.com)

4.1 RPE Functions

RPE is involved in a variety of functions which includes phagocytosis of shed outer segments, transport of vitamin A to the photoreceptors and maintenance of normal physiology of the choriocapillaries (Bok *et al* 1993). RPE transports electrolytes and water from the subretinal space to the choroid, also transports glucose and other nutrients from the blood to the photoreceptors.

a) Light absorption – RPE increases optical quality by helping in absorption of the scattered light. RPE pigmentation is very critical to maintain visual function. It contains a complex composition of various pigments (melanin, lipofuscin) which absorb different wavelengths of light. Melanin is the main pigment of RPE present within cytoplasmic granules called melanosomes. It absorbs stray light and minimizes light scattering within the eye. The retina has a direct and frequent exposure to light which causes the photo-

oxidation of lipids, which can be extremely toxic to retinal cells (Girotti *et al* 2004). The retina also generates large amounts of reactive oxygen species (ROS) due to its high oxygen consumption. RPE counterbalances the high oxidative stress present in the retinal cells by maintaining large amounts of enzymes like superoxide dismutase (SOD) and catalase (Frank *et al* 1999; Tate *et al* 1995) and non enzymatic antioxidants like ascorbate, lutein and zeaxanthin (Newsome *et al* 1994; Beatty *et al* 2000), which act as a defence system against the oxidative stress.

b) Transport nutrients and ions – RPE transports nutrients like glucose, retinol and fatty acids from blood to the photoreceptors. It has large numbers of glucose transporters GLUT 1 and GLUT 3 in its apical and basolateral membranes (Ban *et al* 2000). With the help of these glucose transporters, RPE transfers glucose from the blood to the photoreceptors. GLUT1 induces glucose transport in response to mitogens and hence adapts glucose transport according to the metabolic needs of the retina. During the visual cycle, the bulk of retinal is exchanged between RPE and the photoreceptors. The RPE takes all-*trans* retinol from the photoreceptors, oxidizes and isomerizes it to 11-*cis* retinal and redelivers it to the photoreceptors (Baehr *et al* 2003). Docosahexaenoic acid (DHA) is an essential omega 3 fatty acid which is required as a structural element of photoreceptor and neuron membranes, however, DHA cannot be synthesized by the neural tissues and is hence transported by RPE from blood to the photoreceptors (Anderson *et al* 1992).

Due to the high metabolic turnover in the photoreceptors, a large amount of water is produced in the retina. Also, there is movement of water from the vitreous body to the retina due to intraocular pressure (Marmor *et al* 1990; Hamann *et al* 2002). Hence, there is a constant need for removal of water from the retina. RPE transports water and ions from the subretinal space to the blood (Hughes *et al* 1998). It also eliminates metabolic end products of the photoreceptors. Photorecpetor outer segments produce lactic acid and its subretinal concentration is estimated to be around 19 mM (Adler *et al* 1992; Hsu *et al* 1994). RPE removes lactic acid from the subretinal space through lactate-H^+ cotransporter MCT1 (Lin *et al* 1994; Philip *et al* 1998) and Na^+ dependent transporter for

organic acids (Kenyon *et al* 1994). The Na^+-K^+-ATPase, which is located in the apical membrane, provides the energy for transepithelial transport (Marmorstein *et al* 2001).

c) Phagocytosis – When the photoreceptors are exposed to high intensities of light, there is an increase in concentration of light induced toxic substances like photo oxidative radicals and photo damaged proteins and lipids, in the photoreceptors (Beatty *et al* 2000). To maintain the excitability of the photoreceptors, the photoreceptor outer segments undergo a constant renewal process (Young *et al* 1969; Nguyen-Legros *et al* 2000). The highest concentration of these toxic substances is present in the tips of the photoreceptor outer segments. Hence, these tips are shed from the photoreceptors and new tips are formed from the base of outer segments, at the cilium. The shedding of tips and the formation of new tips is very well coordinated, so that the length of photoreceptor outer segments is maintained. The shed tips are phagocytosed and digested by RPE. Retinal and docosahexaenoic acid are transported back to the photoreceptors to rebuild the outer segments (Bok *et al* 1993; Bibb *et al* 1974).

d) Secretion – RPE secretes a large number of growth factors which are essential for the maintenance of the structural integrity of the retina. It secretes fibroblast growth factors (FGF-1, FGF-2 and FGF-5), insulin like growth factor-1 (IGF-1), VEGF, pigment epithelium derived factor (PEDF), platelet derived growth factor (PDGF) and lens epithelium derived growth factor (LEDGF).

Although VEGF is secreted in very low quantities by RPE, it plays an important role in maintaining intact endothelium of the choriocapillaries (Adamis *et al* 1993; Burns *et al* 1992). A neuroprotective factor PEDF secreted by RPE protects neurons against glutamate and hypoxia induced apoptosis (Cao *et al* 2001). It stabilizes the endothelium of choriocapillaries (King *et al* 2000) and plays an important role in the embryonic development of the eye (Behling *et al* 2002). Another peptide secreted by RPE is somatostatin, which plays an important role in retinal homeostasis. Somatostatin acts as a neuromodulator through different pathways including intracellular calcium signalling (Johnson *et al* 2001) and glutamate release from the photoreceptors (Akopian *et al* 2000).

e) Retinoid cycle – One of the most important functions of RPE is its role in the visual or retinoid cycle, which involves repeated movement of retinoid and its derivatives between photoreceptors and RPE (Bok *et al* 1993). The light is absorbed by rhodopsin, which is composed of the G-coupled receptor protein opsin and chromophore 11-*cis* –retinal. After light absorption, 11-*cis*-retinal is converted into all-*trans* retinal. The photoreceptors lack *cis*-*trans* isomerase function for retinal and are unable to regenerate 11-*cis*-retinal from all-*trans*-retinal. The main purpose of the visual cycle is to regenerate 11-*cis* retinal, which acts as a chromophore for the visual pigments of outer segments of photoreceptors. All-*trans*-retinal is reduced to all-*trans*-retinol and is transported to RPE. The isomerisation is the first step in phototransduction and takes place in RPE. In RPE, retinol is oxidized and reisomerized to 11-*cis*-retinal by the enzyme retinal pigment epithelium-specific proten (RPE65) and is delivered back to the photoreceptors (Hargrave *et al* 2001; Pang *et al* 2006; Bernstein *et al* 1987). Interphotoreceptor retinoid binding protein (IRBP) mediates the transport of retinoids between RPE and photoreceptors. IRBP is a large glycoprotein present in the RPE endosomes and interphotoreceptor matrix (IPM) (Cunningham *et al* 2003; Wu *et al* 2007; Gonzalez-Fernandez *et al* 2008). IRBP solubilises retinal and retinol and mediates the direction of transport of these compounds (Okajima *et al* 1989; Pepperberg *et al* 1991).

4.2 RPE ageing and diseases

A variety of structural and biochemical changes occur in RPE with increasing age. There is increase in atrophy, hyperpigmentation and loss in cell shape. With advancing age, there is also a decrease in the concentration of RPE cells in the posterior pole. The melanin content of RPE also decreases with age (Salvi *et al* 2006). Senescent RPE accumulate metabolic debris from remnants of incomplete degradation of phagocytized rod and cone membranes (Ciulla *et al* 2001). Ingestion of outer segments of photoreceptors puts a heavy phagocytic burden on RPE, which results in the accumulation of lipofuscin between RPE and Bruch's membrane. Lipofuscin is an undegradable byproduct of outer segment photoreceptor metabolism which increases in RPE over time. The accumulation of lipofuscin is involved in the pathogenesis of various

retinal diseases like age related macular degeneration (AMD) and is one of the major characteristic features of ageing in RPE. Lipofuscin is continuously exposed to light and high oxygen tension, which leads to production of reactive oxygen species (ROS) and causes oxidative damage to mitochondria and mitochondrial DNA. The production of antioxidants, which RPE produces to counteract oxidative stress, also decreases with age (Liang *et al* 2003). Mitochondrial damage affects the cellular and physiological functioning of RPE. This leads to decrease in energy production and subsequently signals apoptosis eventually decreasing the number of RPE (Zarbin *et al* 2004).

Under normal conditions, RPE secretes various growth factors which can protect photoreceptors from damage. There is constant balance between angiogenic and anti-angiogenic growth factors within the eye. Imbalance between the secretion of these growth factors leads to choroidal neovascularisation (Bhutto *et al* 2006). PEDF and VEGF are two growth factors secreted by RPE, which cross regulate each other. VEGF gene expression increases angiogenesis whereas PEDF acts as an antagonist and inhibits angiogenesis (Tsai *et al* 2006; Dawson *et al* 1999). To regulate angiogenesis in the retina, balance between these two growth factors is very essential (Tong *et al* 2006). Previous studies have shown that VEGF is upregulated in RPE and choroid complex in patients suffering from AMD (Tsai *et al* 2006). Decreased PEDF levels in the vitreous samples of AMD patients have also been reported (Holekamp *et al* 2002).

4.2.1 Age related macular degeneration (AMD) – AMD is the major cause of blindness in elderly people. The atrophic or dry form of AMD is caused by progressive degradation of RPE and the photoreceptors. In AMD, vision loss occurs as a result of photoreceptor damage in the central retina; however the initial pathogenesis involves RPE degeneration (Zarbin *et al* 1998). Since RPE is involved in the metabolic and nutritional aspects of the photoreceptors, RPE dysfunction can cause secondary degeneration of the photoreceptors. Age-related processes that occur in the retinal pigment epithelium-Bruch's membrane-choriocapillaris complex can precede the development of AMD (Liang *et al* 2003). AMD is associated with an accumulation of lipofuscin, a pigment formed in tissues with high levels of oxidative stress. Early AMD is characterized by thickening and loss of normal

architecture within Bruch's membrane, lipofuscin accumulation in the RPE, and drusen formation beneath the RPE in Bruch's membrane. The primary clinical characteristic of late stage dry AMD is the appearance of RPE atrophy. It is characterized by roughly oval areas of hypopigmentation and is usually the consequence of RPE cell loss. Loss of RPE cells which provide nutrition to the photoreceptors leads to the gradual degeneration of nearby photoreceptors, resulting in a progressive visual impairment.

4.2.2 Retinitis pigmentosa – Retinitis pigmentosa is an inherited form of retinal which is characterized by pigment deposits in the retina. It involves degeneration of photoreceptors rods and cones and deposits in the retinal pigment epithelium. The accumulation of metabolic waste products lead to lipofuscin formation which affects the function of the RPE. The inability of RPE to phagocytose photoreceptor outer segments causes an autosomal recessive form of retinitis pigmentosa (Edwards *et al* 1977; Wang *et al* 2001).

4.2.3 Diabetic retinopathy – Diabetic retinopathy (DR) is one of the leading causes of blindness in developed countries. DR is characterized by decreased levels of glutathione, SOD and ascorbic acid (Madsen-Bouterse *et al* 2008; Silva *et al* 2009; Minamizono *et al* 2006). A recent study has shown that there is a decrease in IRBP production in early diabetic retinopathy (Garcia-Ram´ırez *et al* 2009). IRBP is required for retinoid transport between RPE and photoreceptors and is critical for the visual cycle.

Increased production of VEGF, an angiogenic factor, plays an important role in the pathogenesis of DR. There is a decreased expression of the anti-angiogenic factor, PEDF, by elevated glucose concentration in cultured human RPE cells (Yao *et al* 2003). New therapeutic approaches for DR which involve blocking VEGF and stimulating PEDF have been proposed. The development of DR is also favoured by the decreased expression of somatostatin (Carrasco *et al* 2007). Somatostatin plays an important role in preventing neovascularisation and fluid accumulation within the retina. These functions are greatly impaired due to downregulation of somatostatin expression, thus leading to development of DR (Hern´andez *et al* 2005; Sim *et al* 2007).

References

Adamis AP, Shima DT, Yeo KT, Yeo TK, Brown LF, Berse B, D'Amore PA and Folkman J. Synthesis and secretion of vascular permeability factor/vascular endothelial growth factor by human retinal pigment epithelial cells. Biochem Biophys Res Commun 1993; 193: 631–638.

Adler AJ and Southwick RE. Distribution of glucose and lactate in the interphotoreceptor matrix. Ophthalmic Res 1992; 24: 243–252.

Akopian A, Johnson J, Gabriel R, Brecha N and Witkovsky P. Somatostatin modulates voltage-gated K^+ and Ca^{2+} currents in rod and cone photoreceptors of the salamander retina. Journal of Neuroscience 2000; 20 (3): 929–936.

Albuquerque ML, Waters CM, Savla U, Schnaper HW and Flozak AS. Shear stress enhances human endothelial cell wound closure in vitro. Am J Physiol Heart Circ Physiol 2000; 279: H293–H302.

Anderson RE, O'Brien PJ, Wiegand RD, Koutz CA and Stinson AM. Conservation of docosahexaenoic acid in the retina. Advances in Experimental Medicine and Biology 1992; 318: 285–294.

Andrews RK, Lopez JA and Berndt MC. Molecular mechanisms of platelet adhesion and activation. Int J Biochem. 1997; 29:91-105.

Andrews RK, Gardiner EE, Shen, Y, Whisstock JC and Berndt MC. Glycoprotein Ib-IX V. Int. J. Biochem. Cell Biol. 2003; 35 (8): 1170-1174.

Badimon L, Turitto V, Rosemark JA, Badimon JJ and Fuster V. Characterization of a tubular flow chamber for studying platelet interaction with biologic and prosthetic materials: deposition of indium 111-labeled platelets on collagen, subendothelium, and expanded polytetrafluoroethylene. J Lab Clin Med. 1987;110(6):706-18.

Baehr W, Wu SM, Bird AC and Palczewski K. The retinoid cycle and retina disease. Vision Research 2003; 43 (28): 2957–2958.

Ban Y and Rizzolo LJ. Regulation of glucose transporters during development of the retinal pigment epithelium. Brain Res 2000; 121: 89–95.

Bao LR, Loda M, Janmey PA, Steward R, Ananapte B and Zatter BR. Thymosin beta 15: a novel regulator of tumor cell motility upregulated in metastatic prostate cancer. Nature Med 1996; 2: 1322-1328.

Barstad RM, Roald HE, Cui Y, Turitto VT and Sakariassen KS. A perfusion chamber developed to investigate thrombus formation and shear profiles in flowing native human blood at the apex of well- defined stenoses. Arterioscler Thromb Vasc Biol 1994; 14:1984-1991.

Baum J and Brodsky B. Folding of peptide models of collagen and misfolding in disease. Curr Opin Struct Biol 1999; 9: 122–128.

Beatty S, Koh H, Phil M, Henson Ds and Boulton M. The role of oxidative stress in the pathogenesis of age-related macular degeneration. Surv Ophthalmol 2000; 45:

115–134.

Behling KC, Surace EM and Bennett J. Pigment epitheliumderived factor expression in the developing mouse eye. Mol Vis 2002; 8: 449–454.

Berndt MC, Ward CM, De Luca M, Facey DA, Castaldi PA, Harris SJ and Andrews RK. The molecular mechanisms of platelet adhesion. Aust.NZ.J Med 1995; 25:822 830.

Bernstein, P.S., W.C. Law and R.R. Rando. Isomerization of all-trans-retinoids to 11-cis retinoids in vitro. Proc. Natl. Acad. Sci. U.S.A. 1987; 84:1849-1853.

Bhutto IA, McLeod DS, Hasegawa T, Kim SY, Merges C, Tong P and Lutty GA. Pigment epithelium-derived factor (PEDF) and vascular endothelial growth factor (VEGF) in aged human choroid and eyes with age-related macular degeneration. Exp Eye Res 2006; 82:99–110.

Bibb C and Young RW. Renewal of fatty acids in the membranes of visual cell outer segments. Journal of Cell Biology 1974; 61 (2): 327–343.

Bock-Marquette I, Saxena A, White MD, Dimaio JM and Srivastva. Thymosin beta 4 activates integrin-linked kinase and promotes cardiac cell migration, survival and cardiac repair. Nature 2004; 432: 466–472.

Bok D. The retinal pigment epithelium: a versatile partner in vision. J Cell Sci Suppl 1993; 17: 189–195.

Born GVR. Quantitative investigations into the aggregation of blood platelets. J Physiol 1962; 162: 67P-68P.

Brown TD 2000 Techniques for mechanical stimulation of cells in vitro: a review. J Biomech 33(1):3-14.

Burns MS and Hartz MJ. The retinal pigment epithelium induces fenestration of endothelial cells in vivo. Curr Eye Res 1992; 11: 863–873.

Campochiaro PA. Retinal and choroidal neovascularization. J Cell Physiol 2000; 184: 301–310.

Cao W, Tombran-Tink J, Elias R, Sezate S, Mrazek D, and McGinnis JF. In vivo protection of photoreceptors from light damage by pigment epithelium-derived factor. Invest Ophthalmol Vis Sci 2001; 42: 1646–1652.

Carrasco E, C. Hern´andez, A. Miralles, P. Huguet, J. Farr´es, and R. Sim´ o. Lower somatostatin expression is an early event in diabetic retinopathy and is associated with retinal neurodegeneration. Diabetes Care 2007; 30(11): 2902–2908.

Chatzizisis YS, Coskun AU, Jonas M, Edelman, Feldman CL and Stone PH. Role of endothelial shear stress in the natural history of coronary atherosclerosis and vascular remodeling. J Am Coll Cardiol 2007; 49:2379-2393.

Chiu JJ, Wang DL, Chien S, Skalak R and Usami S. Effects of disturbed flow on endothelial cells. J Biomech Eng. 1998; 120:2-8.

Ciulla TA, Harris A and Martin BJ. Ocular perfusion and age related macular degeneration. Acta Ophthalmol Scand 2001; 79:108–15.

Communi D, Janssens R, Suarez-Huerta N, Robaye B and Boeynaems JM. Advances in

signaling by extracellular nucleotides: the role and transduction mechanisms of P2Y receptors. Cell Signal 2000; 12: 351–360.

Cunningham LL and F. Gonzalez-Fernandez. Internalization of interphotoreceptor retinoid-binding protein by the Xenopus retinal pigment epithelium. Journal of Comparative Neurology 2003; 466 (3): 331–342.

Dardik A, Chen L, Frattini J, Asada H, Aziz F, Kudo FA, Sumpio BE. Differential effects of orbital and laminar shear stress on endothelial cells. Journal of Vascular Surgery 2005; 41, 869-880.

Davies PF. Flow-mediated endothelial mechanotransduction. Physiol. Rev. 1995; 75, 519–560.

Dawson DW, Volpert OV, Gillis P, Crawford SE, Xu H, Benedict W and Bouck NP. Pigment epithelium-derived factor: a potent inhibitor of angiogenesis. Science. 1999 Jul 9; 285(5425):245-8.

Dewey CF Jr, Bussolari SR, Gimbrone MA Jr, Davies PF. The dynamic response of vascular endothelial cells to fluid shear stress. Journal of Biomechanical Engineering 1981; 103: 177-185.

Dimmeler S, Haendeler J, Rippmann V, Nehls M and Zeiher AM. Shear stress inhibits apoptosis of human endothelial cells. FEBS Lett. 1996; 399:71-74.

Edwards RB and Szamier RB. Defective phagocytosis of isolated rod outer segments by RCS rat retinal pigment epithelium in culture. Science 1977;197: 1001–1003.

Faktorovich EG, Steinberg RH, Yasumura D, Matthes MT and LaVail MM. Photoreceptor degeneration in inherited retinal dystrophy delayed by basic fibroblast growth factor. Nature 1990; 347:83-86.

Farndale RW, Sixma JJ, Barnes MJ and DeGroot PG. The role of collagen in thrombosis and hemostasis. J Thromb Haemost. 2004; 2: 561-573.

Frank RN, Amin RH and Puklin JE. Antioxidant enzymes in the macular retinal pigment epithelium of eyes with neovascular age-related macular degeneration. American Journal of Ophthalmology 1999; 127 (6): 694– 709.

Frank RN. Growth factors in age-related macular degeneration: pathogenic and therapeutic implications. Ophthalmic Res 1997; 29: 341– 353.

Fukuyama M, Satai K,Itagaki I, Kawano K, Murata M, Kawai Y, Watanabe K, Handa M and Ikeda Y. Continuous measurement of shear induced platelet aggregation. Thrombosis Research 1989; 54: 253-260.

Garcia-Ram´ırez M, Hern´andez C, Villarroel M, Canals F, Alonso M, Fortuny R, Masmiquel L, Navarro A, García-Arumí J, Simó R. Interphotoreceptor retinoid binding protein (IRBP) is downregulated at early stages of diabetic retinopathy. Diabetologia 2009; 52 (12): 2633–2641.

Gawaz M. Role of platelets in coronary thrombosis and reperfusion of ischemic myocardium. Cardiovasc Res. 2004; 61: 498-511.

Girard, P.R., and Nerem RM. Shear stress modulates endothelial cell morphology and F actin organization through the regulation of focal adhesion-associated proteins. J.

Cell. Physiol. 1995; 163, 179–193.

Girotti AW and T. Kriska T. Role of lipid hydroperoxides in photo-oxidative stress signalling. Antioxidants and Redox Signaling 2004; 6 (2): 301–310, 2004.

Gonzalez-Fernandez F and D. Ghosh. Focus on molecules: interphotoreceptor retinoid binding protein (IRBP). Experimental Eye Research 2008; 86 (2):169–170.

Goto S, Salomon DR, Ikeda Y and Ruggeri ZM. Characterization of the unique mechanisms mediating the shear-dependent binding of soluble von Willebrand factor to platelets. J Biol Chem 1995; 270:23353-23361.

Goto S, Tamura N, Eto K, Ikeda Y and Handa S. Functional significance of adenosine 5¢ diphosphate receptor ($P2Y_{12}$) in platelet activation initiated by binding of von Willebrand factor to platelet GP Iba induced by conditions of high shear rate. Circulation. 2002; 105:2531-2536.

Goto, S., Y. Ikeda, E. Saldivar and Z. M. Ruggeri. Distinct mechanisms of platelet aggregation as a consequence of different shearing flow conditions. J. Clin. Invest. 1998; 101:479–486.

Grabowski EF, Jaffe EA and Weksler BB. Prostacyclin production by cultured endothelial cell monolayers exposed to step increases in shear stress. J Lab Clin Med. 1985; 105(1):36-43.

Grant DS, Kinsella JL, Kibbey MC, LaFlamme S, Burbelo PD, Goldstein AL and Kleinman HK. 1995. Matrigel induces thymosin beta 4 gene in differentiating endothelial cells. J. Cell Sci. 1995; 108: 3685–3694.

Grant DS, Rose W, Yaen C, Goldstein A, Martinez J and Kleinman H. 1999. Exogenous Thymosin beta 4 enhances endothelial differentiation and angiogenesis. Angiogenesis 1999; 3: 125–135.

Gruner S, ProstrednaM, Schulte V, Krieg T, Eckes B, Brakebusch C and Nieswandt B. Multiple integrin-ligand interactions synergize in shear resistant platelet adhesion at sites of arterial injury in vivo. Blood 2003; 102: 4021–7.

Gutierrez E, Petrich BG, Shattil SJ, Ginsberg, Groisman A and Kasirer-Friede A. Microfluidic devices for studies of shear dependent platelet adhesion. Lab Chip 2008; 8(9): 1486-1495.

Hamann S. Molecular mechanisms of water transport in the eye. Int Rev Cytol 2002; 215: 395–431.

Hanada T, Hashimoto M, Nosaka S, Sasaki T, Nakayama K, Masumura S, Yamauchi M and Tamura K. Shear stress enhances prostacyclin release from endocardial endothelial cells. Life Sci. 2000; 66(3):215-20.

Hannappel E and Leibold W. Biosynthesis rates and content of thymosin beta 4 in cell lines. Arch.Biochem.Biophys. 1985; 240: 236-241.

Hannappel E and Van Kampen M. Determination of thymosin beta 4 in human blood cells and serum. J Chromatogr. 1987: 397; 279-285.

Hannappel, E and Wartenberg F. Actin-sequestering ability of thymosin $ß_4$, thymosin $ß_4$ fragments, and thymosin $ß_4$-like peptides as assessed by the DNase I inhibition

assay. *Biol. Chem. Hoppe-Seyler* 1993; **374**,117-122

Hargrave PA. Rhodopsin structure, function, and topography: the Friedenwald lecture. Investigative Ophthalmology and Visual Science 2001; 42 (1): 3–9.

Hern´andez C, Carrasco E, Casamitjana R, Deulofeu R, Garc´ıa-Arum´ı J and Sim´ o R. Somatostatin molecular variants in the vitreous fluid: a comparative study between diabetic patients with proliferative diabetic retinopathy and nondiabetic control subjects. Diabetes Care 2005; 28 (8): 1941–1947.

Hinkel R, El-Aouni C, Olson T, Horstkotte J, Mayer S, Müller S, Willhauck M, Spitzweg C, Gildehaus FJ, Münzing W, Hannappel E, Bock-Marquette I, DiMaio JM, Hatzopoulos AK, Boekstegers P and Kupatt C.. Thymosin beta 4 is an essential paracrine factor of embryonic endothelial progenitor cell-mediated cardioprotection. Circulation 2008; 117: 2232–2240.

Ho JH, Su Y, Chen KH and Lee OK. Protection of thymosin beta-4 on corneal endothelial cells from UVB-induced apoptosis. Chin J Physiol. 2010 Jun 30; 53(3):190-5.

Ho JHC, Chuang CH, Ho CY, Shih YRV, Lee OKS and Su Y. Internalization is essential for the antiapoptotic effects of exogenous thymosin beta-4 on human corneal epithelial cells. Investigative Ophthalmology & Visual Science. 2007; 48: 27-33.

Holekamp NM, Bouck N and Volpert O. Pigment epithelium-derived factor is deficient in the vitreous of patients with choroidal neovascularisation due to age-related macular degeneration. Am J Ophthalmol 2002; 134:220–7.

Holz FG, Pauleikhoff D, Klein R and Bird AC. Pathogenesis of lesions in late age-related macular disease. Am J Ophthalmol 2004; 137: 504–510.

Hsu PP, Li S, Li YS, Usami S, Ratcliffe A, Wang X and Chien S. Effects of flow patterns on endothelial cell migration into a zone of mechanical denudation. Biochem Biophys Res Commun 2001; 285:751–759.

Hsu SC and Molday RS. Glucose metabolism in photoreceptor outer segments. Its role in phototransduction and in NADPH-requiring reactions. J Biol Chem 1994; 269: 17954–17959.

Hudspeth AJ and Yee AG. The intercellular junctional complexes of retinal pigment epithelia. Invest Ophthalmol Vis Sci 1973;12: 354-365.

Huff T, Otto AM, Muller CS, Meier M and Hannappel E. Thymosin β 4 is released from human blood platelets and attached by factor XIIIa (transglutaminase) to fibrin and collagen. FASEB J 2002; 16:691–696.

Huff T, Müller CSG, Otto AM, Netzker R and Hannappel E. ß-Thymosins: small, acidic peptides with multiple functions. *Int. J. Biochem. Cell Biol.* 2001; **33**,205-220.

Hughes BA, Gallemore RP and Miller SS. Transport mechanisms in the retinal pigment epithelium. In: The Retinal Pigment Epithelium, edited by Marmor MF and Wolfensberger TJ. New York: Oxford Univ. Press 1998: 103–134.

Ikeda Y, Handa M, Kawano K, Kamata T, Murata M, Araki Y, Anbo H, Kawai Y, Watanabe K, Itagaki I, Sakai K and Ruggeri ZM. The role of von Willebrand factor and fibrinogen in platelet aggregation under varying shear stress. J Clin

Invest 1991; 87: 1234–40.

Jacobs ER, Cheliakine C, Gebremedhin D, Birks EK, Davies PF and Harder DR. Shear activated channels in cell-attached patches of cultured bovine aortic endothelial cells. Pflugers Arch 1995; 431: 129-131.

Jin J and Kunapuli SP. Coactivation of two different G proteincoupled receptors is essential for ADP-induced platelet aggregation. Proc Natl Acad Sci U S A 1998; 95:8070–8074.

Johnson J, Caravelli ML and Brecha NC. Somatostatin inhibits calcium influx into rat rod bipolar cell axonal terminals. Visual Neuroscience 2001;18 (1): 101–108.

Kenyon E, Yu K, La Cour M and Miller SS. Lactate transport mechanisms at apical and basolateral membranes of bovine retinal pigment epithelium. Am J Physiol Cell Physiol 1994;267: C1561–C1573.

Kim S and Kunapuli SP. P2Y12 receptor in platelet activation. Platelets 2011; 22(1): 56 60.

King GL and Suzuma K. Pigment-epithelium-derived factor—a key coordinator of retinal neuronal and vascular functions. N Engl J Med 2000; 342: 349–351.

Kroll MH, Hellums JD, McIntire LV, Schafer AL and Moake JL. Platelets and shear stress. Blood 1996; 88:1525–1541.

Languino LR, Plescia J, Duperray A, Brian AA, Plow EF, Geltosky JE and Altieri DC. Fibrinogen mediates leukocyte adhesion to vascular endothelium through an ICAM- I -dependent pathway. Cell 1993; 73:1423-1434.

Levesque MJ, Nerem RM and Sprague EA. Vascular endothelial cell proliferation in culture and the influence of flow. Biomaterials 1990; 11:702-707.

Levesque MJ and Nerem RM. The elongation and orientation of cultured endothelial cells in response to shear stress. J Biomech Eng. 1985; 107(4):341-347.

Li C, Zeng Y, Hu J and Yu H. Effects of fluid shear stress on expression of proto oncogenes c-fos and c-myc in cultured human umbilical vein endothelial cells. Clin Hemorheol Microcirc. 2002; 26(2):117-23.

Li S, Butler P, Wang Y, Hu Y, Han DC, Usami S, Guan JL and Chien S. The role of the dynamics of focal adhesion kinase in the mechanotaxis of endothelial cells. Proc Natl Acad Sci USA 2000; 99:3546–3551.

Li S, Kim M, Hu YL, Jalali S, Schlaepfer DD, Hunter T, Chien S, Shyy JY. Fluid shear stress activation of focal adhesion kinase. Linking to mitogen-activated protein kinases. J. Biol. Chem. 1997; 272, 30455–30462.

Liang FQ and Godley BF. Oxidative stress-induced mitochondrial DNA damage in human retinal pigment epithelial cells: a possible mechanism for RPE aging and age related macular degeneration. Experimental Eye Research 2003; 76:397–403.

Lin H, la Cour M, Andersen MV, and Miller SS. Proton-lactate cotransport in the apical membrane of frog retinal pigment epithelium. Exp Eye Res 1994; 59: 679–688.

Liu Y, Chen BP, Lu M, Zhu Y, Stemerman MB, Chien S and Shyy JY. Shear stress activation of SREBP1 in endothelial cells is mediated by integrins. Arterioscler

Thromb Vasc Biol 2002;22:76-81.

Loncar R, Kalina U, Stoldt V, Thomas V, Scharf RE and Vodovnik A. Antithrombin significantly influences platelet adhesion onto immobilized fibrinogen in an in vitro system simulating low flow. Thrombosis Journal 2006, 4:19-26.

Low TL, Hu SK and Goldstein AL. Complete amino acid sequence of bovine thymosin beta 4: a thymic hormone that induces terminal deoxynucleotidyl transferase activity in thymocyte populations. PNAS 1981; 78: 1162-1166.

Madsen-Bouterse SA and R. A. Kowluru. Oxidative stress and diabetic retinopathy: pathophysiological mechanisms and treatment perspectives. Reviews in Endocrine and Metabolic Disorders 2008; 9 (4): 315–327.

Makogonenko E, Goldstein AL, Bishop PD and Medved L. Factor XIIIa incorporates thymosin b4 preferentially into the fibrin(ogen) aC-domains. Biochemistry 2004; 43:10748–10756.

Malek AM, Alper SL and Izumo S. Hemodynamic shear stress and its role in atherosclerosis. JAMA. 1999; 252:2035–2042.

Malek AM and Izumo S. Mechanism of endothelial cell shape change and cytoskeletal remodeling in response to fluid shear stress. J. Cell Sci. 1996; 109 (4), 713–726.

Malinda KM, Sidhu GS, Mani H, Banaudha K, Maheshwari RK, Goldstein AL and Kleinman HK. Thymosin ß$_4$ accelerates wound healing. J. Invest. Dermatol. 1999; 113,364-368.

Malinda KM, Goldstein AL and Kleinman HK. Thymosin β4 stimulates directional migration of human umbilical vein endothelial cells. FASEB J 1997; 11: 474–481.

Marmor MF. Control of subretinal fluid: experimental and clinical studies. Eye 1990;4: 340–344.

Marmorstein AD. The polarity of the retinal pigment epithelium. Traffic 2001; 2 (12):867–872.

Massberg S, Brand K, Gruner S, Page S, Muller E, Muller I, Bergmeier W, Richter T, Lorenz M, Konrad I, Nieswandt B and Gawaz M. A critical role of platelet adhesion in the initiation of atherosclerotic lesion formation. J Exp Med 2002; 196: 887-96.

McDonald DA. Blood flow in arteries. Baltimore: The Williams and Wilkins Co. 1974: 356-378.

Minamizono A, Tomi M, and Hosoya KI. Inhibition of dehydroascorbic acid transport across the rat blood-retinal and -brain barriers in experimental diabetes. Biological and Pharmaceutical Bulletin 2006; 29 (10): 2148–2150.

Modderman PW, Admiraal LG, Sonnenberg A and Von dem Borne AE. Glycoproteins V and Ib-IX form a noncovalent complex in the platelet membrane. J.Biol.Chem. 1992; 267: 364-369.

Mondy JS, Lindner V, Miyashiro JK, Berk BC, Dean RH and Geary RL. Platelet-derived growth factor ligand and receptor expression in response to altered blood flow in vivo. Circ Res. 1997; 81:320-327.

Moroi M, Jung SM, Nomura S, Sekiguchi S, Ordinas A and Diaz-Ricart M. Analysis of the involvement of the von Willebrand factor-glycoprotein Ib interaction in platelet adhesion to a collagen-coated surface under flow conditions. Blood. 1999; 90: 4413-4424.

Mustard JF, Jorgensen L, Hovig T, Glynn MF and Rowsell HC. Role of platelets in thrombosis. Thromb Diath Haemorrh Suppl 1966; 21:131–58.

Nachmias VT, Cassimeris L, Golla R and Safer D. Thymosin beta 4 (T) in activated platelets. European Journal of Cell Biology 1993; 61: 314-320.

Nerem RM. Hemodynamics and the vascular endothelium. J. Biomech. Eng. 1993; 115:510 –514.

Newsome DA, Miceli MV, Liles MR, Tate Jr. DJ, and Oliver PD. Antioxidants in the retinal pigment epithelium. Progress in Retinal and Eye Research 1994; 13 (1):101– 123.

Nguyen-Legros J and Hicks D. Renewal of photoreceptor outer segments and their phagocytosis by the retinal pigment epithelium. Int Rev Cytol 2000; 196: 245 313.

Nieswandt B, Varga-Szabo D and Elvers M. Integrins in platelet activation. Journal of Thrombosis and Haemostasis 2009; 7 (Suppl. 1): 206–209.

Nieswandt B, Watson SP. Platelet collagen interaction: is GPVI the central receptor? Blood 2003; 102: 449-61.

Noria S, Xu F, McCue S, Jones M, Gotlieb AI and Langille BL. Assembly and reorientation of stress fibers drives morphological changes to endothelial cells exposed to shear stress. American Journal of Pathology 2004; 164 (4): 1211-1223.

Okajima TI, Pepperberg DR, Ripps H, Wiggert B and Chader GJ, Interphotoreceptor retinoid-binding: role in delivery of retinol to the pigment epithelium. Experimental Eye Research 1989; 49 (4): 629–644.

Olesen SP, Clapham DE and Davies PF. Haemodynamic shear stress activates a K+ current in vascular endothelial cells. Nature 1988; 331: 168-170.

Osawa M, Masuda M, Harada N, Lopes RB and Fujiwara K. Tyrosine phosphorylation of platelet endothelial cell adhesion molecule-1 (PECAM-1, CD31) in mechanically stimulated vascular endothelial cells. Eur. J. Cell Biol. 1997; 72: 229–237.

Pang JJ, Chang B, Kumar A, Nusinowitz S, Noorwez SM, Li J, Rani A, Foster TC, Vhiodo VA, Doyle T, Li H, Malhotra R, Teusner JT, McDowell JH, Min SH, Li Q and Kaushal S. Gene therapy restores vision-dependent behavior as well as retinal structure and function in a mouse model of RPE65 leber congenital amaurosis. Molecular Therapy 2006; 13 (3): 565–572.

Pepperberg DR, Okajima TL, Ripps H, Chader GJ and Wiggert B. Functional properties of interphotoreceptor retinoid-binding protein. Photochemistry and Photobiology 1991; 54 (6):1057–1060.

Philp NJ, Yoon H and Grollman EF. Monocarboxylate transporter MCT1 is located in the apical membrane and MCT3 in the basal membrane of rat RPE. Am J Physiol

Regul Integr Comp Physiol 1998; 274: R1824–R1828, 1998.

Philp D, Nguyen M, Scheremeta B, St-Surin S, Villa AM, Orgel A, Kleinman HK and Elkin M. Thymosin increases hair growth by the activation of clonogenic hair follicle stem cells. FASEB J 2004; 18: 385–387.

Rivera J, Lozano ML, Navarro-Núñez L and Vicente V. Platelet receptors and signalling in the dynamics of thrombus formation. Haematologica 2009; 94:700-711.

Roux SP, Sakariassen KS and Turitto VT. Effect of aspirin and epinephrine on experimentally induced thrombogenesis in dogs. A parallelism between in vivo and ex vivo thrombosis models. Arterioscler Thromb. 1991; 11: 1182-1191.

Ruel J, Lemay J, Dumas G, Doillon C and Charara J. Development of a parallel plate flow chamber for studying cell behavior under pulsatile flow. ASAIO Journal 1995; 41: 876-883.

Ruggeri ZM, Orje JN, Habermann R, Federici AB and Reininger AJ. Activation independent platelet adhesion and aggregation under elevated shear stress. Blood 2006; 108: 1903–10.

Ruggeri ZM. Von Willebrand Factor. Curr.Opin.Hematol. 2003;10: 142-149.

Salvi SM, Akhtar S and Currie Z. Ageing changes in the eye. Postgrad Med J 2006; 82:581–7.

Santelli G, Califano D, Chiappetta G, Vento MT, Bartoli PC, Zullo F, Trapasso F, Viglietto G and Fusco A. Thymosin beta 10 gene overexpression is a general event in human carcinogenesis. Am J Pathol 1999; 155: 799-804.

Sarratt KL, Chen H, Zutter MM, Santoro SA, Hammer DA and Kahn ML. GPVI and $\alpha_2\beta_1$ play independent critical roles during platelet adhesion and aggregate formation to collagen under flow. Blood 2005; 106:1268-77.

Savage B, Almus-Jacobs F and Ruggeri ZM. Specific synergy of multiple substrate receptor interactions in platelet thrombus formation under flow. Cell. 1998; 94:657–666.

Savage B, Saldı´var E, and Ruggeri ZM. Initiation of platelet adhesion by arrest onto fibrinogen or translocation on von Willebrand factor. Cell 1996; 84: 289–297.

Shames IH. Mechanics of fluids. 4th ed. Boston: McGraw-Hill; 2003.

Silva KC, Rosales MAB, Biswas SK, Lopes de Faria JB, and Lopes de Faria JM. Diabetic retinal neurodegeneration is associated with mitochondrial oxidative stress and is improved by an angiotensin receptor blocker in a model combining hypertension and diabetes. Diabetes 2009; 58 (6): 1382–1390.

Sim´ o R, Carrasco E, Fonollosa A, Garc´ıa-Arum´ı J, Casamitjana R and Hern´andez C. Deficit of somatostatin in the vitreous fluid of patients with diabetic macular edema. Diabetes Care 2007; 30 (3): 725–727.

Simmons D, Makgoba MW and Seed B. ICAM, an adhesion ligand of LFA-1, is homologous to the neural cell adhesion molecule NCAM. Nature 1988: 331:624 627.

Sixma JJ, van Zanten GH, Huizinga EG, van der Plas RM,Verkley M, Wu YP, Gros P

and de Groot PG. Platelet adhesion to collagen: an update. Thromb Haemost 1997; 78: 434–438.

Smart N, Riseboro CA, Melville AA, Moses K, Schwartz RJ, Chien KR and Riley PR. Thymosin beta 4: induces adult epicardial progenitor mobilization and neovascularization. Nature 2007; 445: 177–182.

Sosne G, Xu L, Prach L, Mrock KL, Kleinman KL, Letterio JJ, Hazlett LD and Kurpakuz-Wheater M. Thymosin β4 stimulates laminin-5 production independent of TGF-beta. Exp. Cell Res. 2004; 293:175–183.

Sosne G, Siddiqi A and Kurpakus-Wheater M. Thymosin-β4 Inhibits Corneal epithelial cell apoptosis after ethanol exposure. Invest. Ophthalmol. Vis. 2004; 45:1095 1100.

Sosne G, Szliter EA, Barrett R, Kernacki KA, Kleinman KH and Hazlett LD. Thymosin beta 4 promotes corneal wound healing and decreases inflammation in vivo following alkali injury. Exp. Eye Res. 2002; 74: 293–299.

Sosne G, Christopherson I, Barrett RP and Fridman R. Thymosin β4: modulates corneal matrix metalloproteinase levels and polymorphonuclear cell infiltration after alkali injury. Invest. Ophthalmol. Vis. Sci. 2005; 46: 2388– 2394.

Sosne G, Qiu P, Christopherson PL and Wheater MK. Thymosin beta 4 suppression of corneal NFkappaB: a potential anti-inflammatory pathway. Exp. Eye Res. 2007; 84: 663–669.

Sugase K, Dyson HJ and Wright PE. Mechanism of coupled folding and binding of an intrinsically disordered protein. Nature 2007; 447:1021–1025.

Tate Jr. DJ, Miceli MV and Newsome DA. Phagocytosis and H2O2 induce catalase and metallothionein gene expression in human retinal pigment epithelial cells. Investigative Ophthalmology and Visual Science 1995; 36 (7): 1271– 1279.

Tokura Y, Nakayama Y, Fukada S, Nara N, Yamamoto H, Matsuda R and Hara T. Muscle injury-induced thymosin β4 acts as a chemoattractant for myoblasts. J Biochem. 2011 Jan; 149(1):43-8.

Tong JP and Yao YF. Contribution of VEGF and PEDF to choroidal angiogenesis: a need for balanced expressions. Clin Biochem. 2006; 39(3):267-76.

Traub O and Berk BC. Laminar shear stress: mechanisms by which endothelial cells transduce an atheroprotective force Arterioscler Thromb Vasc Biol 1998; 18:677 685.

Traub O, Monia BP, Dean NM, Berk BC. 1997. PKC-epsilon is required for mechanosensitive activation of ERK1/2 in endothelial cells. J. Biol. Chem. 272, 31251–31257.

Tsai DC, Charng MJ, Lee FL, Hsu WM and Chen SJ. Different plasma levels of vascular endothelial growth factor and nitric oxide between patients with choroidal and retinal. Ophthalmologica. 2006; 220(4):246-51.

Tseng H, Peterson TE and Berk BC. Fluid shear stress stimulates mitogenactivated protein kinase in endothelial cells. Circ. Res. 1995; 77, 869–878.

Tsuji S, Sugimoto M, Miyata S, Kuwahara M, Kinoshita S and Yoshioka A. Real-time analysis of mural thrombus formation in various platelet aggregation disorders: distinct shear-dependent roles of platelet receptors and adhesive proteins under flow. Blood 1999; 94: 968–75.

Turitto VT and Baumgartner HR. Platelet interaction with subendothelium in flowing rabbit blood: effect of blood shear rate. Microvasc Res 1979; 17: 38–54.

Walpola PL, Gotlieb AI, Cybulsky MI and Langille BL. Expression of ICAM-1 and VCAM-1 and monocyte adherence in arteries exposed to altered shear stress [published correction appears in Arterioscler ThrombVasc Biol. 1995;15:429]. Arterioscler Thromb Vasc Biol. 1995; 15:2-10.

Walpola PL, Gotlieb AI and Langille BL. Monocyte adhesion and changes in endothelial cell number, morphology, and F-actin distribution elicited by low shear stress in vivo. Am J Pathol. 1993; 142:1392-1400.

Wang Q, Chen Q, Zhao K, Wang L and Traboulsi EI. Update on the molecular genetics of retinitis pigmentosa. Ophthalmic Genet 2001; 22: 133–154.

Weisel JW. Fibrinogen and fibrin. Adv. Protein Chem. 2005; 70: 247-299.

Wu Q, Blakeley LR, Cornwall MC, Crouch RK, Wiggert BN, and Koutalos Y. Interphotoreceptor retinoidbinding protein is the physiologically relevant carrier that removes retinol from rod photoreceptor outer segments. Biochemistry 2007; 46 (29): 8669–8679.

Yao Y, Guan M, Zhao XQ and Huang YF. Downregulation of the pigment epithelium derived factor by hypoxia and elevated glucose concentration in cultured human retinal pigment epithelial cells. Zhonghua yi xue za zhi 2003; 83 (22):1989–1992.

Yoshikawa N, Ariyoshi H, Ikeda M, Sakon M, Kawasaki T and Monden M. Shear stress causes polarized change in cytoplasmic calcium concentration in human umbilical vein endothelial cells (HUVECs). Cell Calcium 1997; 22, 189–194.

Young RW and Bok D. Participation of the retinal pigment epithelium in the rod outer segment renewal process. J Cell Biol 1969; 42: 392–403.

Yu FX, Lin SC, Morrison-Bogorad M and Yin HL. Effects of thymosin beta 4 and thymosin beta 10 on actin structures in living cells. Cell Motil. Cytoskeleton 1994; 27; 13-25.

Yu H, Zeng Y, Hu J and Li C. Fluid shear stress induces the secretion of monocyte chemoattractant protein-1 in cultured human umbilical vein endothelial cells. Clin Hemorheol Microcirc. 2002; 26(3):199-207.

Zarbin MA. Current concepts in the pathogenesis of age related macular degeneration. Arch Ophthalmol 2004; 122:598–614.

Zarbin MA. Age-related macular degeneration: review of pathogenesis. Eur. J. Ophthalmol. 1998; 8: 199-206.

Zarbock J, Oschkinat H, Hannappel E, Kalbacher H, Voelter W and Holak TA. Solution conformation of thymosin beta 4: A nuclear magnetic resonance and simulated annealing study. Biochemistry 1990; 29:7814–7821.

Zeng Y, Qiao Y, Zhang Y, Liu X, Wang Y and Hu J. Effects of fluid shear stress on apoptosis of cultured human umbilical vein endothelial cells induced by LPS. Cell Biol Int. 2005; 29(11):932-5.

Zhang Y and Neelamegham S. An analysis tool to quantify the efficiency of cell tethering and firm-adhesion in the parallel-plate flow chamber. J Immunol Methods 2003; 278(1-2):305-17.

Zucker MB and Nachmias VT. Platelet activation. Arterioscler Thromb Vasc Biol 1985; 5:2-18.

CHAPTER 2

Development of flow device to study effects of shear stress on endothelial cells and its applications

Introduction

Endothelial cells are exposed to various mechanical stimuli such as shear stress, hydrostatic pressure and cyclic stretch due to vessel deformation. These stimuli alter endothelial cell morphology, initiate cytoskeletal changes and activate various signalling pathways. The nature and magnitude of these hemodynamic forces has an important role in maintaining vascular homeostasis.

Laminar shear stress is one of the most potent endothelial stimulators, which is very critical for normal vascular functioning. It plays an important role against inflammatory activation and apoptosis (Tricot *et al* 2010; Chien *et al* 2008). Disturbed shear stress has been implicated in the pathogenesis of various diseases including atherosclerosis and cardiovascular diseases (Traub *et al* 1998).

In the past few years, physiological and pathological shear stress has been studied extensively to understand the development and progression of vascular diseases. To understand the effects of these hemodynamic forces *in vitro*, engineered devices are required that can maintain the endothelial cells in a controlled *in vivo* like environment. The fluid flow must be predictable in these devices so that shear stress over endothelial cells can be properly controlled.

Many *in vitro* flow systems have been developed to study endothelial cells under shear stress. These flow devices require a large population of endothelial cells which needs more chemicals and reagents. Recently, many studies have reported the development of microfluidic flow chambers. Some of these designs have multiple microchannels to study different cell types and shear rates at the same time (Young *et al* 2007). A major drawback of such flow devices is cross contamination between different channels. Some of these flow devices and microfluidic devices have been custom laboratory prototypes, while others are commercially available.

In the present study, we describe the construction and testing of a simple and robust parallel plate flow chamber. The aim of this study was to develop an *in vitro* model using a parallel-plate flow chamber to simulate *in vivo* fluid shear stresses on endothelial cells exposed to dynamic fluid flow in their physiological environment. A computational fluid dynamics (CFD) template was developed for simulation and prediction of flow

induced shear rates on the endothelium, while an *in vitro* model was used to investigate the subsequent cellular biological responses.

The flow chamber was validated by determining changes in the production of nitric oxide and caveolin-1 expression in bovine endothelial cells exposed to shear stress.

Experimental Methods

Cell culture

Bovine aortic endothelial cells (BAECs) were purchased from Coriell Institute for Medical Research. The cells were cultured in DMEM F-12 media containing 10% fetal calf serum (FCS, Gibco) and penicillin-streptomycin, at 37°C in a humidified atmosphere of 95% air and 5% CO_2.

Parallel plate flow chamber configuration

The flow apparatus used in this study is a parallel plate flow chamber with a closed loop system (Figure 1).

CFD simulation and viscosity measurement

In order to use the velocity gradient templates as shear stress templates, the viscosity of the media at 37ºC was required. A viscometer (Canon Instruments, Model 2085, PA, USA) and viscosity bath, set to 37ºC, were used. The media was injected into the viscometer and allowed to reach equilibrium conditions before being suctioned to the top of the viscometer and then released while the time it takes the fluid to flow through a defined section was measured. Using equipment specific correlations, the viscosity was calculated based on the time taken to pass through a defined section. This process was repeated five times and an average viscosity was calculated and used in the shear stress calculations. The specific gravity of the media was determined by using a calibrated hydrometer. The average viscosity was 0.753 cP (0.00753 Pa·s).

Calculation of shear stress

Shear stress was calculated according to the following formula:

$$\tau = \mu \frac{dy}{dz}$$

Where μ is the viscosity of the media and dy/dz is the velocity gradient of the flow. From the templates generated in FLUENT the values of the velocity gradients at various regions on the plate are known. Since the viscosity of the media has been measured, the shear stress can be directly calculated and an average shear stress for each region on the

template can be defined. The shear stress values used in our investigations ranged from 0.05 to 1.47 Pa, which is within the physiological range for aortas (~0.002 Pa) and veins (~0.01 Pa).

Shear stress studies

Bovine endothelial cells were grown on coverslips in 35mm cell culture plates. The cells were exposed to shear stress using a peristaltic pump (Reglo Digital MS 4/6, model ISM 833, Ismatec). PTFE tubing (Scientific Products & Equipment, Canada) was used to link the pump and the flow chamber. Shear stress experiments were performed for 16 hours in complete media in 5% CO_2 incubator at 37°C.

Measurement of NO production

To determine changes in NO production, endothelial cell monolayers were incubated with cell culture medium containing 5 μM 4,5-diaminofluorescein diacetate (DAF-DA , Invitrogen) at 37°C in a 95% air/5% CO_2 incubator for 30 min. Cells were then washed 3X with phosphate buffered saline (PBS) and mounted on the stage of an Axiovert 200 inverted fluorescence microscope. DAF-DA fluorescence was monitored using excitation and emission wavelengths of 485 and 538 nm, respectively.

BAECs were grown under shear stress and static cells were used as control. After incubation for 24 hours, media containing 100μM of acetylcholine was injected into the flow chamber. The cells were incubated again and after 1 hr, 200 uL of media was withdrawn with a Hamilton gastight syringe and directly injected into the purge vessel of a Sievers Nitric Oxide Analyzer (Model 280i) which contained acetic acid and sodium iodide.

Immunofluorescence

BAEC cells were grown on coverslips in 35mm cell culture dishes. The cells were grown under shear stress for 16 hours and static cells were used as control. After incubation, the cells were washed with PBS and fixed in 3% paraformaldehyde for 10 min. The cells were then permeabilized with 0.025% Triton X for 10 min. Rabbit polyclonal antibody against Ser 1177 phospho eNOS (1:200 dilution; Cell Signal) and anti-mouse caveolin-1

(1:100) were used as primary antibodies. Alexa Fluor 488 -labelled goat anti-rabbit IgG and Alexa Fluor 568 conjugated anti-mouse IgG were used as a secondary antibodies (1:500 dilution; Molecular Probes, Canada). Cells were also stained with either propidium iodide (PI) or DAPI for the localization of nuclei. Preparations were mounted in fluoromount G (Southern Biotech) and examined by fluorescence microscopy.

Statistical analysis

Data is expressed as an average of all trials and statistical analysis was done by Student's *t* test. The quantification of the fluorescence intensity was done using Image J software.

Results

Flow chamber

The parallel plate flow chamber described herein was designed to minimize solution volumes, to be operationally robust and precise, simple to set up, and inexpensive. Also critical to the design was the ability of the chamber to be mounted on a microscope stage to facilitate visualization experiments. The chamber pictured in Figure 1 is 64 mm in diameter and 28 mm in height. It was machined out of surplus aluminum and acrylic stock. The unit consists of three principal elements, an inner acrylic "puck" that forms the chamber, an interchangeable gasket that creates the channel geometry, and an aluminum clamping fixture that holds it all together. A special low cost thermoset plastic has been adapted for use as a chamber gasket. A simple series of die punches provide a variety of channel geometries. The unit can also accept commercially available gaskets like those produced by Glycotech (Rockville Maryland). Channel depth is set by the clamping fixture and the thickness of gasket utilized. The two halves of the clamping fixture thread together to compress the gasket to provide the chamber seal. To ensure proper channel depth, two interchangeable locator pins prevent the fixture from being over tightened. Inlet and outlet ports were machined into the top of the acrylic chamber. Each is threaded to accept standard commercially available fittings. The ports are chamfered with a smooth Gaussian shaped profile to minimize flow disturbances during flow entrance and exit.

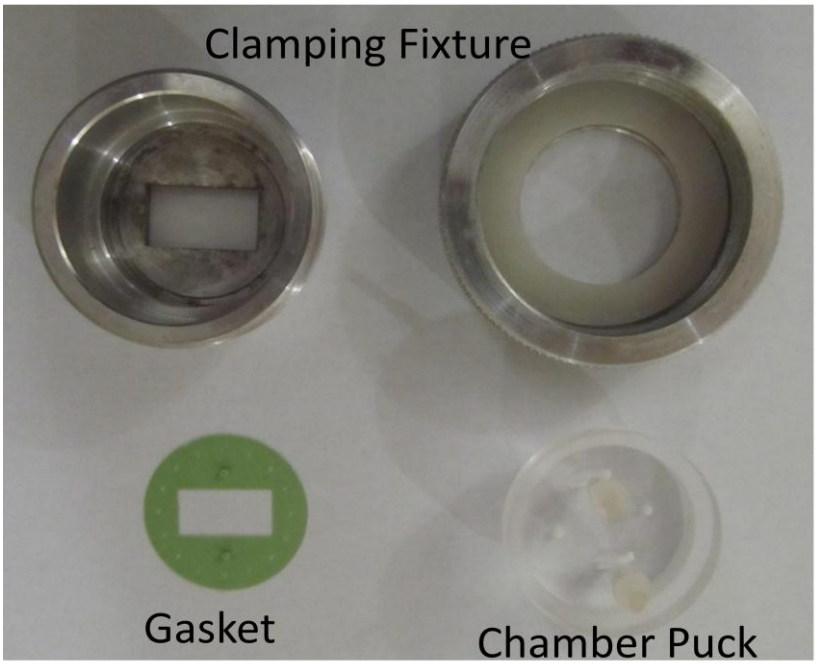

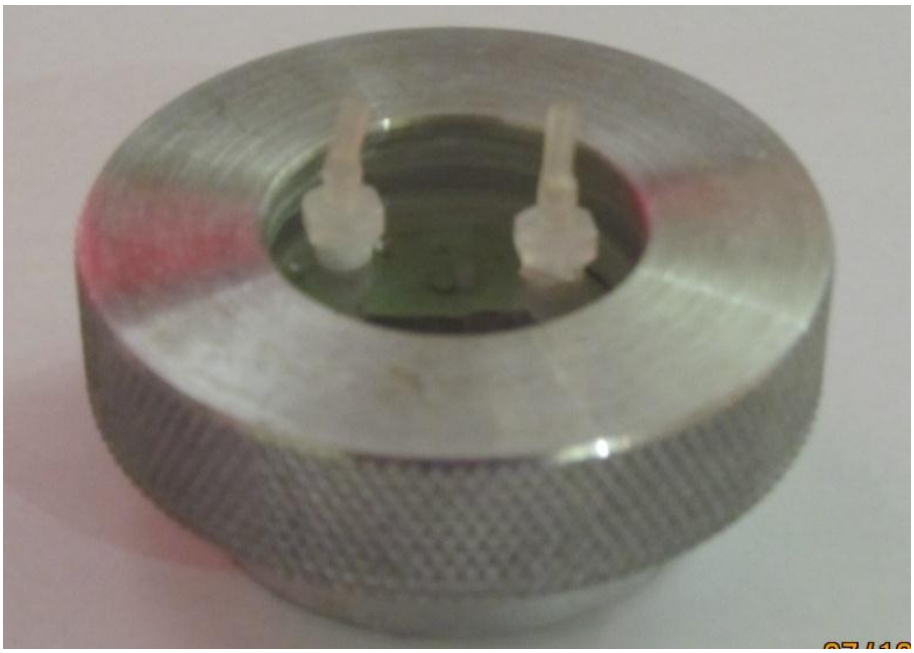

Assembled Chamber

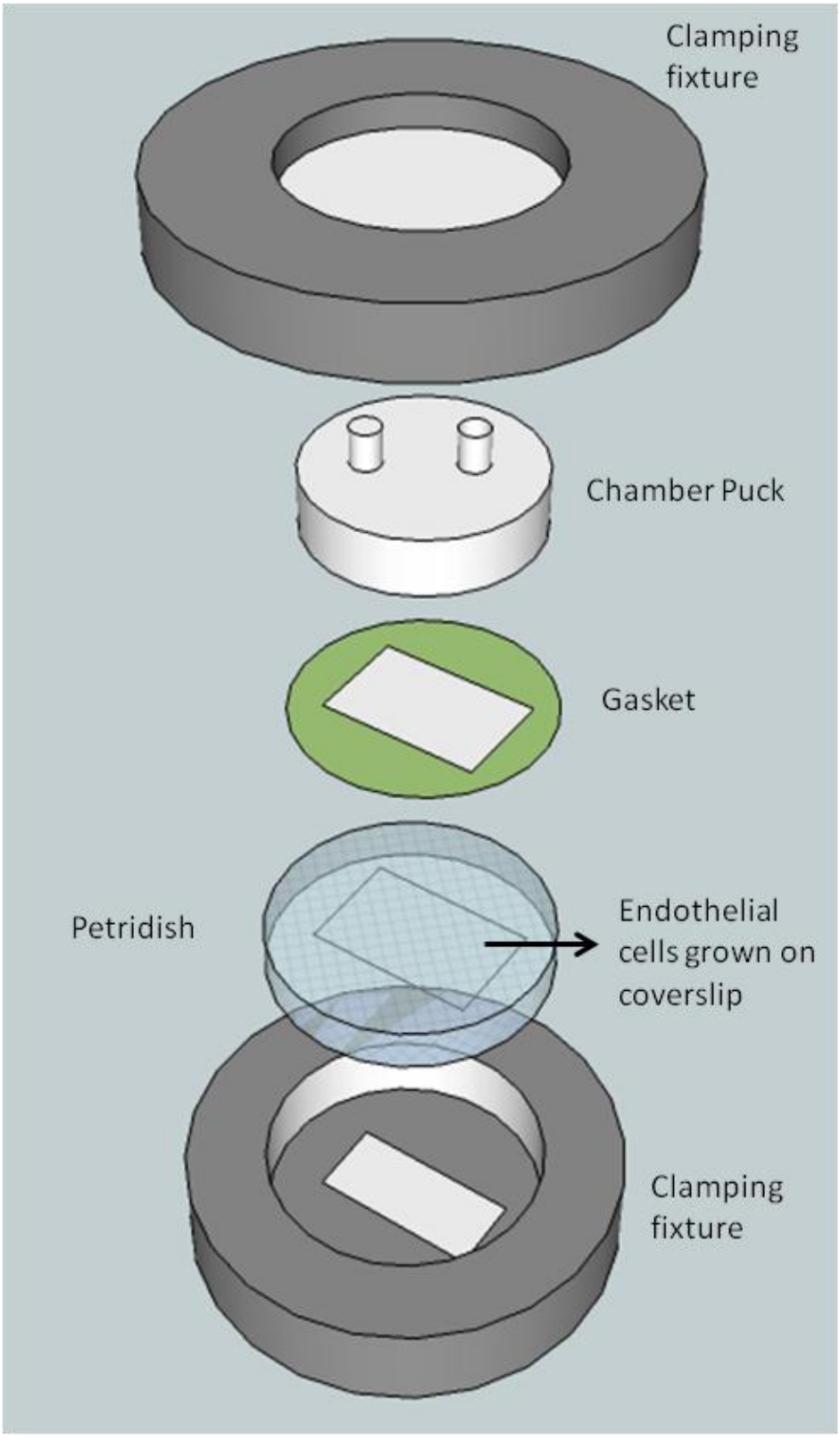

Figure 1 – Schematic diagram of the parallel plate flow chamber.

Computational fluid dynamics

To simulate the flow in the chamber and estimate the shear stress for the testing program, a computational model of the flow channel was developed. The commercial finite volume solver, Fluent 6.1 was utilized for this study. Free outflow and mass flow inlet boundary conditions were assumed at the outlet and inlet of the channel respectively in the steady, laminar simulation. The material properties of the solution were approximated to be that of water. The inlet/outlet ports and flow channel [19 mm long X 5 mm wide X 0.25 mm deep] was discretized by tetrahedral elements. Three mesh densities were tested, consisting of 83,000, 196,000, and 454,000 elements. Values of the flow velocity assessed at 5 locations across the domain changed by no more than 2% when the mesh density increased from 196,000 to 454,000. Thus the medium mesh density was chosen for the test runs.

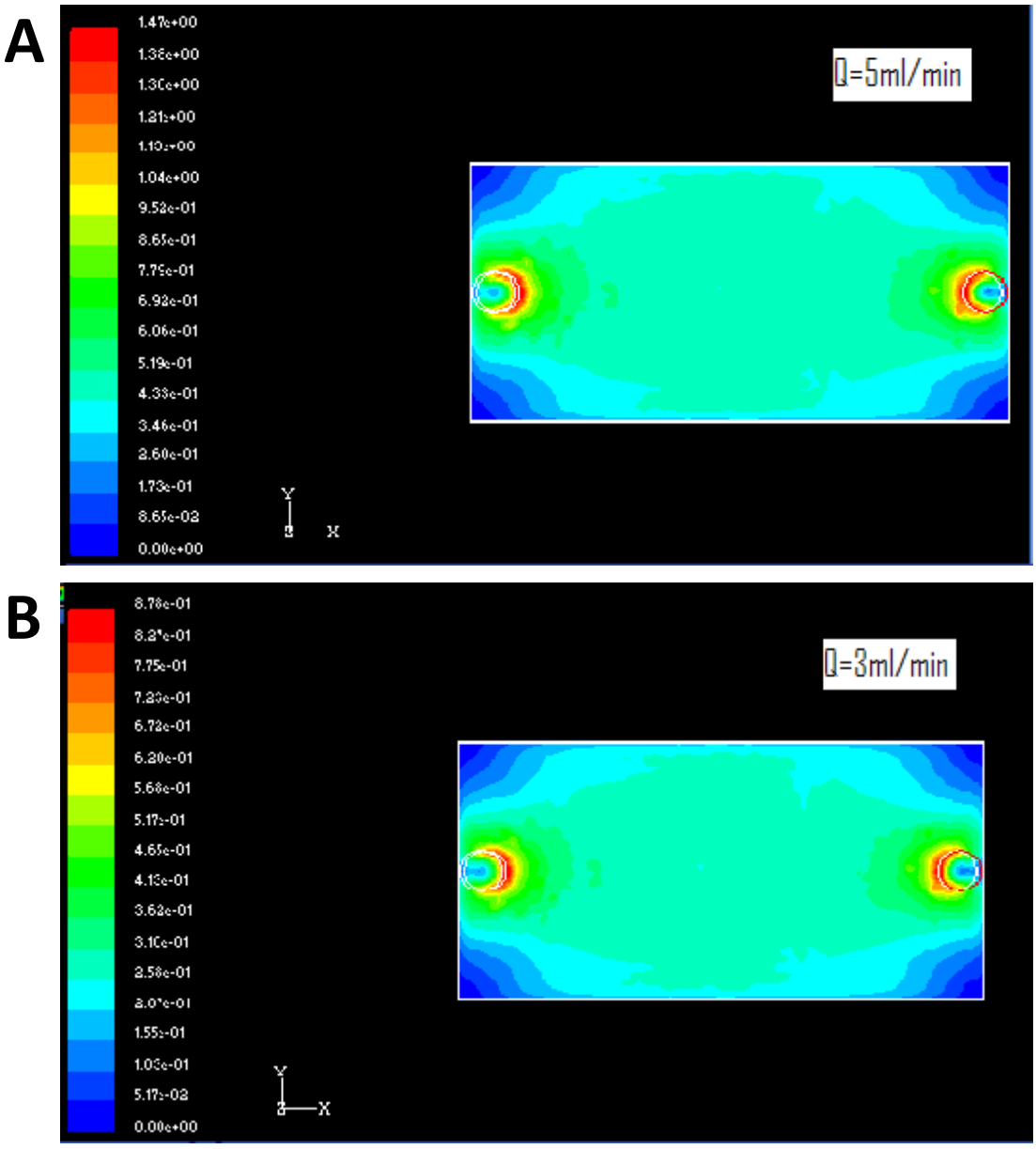

Figure 2 – Velocity gradient template.

Validation of the flow chamber

In the present study, we first examined the morphological changes of endothelial cells associated with exposure to physiologically relevant shear stress using this flow chamber. Bovine aortic endothelial cells were either maintained in static condition or exposed to laminar flow at a shear stress of 5 dyne/cm^2 for 16 h. As shown in Figure 3, fluid shear stress induced dramatic morphological changes such as cell elongation and alignment with the direction of flow. In contrast, there is no significant cell orientation in cells under static conditions.

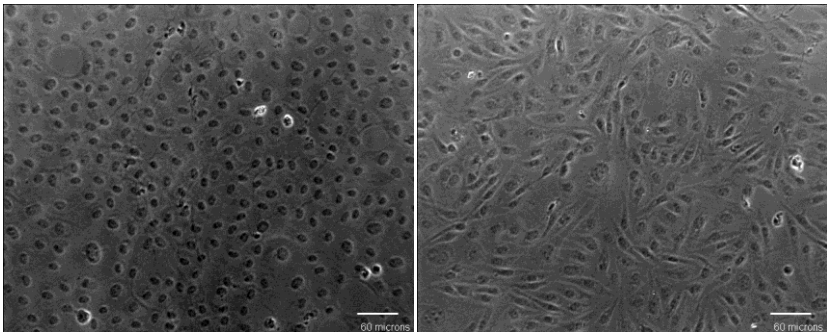

Control **5 dyne/cm^2**

Figure 3 – Effect of shear stress on morphology of bovine endothelial cells. Bovine aortic endothelial cells were maintained either under static conditions or under shear stress (5 dyne/cm^2). After incubation for 16 hours, the morphological changes were visualized using 20X objective of a Zeiss Axiovert 200 microscope.

Nitric oxide production and eNOS phosphorylation in response to shear stress

In order to validate whether this flow chamber can be employed for studies in the areas of biomedical research, the effect of fluid shear stress on nitric oxide production in endothelial cells was examined. In the present study, nitric oxide production in bovine aortic endothelial cells was determined by a membrane-permeable fluorescent probe 4, 5-diaminofluorescein diacetate (DAF-2 DA). A significant upregulation (~ 3.6 fold) of NO was observed in endothelial cells which were exposed to laminar flow at a shear stress of 5 dyne/cm^2 for 16 hours, compared with those maintained in static condition (Fig. 4 A, B). A qualitative examination of the data revealed that nitric oxide production increased by 7 fold as compared to the static cells when the endothelial cells were exposed to a shear rate of 15 dyne/cm^2 (Fig. 4 A, B). A significant upregulation (~ 2.5 fold) of authentic NO (as determined with NO analyzer) was also observed in endothelial cells which were exposed to laminar flow at a shear stress of 5 dyne/cm^2 for 16 hours, compared with those maintained in static condition (Fig. 4C).

A

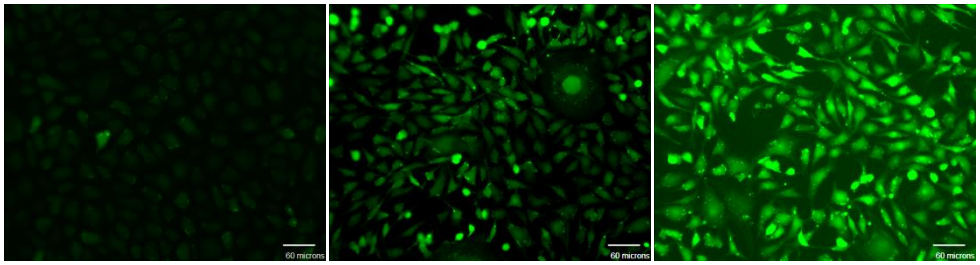

Control **5 dyne/cm^2** **15 dyne/cm^2**

B

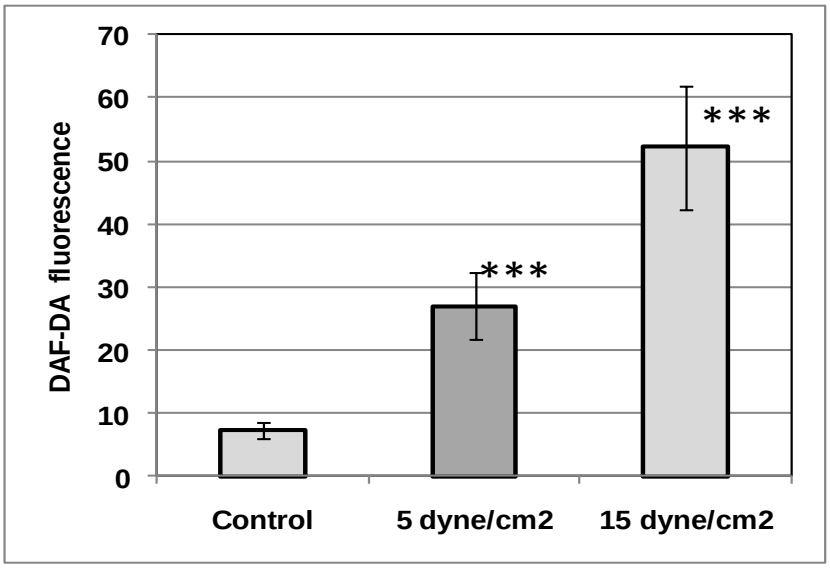

C

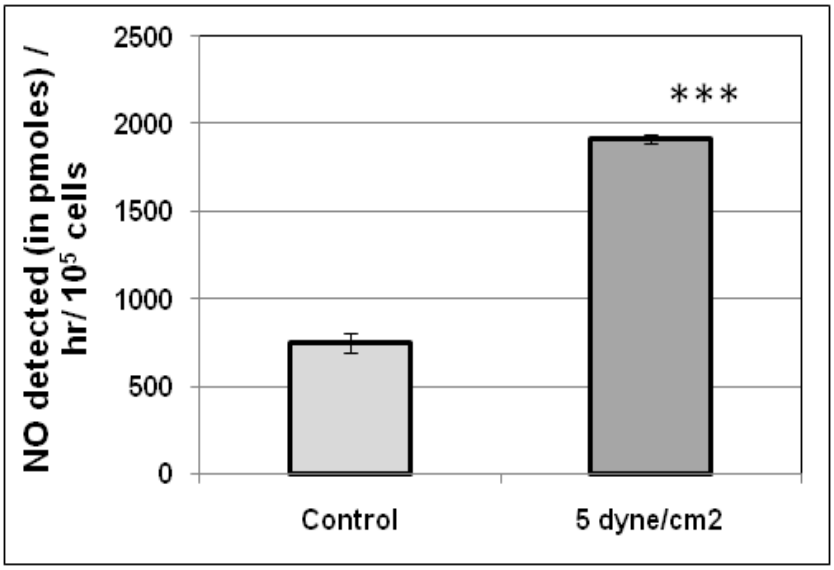

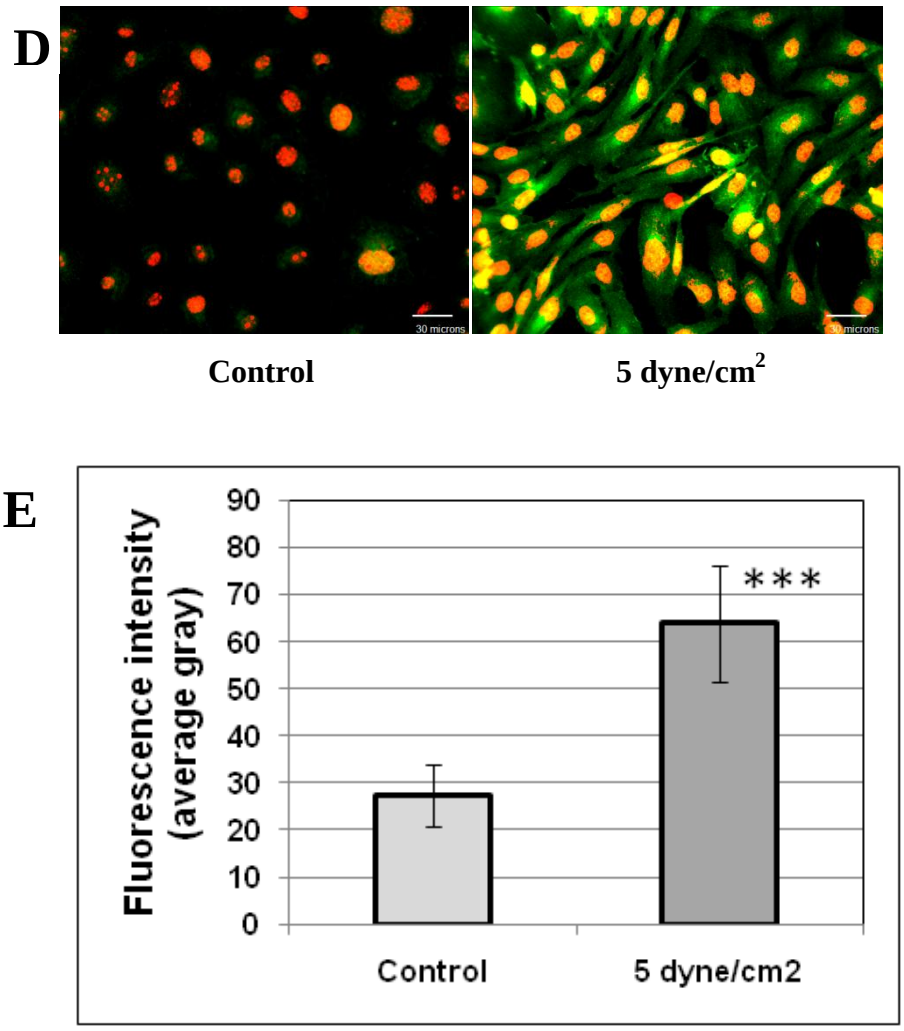

Figure 4 – Nitric oxide production and eNOS phosphorylation in response to shear stress. (A) The bovine endothelial cells grown under static conditions and shear stress for 16 hours were incubated with 5µM DAF-DA for 30 min. The cells were washed with PBS and viewed under Zeiss Axiovert fluorescence microscope using 20X objective. (B) The graph represents average of DAF-DA fluorescence taken from 4 independent experiments (± SD). *** $P < 0.001$ (C) Total nitrite was measured in control cells and cells under shear stress using NO analyzer. The bovine endothelial cells were grown under shear stress for 16 hours after which the cells were stimulated with acetylcholine for 1 hour and total nitrite was measured. The data shown is average of 3 independent experiments (± SD). (D) The cells maintained under static conditions and exposed to shear stress for 16 hours were fixed with paraformaldehyde and incubated with anti-rabbit Ser1177 phospho eNOS antibody. Alexa Fluor 488 conjugated anti-rabbit IgG was used as secondary antibody and the nuclei were stained with PI. The slides were viewed under oil immersion 40X objective. (E) Average gray values (immunofluorescence intensity) of phospho eNOS levels in static and shear stress exposed cells. The values (average ± SD) were calculated from at least 10 different microscopic fields in each slide (n=3). *** $P < 0.001$.

Change in caveolin-1 expression after shear stress induction

The changes in caveolin-1 expression and distribution were determined by indirect immunofluorescence. As shown in Fig. 5, the cells exposed to shear stress showed a ~ 2.7 fold increase in caveolin-1 expression as compared to static cells. In static cells, caveolin-1 is present mostly in the plasma membrane, whereas in cells under shear stress caveolin-1 is also found in the cytoplasm.

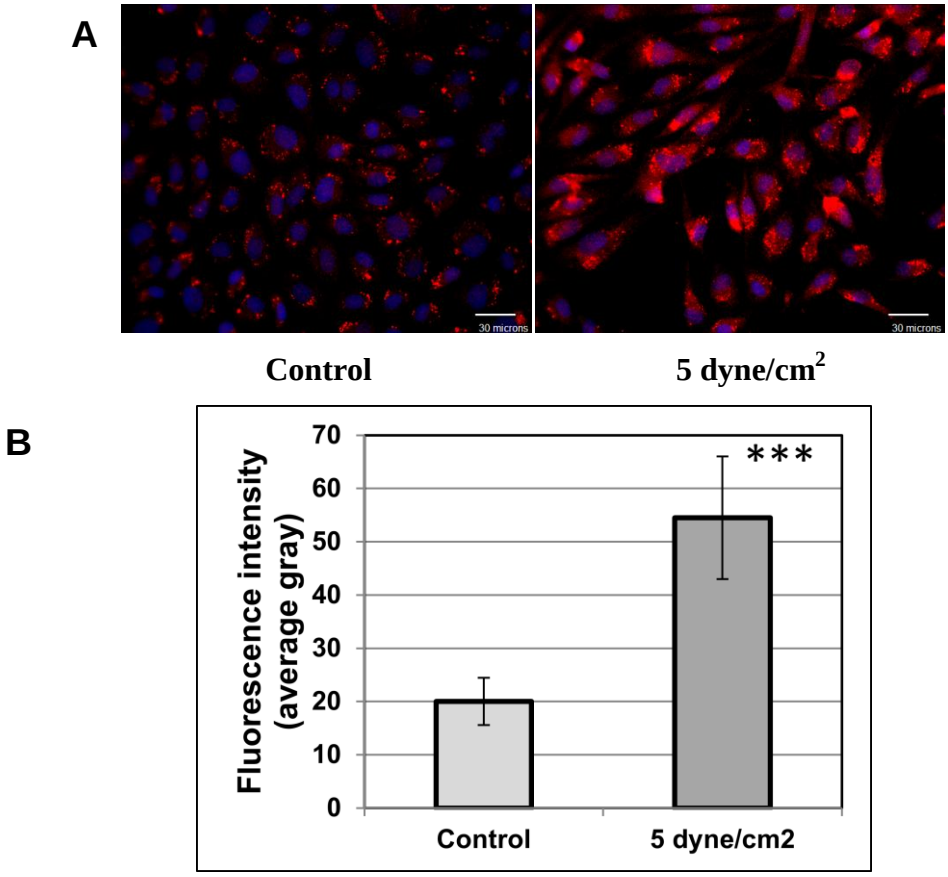

Figure 5 – Shear stress upregulates caveolin-1 expression in bovine endothelial cells. (A) BAECs were exposed to shear stress for 16 hours and static cells were used as controls. Caveolin-1 expression and distribution (red) was determined by indirect immunofluorescence. The nuclei were stained with DAPI (blue). The images were taken by 40X oil emersion objective using Zeiss Axiovert 200 microscope. (B) Average gray values (immunofluorescence intensity) of caveolin-1 levels in cells maintained under static and shear stress. The values (average ± SD) were calculated from at least 10 different microscopic fields in each slide (n=3). *** $P < 0.001$.

Discussion

Parallel plate flow chambers have been used for years in the study of hemodynamics and cellular mechanotransduction (Frangos *et al* 1985; Levesque *et al* 1985; Galbraith *et al* 1998; McCann *et al* 2005; Bacabac *et al* 2005). The majority of chambers documented in the literature were developed for specific research applications and were not mass-produced for commercial use. The bulk of chambers presently available off the shelf can cost upwards of $500 for a pump-ready apparatus. They often require the use of a vacuum line or pump and delicate gaskets to maintain chamber seals and prevent leaks.

This flow device introduced in this study provides a leak proof and contamination free environment to the cells. It can also be used for real time monitoring of the live cells, to study the dynamics of endothelial cell response to shear. The materials used for making this flow device are chemical resistant. Advantages of this system include its simplicity of use and small number of cells required to run a simulation. The fabrication is convenient, versatile and economical.

The reorganization of the endothelial cell morphology is one of the earliest responses in the endothelial cells that are exposed to fluid shear stress. Previous *in vivo* and *in vitro* studies have shown that the endothelial cells elongate and align parallel to the direction of flow (Azuma *et al* 2001; Wojciak-Stothard *et al* 2003). Our results also showed change in morphology of the endothelial cells, which are in agreement with the previous reports by other groups (Topper *et al* 1999; Wang *et al* 2001; Kadohama *et al* 2006).

Shear stress is one of the most important physiological stimuli which modulate many physiological and pathological processes associated with endothelium, such as inflammatory response, vasodilation and endothelial cell proliferation (Davies *et al* 1995). It acts as a potent stimulus for endothelium-dependent NO production and vasodilation (Kuchan *et al* 1994).

An important step in the validation process was to determine whether our flow chamber was able to discern different shear rates. BAECs were exposed to two different shear rates (5 & 15 dyne/cm^2) and changes in NOx production in response to shear stress were determined. There was a ~ 3.5 fold increase in NOx production at 5 dyne/cm^2 and a

7 fold increase at 15 dyne/cm^2 as compared to the static cells. These results suggest that this flow chamber can be utilized to attain different shear rates. These findings are also in agreement with numerous previous studies which demonstrated nitric oxide upregulation in response of laminar shear stress (Andrews *et al* 2010; Yang *et al* 2007).

Previous studies have shown that increase in shear stress increases eNOS activity by phosphorylation of eNOS at serine 1177 (Corson *et al* 1996; Dimmeler *et al* 1999). The results of this study also illustrated increase in phosphorylation of eNOS at Ser 1177 by 2.3 fold.

Caveolae are small cell surface plasma membrane invaginations, which have important role in cell signaling and cholesterol homeostasis. Cholesterol binding protein caveolin-1 is the main marker of caveolae. Caveolin-1 could mediate the transfer of newly synthesized cholesterol from the ER to the plasma membrane (Smart *et al* 1996). Our results are also in agreement with a previous study which has shown that laminar shear stress increases caveolin-1 expression and it also changes the localization of caveolin-1 (Sun *et al* 2002).

Conclusions

In conclusion, we have introduced a parallel plate flow chamber for shear stress studies *in vitro*. The data provides robust evidence that this parallel plate flow chamber can be used as an effective *in vitro* system to study the effects of fluid shear stress on the structure and function of endothelial cells. The flow rates can be precisely controlled in this laminar flow chamber to induce normal stress and shear stress so as to simulate the hemodynamic environment of human arteries *in vivo.*

References

Andrews AM, Jaron D, Buerk DG, Kirby PL and Barbee KA. Direct, real-time measurement of shear stress-induced nitric oxide produced from endothelial cells in vitro. Nitric Oxide 2010; 23(4): 335-342.

Azuma N, Akasaka N, Kito H, Ikeda M, Gahtan V, Sasajima T and Sumpio BE. Role of p38 MAP kinase in endothelial cell alignment induced by fluid shear stress. Am J Physiol Heart Circ Physiol 2001; 280(1): H189-197.

Bacabac RG, Smit TH, Cowin SC, Van Loon JJ, Nieuwstadt FT, Heethaar R and Klein-Nulend J. Dynamic shear stress in parallel-plate flow chambers. J Biomech 2005; 38(1): 159-167.

Chien S. Role of shear stress direction in endothelial mechanotransduction. Mol Cell Biomech 2008; 5(1): 1-8.

Corson MA, James NL, Latta SE, Nerem RM, Berk BC and Harrison DG. Phosphorylation of endothelial nitric oxide synthase in response to fluid shear stress. Circ Res 1996; 79(5): 984-991.Davies PF. Flow-mediated endothelial mechanotransduction. Physiol Rev, 1995; 75(3): 519-560.

Dimmeler S, Fleming I, Fisslthaler B, Hermann C, Busse R and Zeiher AM. Activation of nitric oxide synthase in endothelial cells by Akt-dependent phosphorylation. Nature,1999; 399(6736): 601-605.

Frangos JA, Eskin SJ, McIntire LV and Ives CL. Flow effects on prostacyclin production by cultured human endothelial cells. Science 1985; 227(4693): 1477-1479.

Galbraith CG, Skalak R and Chien S. Shear stress induces spatial reorganization of the endothelial cell cytoskeleton. Cell Motil Cytoskeleton 1998; 40(4): 317-330.

Kadohama T, Akasaka N, Nishimura K, Hoshino Y, Sasajima T and Sumpio BE. p38 Mitogen-activated protein kinase activation in endothelial cell is implicated in cell alignment and elongation induced by fluid shear stress. Endothelium 2006; 13(1): 43-50.

Kuchan MJ and Frangos JA. Role of calcium and calmodulin in flow-induced nitric oxide production in endothelial cells. Am J Physiol 1994; 266(3 Pt 1): C628-C636.

Levesque MJ and Nerem RM. The elongation and orientation of cultured endothelial cells in response to shear stress. J Biomech Eng 1985; 107(4): 341-347.

McCann JA, Peterson SD, Plesniak MW, Wenstar TJ and Haberstroh KM. Non-uniform flow behavior in a parallel plate flow chamber : alters endothelial cell responses. Ann Biomed Eng 2005; 33(3): 328-336.

Smart EJ, Ying Y, Donzell WC and Anderson RG. A role for caveolin in transport of cholesterol from endoplasmic reticulum to plasma membrane. J Biol Chem 1996; 271(46): 29427-29435.

Sun RJ, Muller S, Stoltz JF and Wang X. Shear stress induces caveolin-1 translocation in cultured endothelial cells. Eur Biophys J 2002; 30(8): 605-611.

Traub O and Berk BC. Laminar shear stress: mechanisms by which endothelial cells transduce an atheroprotective force. Arterioscler Thromb Vasc Biol 1998; 18(5): 677-685.

Tricot O, Mallat Z, Heymes C, Belmin J, Leseche G and Tedgui A. Relation between endothelial cell apoptosis and blood flow direction in human atherosclerotic plaques. Circulation 2000; 101(21): 2450-2453.

Topper JN and Gimbrone MA Jr. Blood flow and vascular gene expression: fluid shear stress as a modulator of endothelial phenotype. Mol Med Today 1999; 5(1): 40-46.

Wang JH, Goldschmidt-Clermont P, Wille J and Tin FC. Specificity of endothelial cell reorientation in response to cyclic mechanical stretching. J Biomech 2001; 34(12): 1563-1572.

Wojciak-Stothard B and Ridley AJ. Shear stress-induced endothelial cell polarization is mediated by Rho and Rac but not Cdc42 or PI 3-kinases. J Cell Biol 2003; 161(2): 429-439.

Yang Z, Tao J, Wang JM, Tu C, Xu MG, Wang Y, Chen L, Luo CF, Tang AL and Ma H. Fluid shear stress upregulated endothelial nitric oxide synthase gene expression and nitric oxide formation in human endothelial progenitor cells. Zhonghua Xin Xue Guan Bing Za Zhi 2007. 35(4): 359-362.

Young EW, Wheeler ER, and Simmons CA. Matrix-dependent adhesion of vascular and valvular endothelial cells in microfluidic channels. Lab Chip 2007; 7(12): 1759-1766.

CHAPTER 3

Real-time kinetic analysis of platelet function in a flow chamber with matrix proteins covalently attached onto a polydimethylsiloxane surface.

Introduction

Platelet adhesion and aggregation is the first step in the physiological defence mechanism of the body in blood vessel injury. Exposure of extracellular matrix at the sites of sub endothelial disruption leads to the capture of platelets to the matrix through various receptors including GPIb-IX-V and GPVI, resulting in platelet activation, followed by thrombi formation. Shear forces generated by blood flow play an important role in platelet adhesion and hence vascular hemostasis.

Several investigations on platelet function have focused on the platelet adhesion to various matrices (fibrinogen, collagen) under flow conditions. In all of these studies, glass slides are coated with fibrinogen, collagen or vWF etc (Turner *et al* 2001; Remijn *et al* 2002) and then used to study platelet aggregation mechanisms. Numerous devices including parallel plate flow chambers, which mimic the *in vivo* conditions (Goncalves *et al* 2003), are available for platelet aggregation studies under various physiological conditions. Some of these flow devices and microfluidic devices have been custom laboratory prototypes, while others are commercially available. There is currently little to no availability of simple, reliable, robust, and inexpensive flow chambers for use in kinetic aggregation studies.

Table 1 – Devices available to study platelet aggregation *in vitro*.

Device	Advantages	Disadvantages	Kinetic/Static
Cone and plate viscometer	High shear rates can be attained	Real time analysis not possible	Static
Parallel plate flow chamber	Easy to use and manufacture,	Cannot be easily modified, requires sizable volumes of reagents	Kinetic
Microfluidic devices	Real time imaging, less sample volumes and cells required	Costly	Kinetic

In the present study, we describe the construction and testing of a parallel plate flow chamber, which fits onto an inverted microscope and permits the optical monitoring of the binding of fluorescently-labelled platelets, in whole blood, onto platelet-binding proteins covalently attached to a small area (~0.8 mm^2) on the flow-device's surface under *in vivo*-like conditions. The flow device was validated by comparing the kinetics of adhesion of resting as well as Ca^{2+}- and ADP-activated platelets from normal and type 2 diabetic subjects onto fibrinogen and collagen covalently attached to the flow devices.

Experimental methods

Subject selection

Healthy human subjects (n=5), ages 25-40 years were chosen to participate in the study only if they showed no overt symptoms of disease and were taking no medication. Diabetic human subjects, ages 25-40 (n=5) on diet therapy alone and achieving stable and satisfactory glycemic control (fasting glycemia and glycosuria variation <15%; post-prandial glycemia variation<25% and HbA1c<7.5%) were chosen for inclusion in the study. None of the patients smoked, had history of alcohol abuse or were taking insulin or any drugs known to lower lipids or interfere with the coagulation and antioxidant systems. The experimental protocols were approved by the University of Windsor Research Ethics Board.

Construction of flow chamber

The flow chamber consisted of a Teflon boundary sealed with 1.5cm microscope coverslips (Figure 1 A). The walls of the flow cell were made of polydimethylsiloxane (PDMS) (Sylgard 184, Dow Corning). A layer of PDMS, ~ 0.96μm thick, was poured on the bottom of the chamber.

Plasma Oxidation of PDMS

To generate silanol groups on inert PDMS (Miyaki *et al* 2007) (Figure 1 B), plasma oxidation was carried out using a Plasma cleaner PDC-32G (Harrick Plasma, USA).

Protein immobilization chemistry

After plasma oxidation, 0.2μl of 2% aminopropyltrimethoxysilane (APTMES) (Sigma, Canada) was added on ~1 mm^2 surface of PDMS, in the centre of the flow chamber. After 10 minutes, a 0.5 μl portion of 0.5mM disuccinimidyl suberate (DSS) (Pierce, USA) solution and 5μM of Type I fibrinogen from bovine plasma (Sigma) solution was added to the APTMES dot in the geometrical centre of the flow chamber. For the experiments with collagen immobilization, 8μM of collagen type I from rat tail (BD Biosciences) was used. The reaction was stopped after 15 minutes by adding Tris buffer pH 8. The immobilization chemistry is shown in Figure 1 B.

Aminolysis of succinimidyl group

DSS has N-hydroxysulfosuccinimide (NHS) esters at each end and during the crosslinking reaction of DSS with primary amines, succinimidyl group is aminolyzed and released. The kinetics of the crosslinking reaction was determined by changes in absorption by succinimidyl group at 260 nm. The reaction was performed in Tris buffer (pH 8) with aminosilane alone, aminosilane and DSS, fibrinogen only, fibrinogen and DSS, collage only or collagen and DSS. All measurements were taken using Agilent 8453 UV-Visible spectrophotometer.

FITC-Fibrinogen labelling and standardization of cross linking time

Fibrinogen was incubated with fluorescein-isothiocyanate (FITC) at room temperature for 2 h in the presence of 1 M bicarbonate buffer pH 9.0. The labelled fibrinogen was run over G25 column in the dark to remove unbound FITC. Protein concentration was determined by bicinchoninic acid (BCA) assay. Aminosilane was added to plasma oxidized PDMS surface as described earlier. FITC-fibrinogen was added onto aminosilane either with DSS or after 10, 20, 30, 40, 50, 60, 70, 80, 90 and 100 sec of DSS addition. After 15 min incubation in dark, excess fibrinogen was washed off with Tris buffer and the bound FITC-fibrinogen was detected by Zeiss Axiovert 200 fluorescence microscope.

SDS washing of immobililized fibrinogen

Fibrinogen was fluorescently labelled with FITC and immobilized on PDMS by the method described above. Fibrinogen-FITC adsorbed on PDMS was used as a control. This was followed by addition of 2% SDS and the samples were incubated in dark for 3 hours. After incubation, the PDMS surface was washed with PBS and images were taken using Zeiss Axiovert 200 fluorescence microscope.

Blood collection and washing of platelets

Platelets were isolated as described previously (Miersch *et al* 2007) and were labelled with 60 μM BODIPY® FL N-(2-aminoethyl) maleimide (Molecular Probes, Canada). After 30 min incubation, platelets were washed twice with HEPES-ACD buffer to remove the excess dye and were put back into whole blood.

Light transmission platelet aggregometry

HEPES ACD was added to BODIPY® FL N-(2-aminoethyl) maleimide labelled and unlabelled platelets to get a final concentration of 1 X 10^7 platelets/mL. 5μM ADP was added as an agonist after ~ 40 sec. The platelet samples without ADP were used as controls. The kinetics of the aggregation reaction were determined by measuring absorbance at 600 nm for 5 min.

Perfusion studies in flow chambers

The flow cell circuit used for this investigation consists of a custom designed flow chamber, PTFE Teflon sterile tubing (0.031" X 0.062"), a medium reservoir, and a peristaltic pump (Reglo Digital MS 4/6, model ISM 833, Ismatec).

Statistical analysis

Data is expressed as an average of all trials and statistical analysis was done by student's *t* test.

Chemical structures in Figure 1 were drawn with ChemDraw 11.0 (Cambridge Software).

RESULTS

Flow chamber geometry and immobilization chemistry

The conventional flow chambers test platelet adhesion and aggregation by coating fibrinogen/collagen on glass slides. In the present study, we plasma-activated an otherwise inert matrix PDMS and used a bifunctional, primary amine-directed crosslinker DSS, to immobilize platelet-binding proteins on the PDMS surface (Figure 1B).

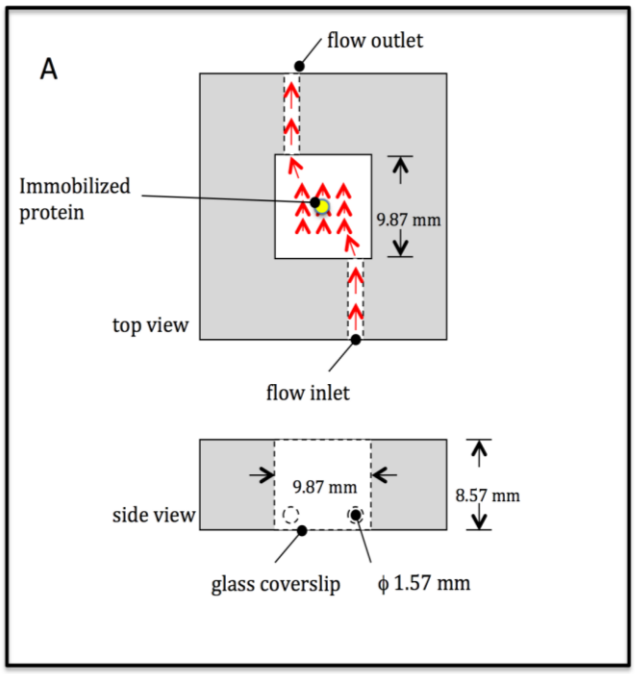

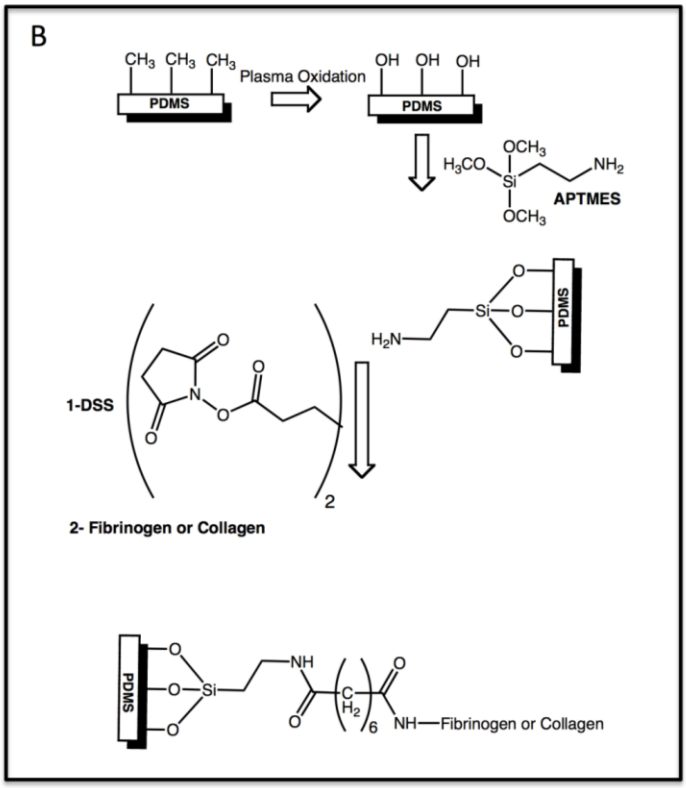

Figure 1 – (A) Geometry of the flow chamber used for perfusion studies. (B) Chemistry of immobilizing fibrinogen and collagen on PDMS. Hydroxyl groups were formed on inert and hydrophobic PDMS by plasma oxidation. Coating of APTMES on polymer surface after plasma oxidation resulted in an amine terminated surface layer. DSS was used as a bi-functional crosslinker which reacts both with the amine terminated surface layer and with the amine groups of the proteins to be immobilized.

Velocity profile

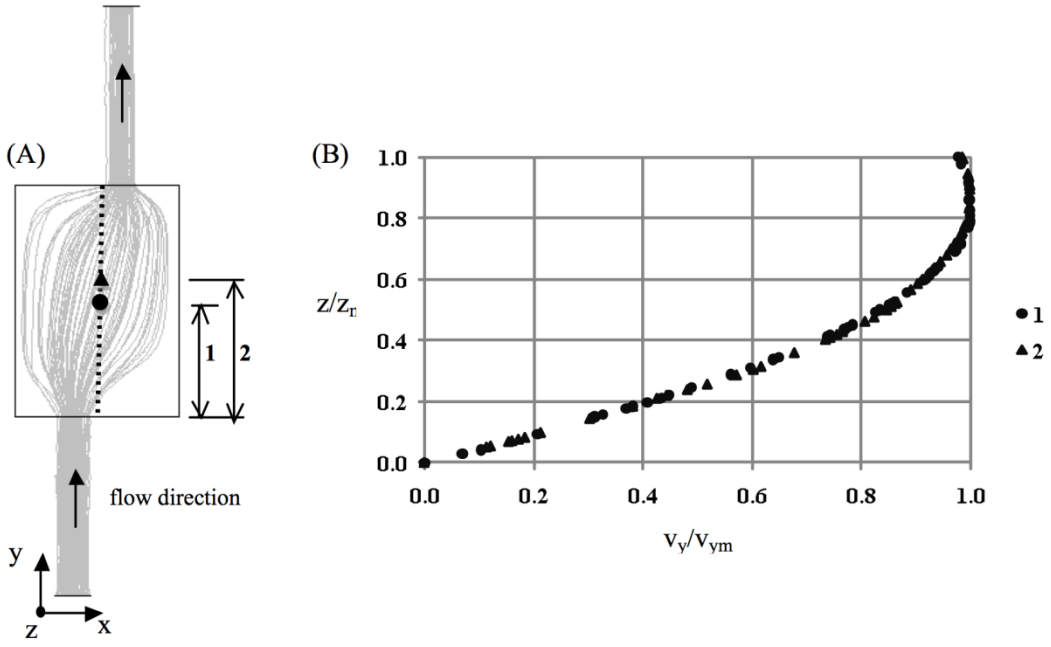

Figure 2 – Velocity profile. The graph shows the velocity profile from the inlet to the two different points in the centre of the flow device. The velocity of flow is zero in the boundary layer and rises monotonically with distance *z* from the wall, reaching maximum at the centre. Z/Zr is the ratio of distance at a given point to the distance to the centre. Vy/Vym is the ratio of the velocity at a given point to the velocity at the centre.

Crosslinking reaction between fibrinogen/collagen/aminosilane and DSS

DSS is a homobifunctional crosslinker which has amine reactive NHS esters at both ends. It reacts with primary amines in slightly alkaline conditions to yield stable amide bonds. This aminolysis reaction releases N-hydroxysuccinimide, which has an absorption maximum at 260 nm. The aminolysis reaction between collagen and DSS and fibrinogen and DSS is shown in Figure 3 A and B respectively.

A

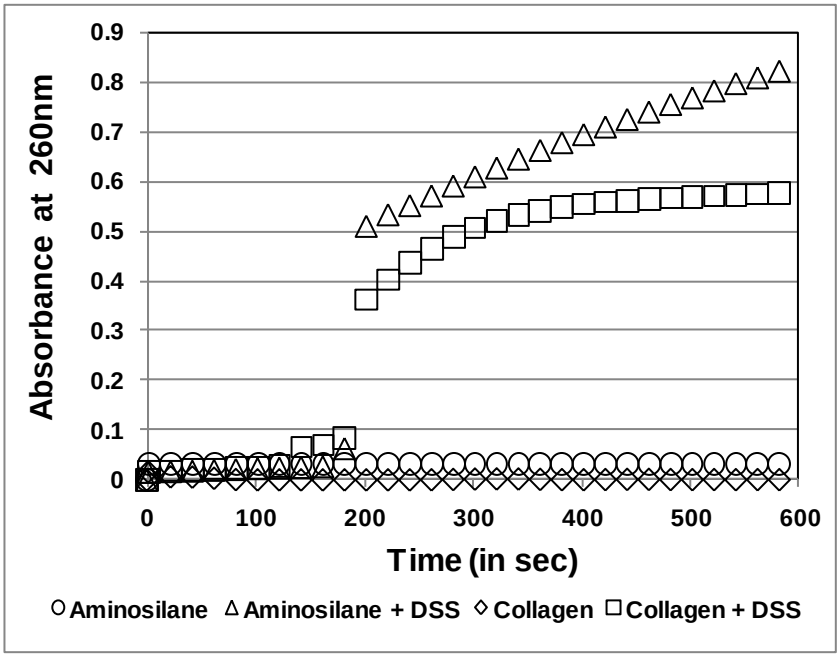

B

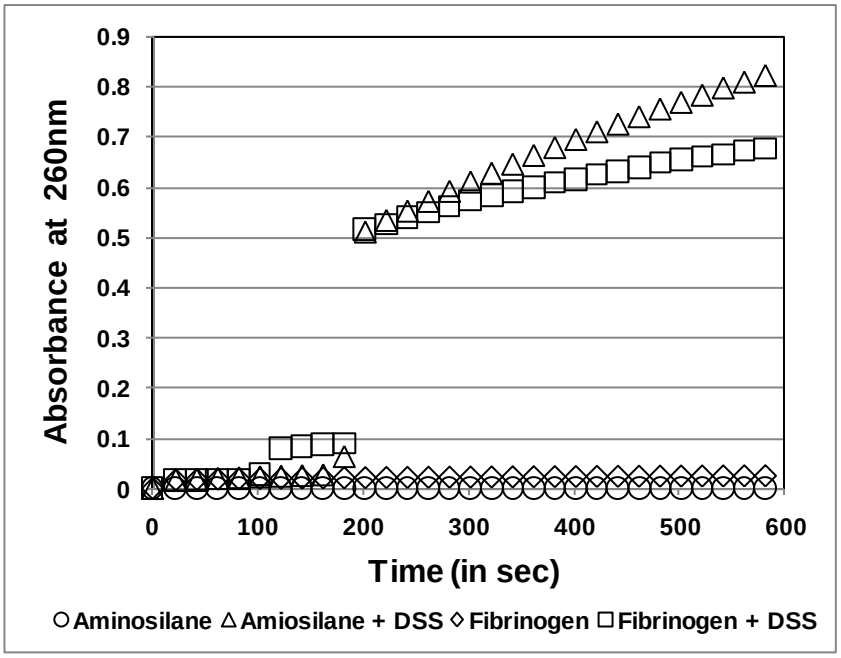

Figure 3 – Kinetic data for aminolysis of DSS. Aminosilane, fibrinogen and collagen were diluted in Tris buffer (pH 8) in different cuvettes. DSS was added after ~ 150 sec and kinetics was measured at 260 nm using UV-Vis spectrophotometer (n=3). Samples without DSS addition were used as controls.

Variations in time point at which fibrinogen/collagen is added to DSS affects immobilization.

Since DSS is a homobifunctional crosslinker, if we add fibrinogen at a later point, all of DSS might react with aminosilnae leading to less protein immobilization. To ensure complete immobilization of fibrinogen onto PDMS surface, the time point at which fibrinogen should be added to DSS has to be determined. FITC labelled fibrinogen was added onto the DSS either with DSS or at different time points. The fluorescence was maximum when DSS and fibrinogen were added together to aminosilane. There was no fluorescence detected when only fibrinogen was added on PDMS surface without any immobilization chemistry.

A

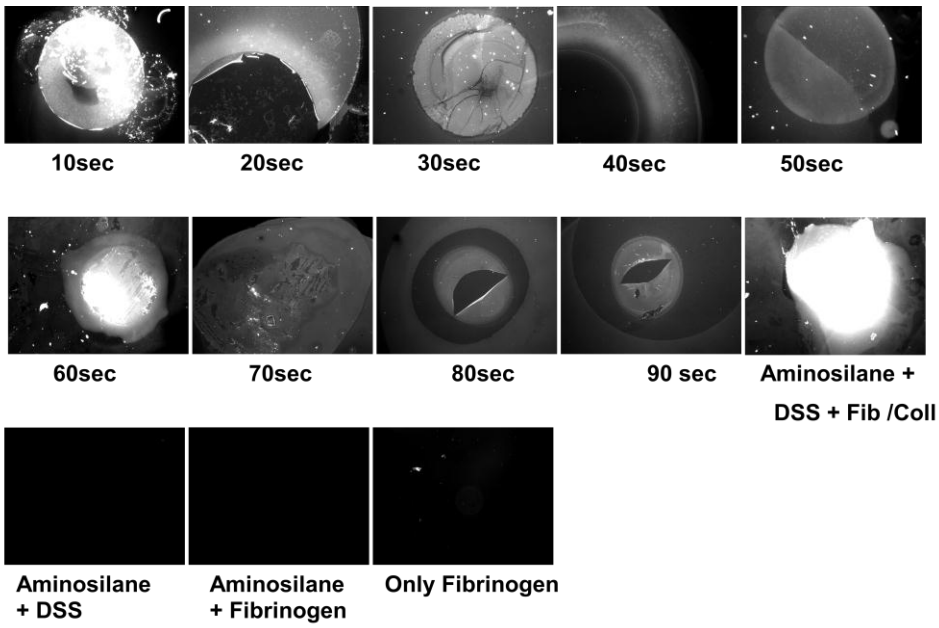

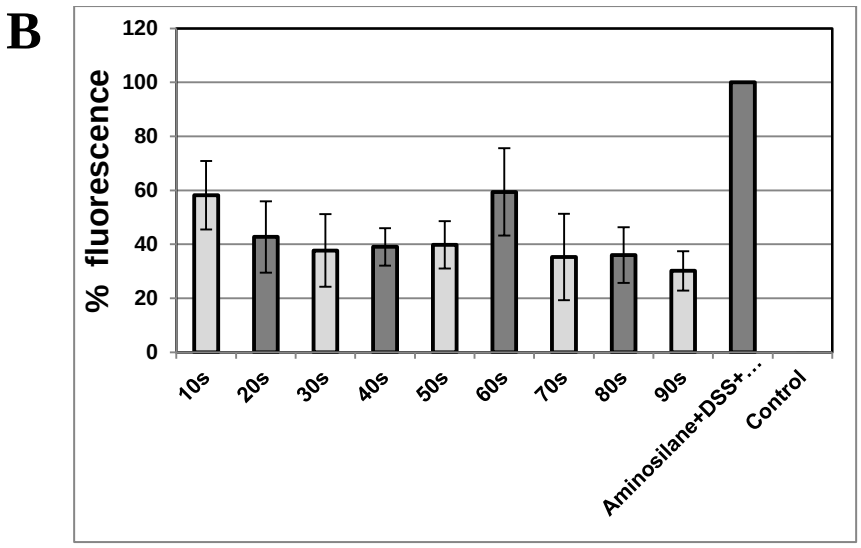

Figure 4 – Variations in time point at which fibrinogen/collagen is added to DSS affects immobilization. (A) The images show FITC-fibrinogen immobilized on PDMS surface where it was added onto aminosilane and DSS at varying time intervals. (B) The bar graph shows average fluorescence intensity for FITC-fibrinogen fluorescence, where each bar represents the mean ± SD from at least three independent experiments.

SDS washing of FITC-fibrinogen

Due to the hydrophobic nature of PDMS, it shows high affinity for proteins. In order to show that the proteins (fibrinogen/collagen) are covalently linked and not adsorbed, the PDMS surface was treated with SDS. Figure 5 illustrates that SDS washes off the protein while about 90% of the protein remains on the PDMS-AS-DSS-Fib surface.

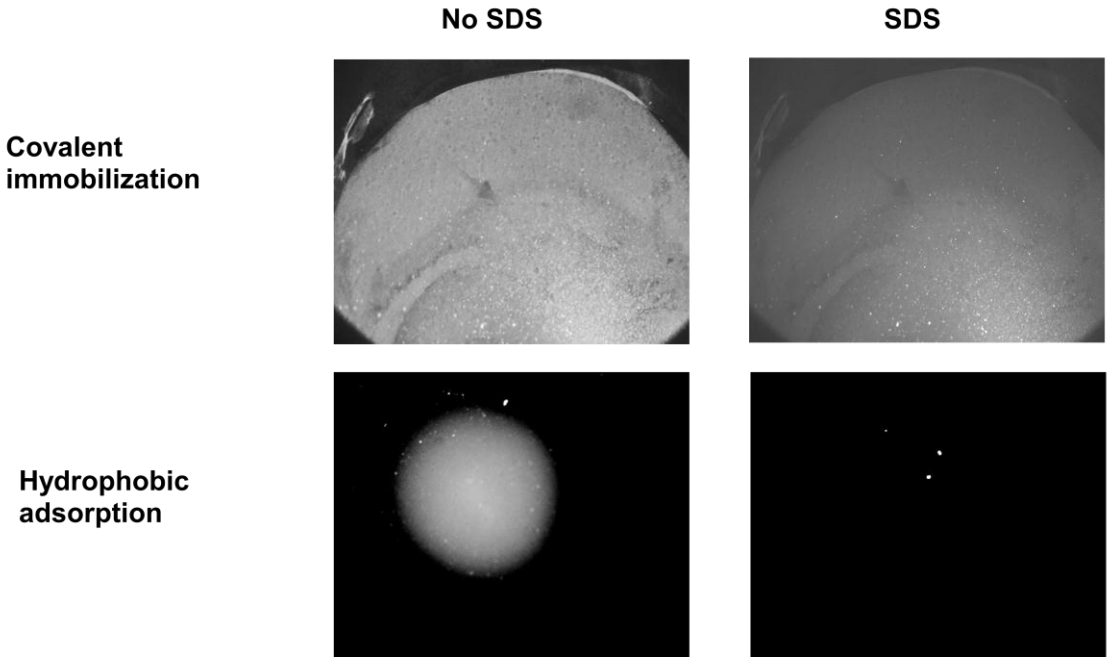

Figure 5 – SDS washing of FITC-fibrinogen. Fibrinogen was labelled with FITC and immobilized on PDMS surface. The surface was incubated with 2% SDS for 3 hours and was washed with Tris buffer. After 3 hours, the covalently linked protein was still there whereas the control showed almost no protein left (n=3).

Effect of bodipy labelling on platelet aggregation

The platelets were fluorescently labelleled with BODIPY FL N-(2-Aminoethyl) maleimide for the further experiments. To analyze the effects of the fluorescent label on platelet aggregation, light transmission aggregometry was done using UV-Vis spectrophotometer. Absorbance at 600 nm was monitored for labelled and unlabelled platelets in the presence and absence of ADP. As can be seen from the optical assessment of aggregation shown in Fig. 6, bodipy-modification at the levels we employ does not interfere with ADP-induced aggregation.

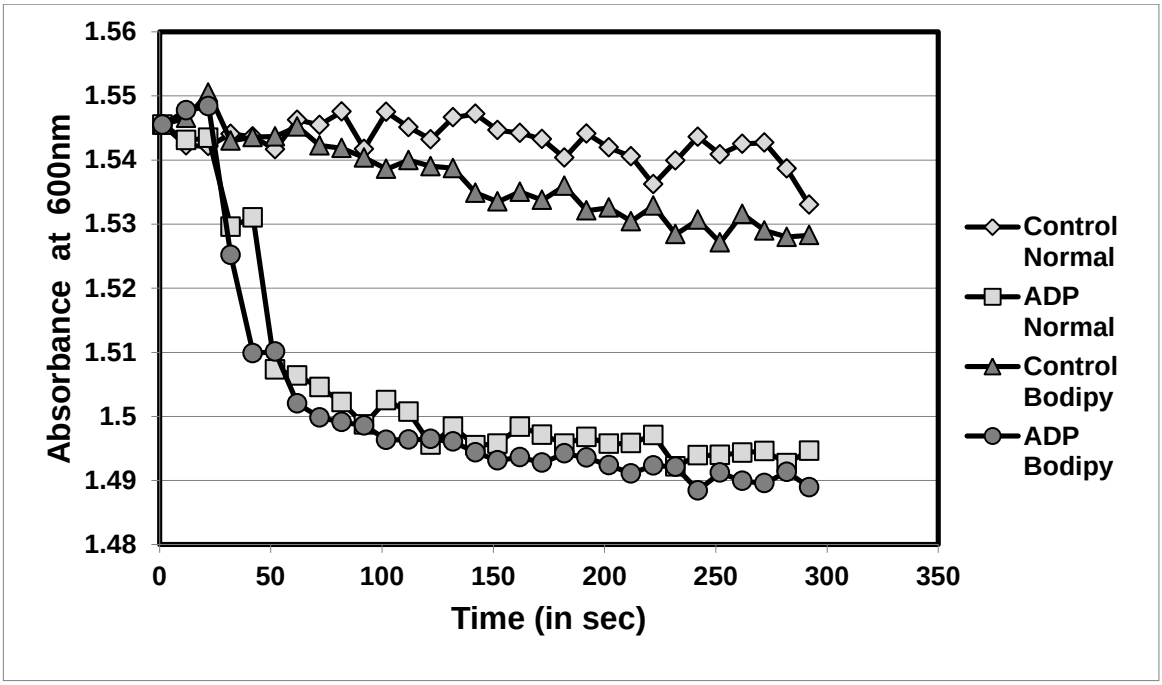

Figure 6 – Effect of bodipy labelling on platelet aggregation. The platelets were diluted in HEPES ACD and 5 µM ADP was added as an agonist after ~ 40 sec. The decrease in absorbance indicates platelet aggregation. The platelets without ADP addition were used as control.

Validation of the flow chambers

In order to assess the suitability of the flow chamber and the immobilization chemistry for platelet adhesion studies, adhesion to collagen and fibrinogen was tested. Flow chambers were placed onto an inverted fluorescence microscope (Zeiss Axiovert 200M. Whole blood containing fluorescently labelled platelets was perfused over the flow chambers containing either PDMS alone or PDMS-immobilized BSA or fibrinogen or collagen. The perfusion rate was 2 ml/min, which generates shear equivalent to that of descending aorta (5 dyne/cm^2). The platelets were either activated by the injection of Ca^{2+} (1 mM) or ADP (20 µM) at t=0. The raw image data, at 40 s intervals, is presented in Figure 7. With the controls, PDMS alone or PDMS-immobilized BSA, there were <50 platelets attached after 200 s of perfusion (Figure 7).

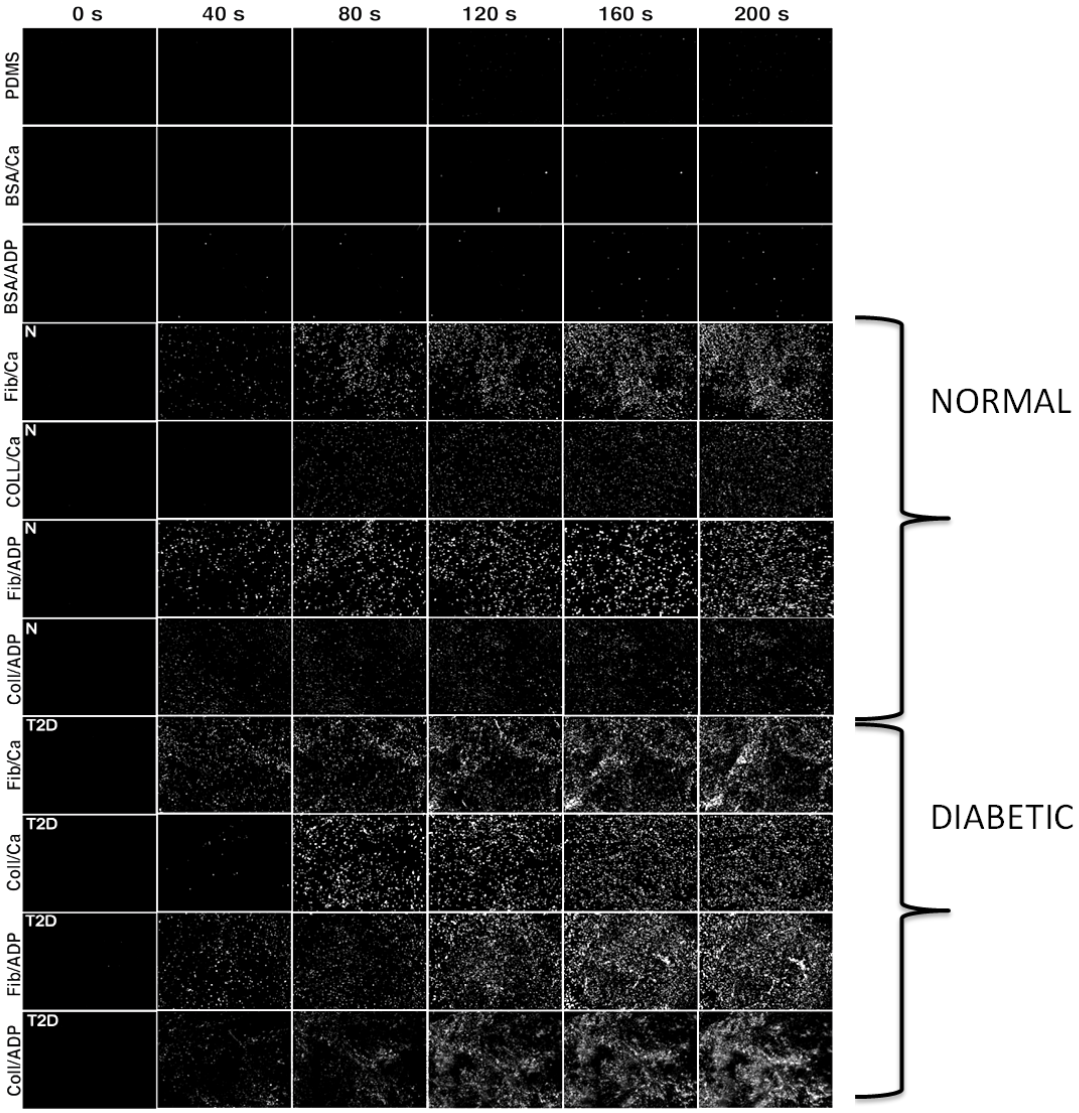
0 s
40 s
80 s
120 s
160 s
200 s
PDMS
BSA/Ca
BSA/ADP
N
Fib/Ca
N
COLL/Ca
N
Fib/ADP
N
Coll/ADP
T2D
Fib/Ca
T2D
Coll/Ca
T2D
Fib/ADP
T2D
Coll/ADP
NORMAL
DIABETIC

Figure 7 – Comparison of platelet aggregation in normal and type 2 diabetic subjects. Whole blood containing fluorescently labelled platelets was passed over PDMS alone and PDMS with immobilized BSA, fibrinogen (Fib) or collagen (Coll) using either 1 mM calcium (Ca^{2+}) or 20 μM ADP as activators. The images show time dependent increase in platelet adhesion to fibrinogen and collagen, with very little adhesion to the controls (PDMS and BSA). The total number of adherent platelets after 200 sec is greater in the case of type 2 diabetic (T2D) subjects as compared to normal (N) subjects, irrespective of the protein/activator used. All experiments were done at 37^{o}C. Images were captured in 20 sec intervals by Zeiss Axiovert 200 microscope with achromat 5X objective (Carl Zeiss), equipped with a Retiga EX cooled monochrome 12 bit camera (Q imaging) and an Xcite series 120 (EXFO,Canada) mercury lamp. Image capture and the quantification of the adhered platelets were facilitated by Northern Eclipse software (Empix, Canada).

Kinetic plots of platelet aggregation

Images over the immobilized protein (fibrinogen or collagen) field were captured every 20 s. The platelets were counted in each frame using Northern Eclipse software and the kinetic plots were constructed (Figure 8). There is an increased rate of platelet aggregation in diabetic subjects as compared to the controls.

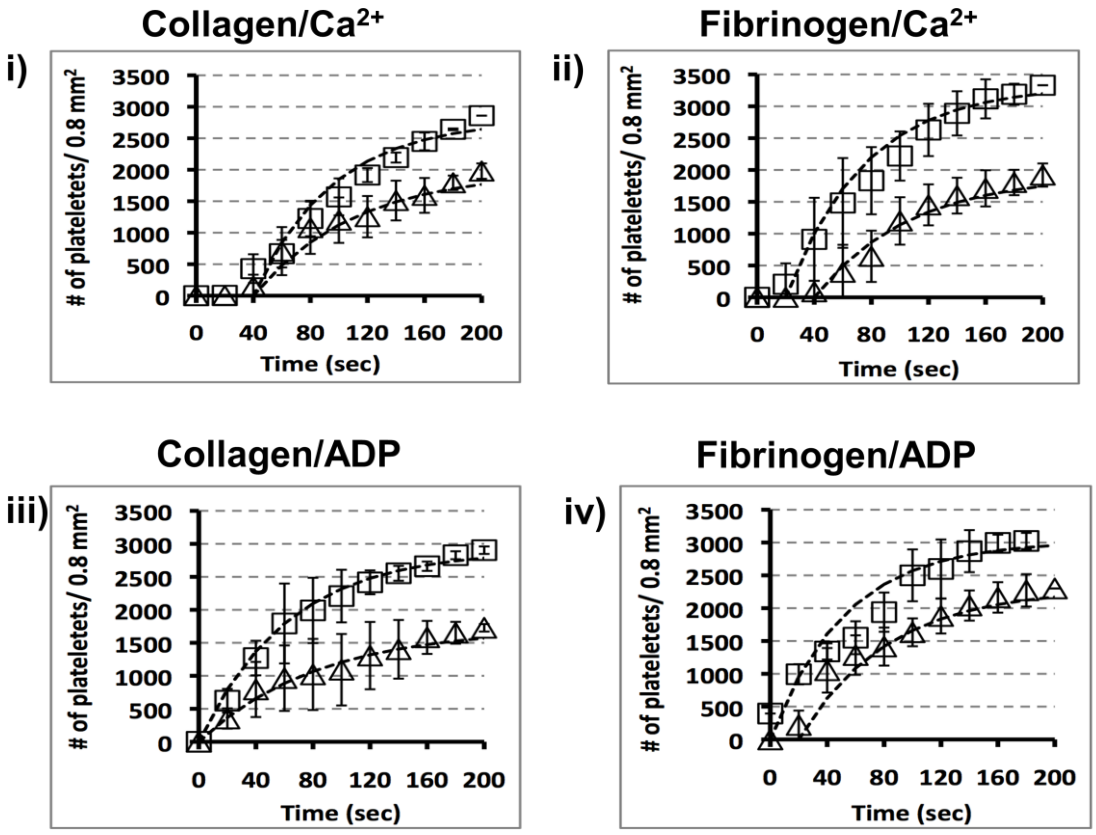

Figure 8 – Kinetic plots of platelets adhered to immobilized fibrinogen and collagen over time. Blood reconstituted with fluorescently labelled platelets from normal and diabetic subjects was perfused through the flow chambers containing immobilized fibrinogen and collagen. Graphs (i) and (ii) show platelets adhered to collagen and fibrinogen, respectively, over time, when calcium was used as an activator. Graphs (iii) and (iv) show increasing number of platelets adhered to collagen and fibrinogen respectively, when ADP was used as an activator. The number of platelets adhering over time is greater in diabetic subjects (squares) as compared to normal subjects (triangles). The platelet binding data is extracted from the entire image data set taken at 20 sec intervals. Each point represents the mean ± SD from at least three independent experiments. The solid lines represent the best fit line for the first order treatment of the binding data: $Y=A\ (1-e^{-kt})$.

The total number of platelets bound to the protein surfaces are summarized in Table 1. In general, the maximum number of platelets bound at saturation (~200 s) was larger for platelets from T2D subjects in comparison to those from the normal subjects, under all conditions examined. The largest ratio between T2D to normal of ~1.73 was obtained with Ca^{2+}-activated platelets on a fibrinogen surface. The smallest ratio of ~1.31 was obtained with ADP-activated platelets on a collagen surface.

Table 1 – Total number of platelets attached

	Normal	T2D	Ratio(T2D:N)
Fib/Ca^{2+}	1920±222	3330±150	1.73
Coll/Ca^{2+}	1978±122	2859±100	1.44
Fib/ADP	2300±110	3024±150	1.31
Coll/ADP	1727±95	2904±57	1.68

Table 1 – The table shows the total number of normal and type 2 diabetic (T2D) platelets ± SD attached to fibrinogen (Fib) and collagen (Coll) after 200 sec, with calcium (Ca^{2+}) and ADP as activators.

Table 2 – First order rate constants (sec^{1})

	Normal	T2D	Ratio(T2D:N)
Fib/Ca^{2+}	0.015±0.0005	0.0183±0.005*	1.22
Coll/Ca^{2+}	0.014±0.0026	0.018±0.0011*	1.28
Fib/ADP	0.016±0.0011	0.018±0.0026	1.12
Coll/ADP	0.012±0.0021	0.016±0.0011*	1.33

Table 2 – The first order rate constants were calculated from the kinetic plots of the platelet adhesion data. The T2D platelets have higher rate constants as compared to the normal (*$P<0.05$).

Discussion

The novel aspect of this study is the surface chemistry, which can be utilized for facile patterning of immobilized proteins on PDMS surface. The design of the flow device and immobilization chemistry introduced here can easily be adapted to microfluidic/lab on chip applications for the analysis of hemostasis. The glass coverslip on the bottom of the flow chamber can be removed, which allows for cheap and reproducible flow chambers for further experiments.

The washing of PDMS with SDS could not remove the immobilized fibrinogen. This indicates that AS-DSS can bind protein more tightly than physiosorption. Light transmission aggregometry illustrated that platelet labeling with Bodipy does not affect the aggregation of platelets in response to agonists'.

When the whole blood was passed over fibrinogen or collagen coated flow devices there was a continuous build up in the adhered platelets over the initial density pattern established in the previous time frames indicating that the interaction was irreversible. At the end of the binding experiments ~10 mL of buffer was pumped through the flow chambers. The number of adhered platelets did not change, which was a further indication of the irreversibility of the interaction with protein matrices covalently attached to the PDMS surface. One observation from the kinetic plots of the data was that when platelets were activated with Ca^{2+}, with either on the collagen or the fibrinogen surface, there was a 20 s to 40 s lag prior to the initiation of platelet binding irrespective of the platelet source (T2D or normal) (Figure 8 i, ii). In contrast, this lag was absent in the ADP-activated platelets (Figure 8 iii, iv).

It is well established that in T2D, the platelets have altered *in vitro* adhesion and aggregation patterns and are hypersensitive to agonists as compared to the normal platelets (Glassman *et al* 1993; Dittmar *et al* 1994; Haouari *et al* 2008; Vinik *et al* 2001). Therefore, an important step in the validation process was to determine whether our flow devices were able to discern functional differences between platelets from normal and T2D subjects. To this end, we compared the adhesion kinetics of Ca^{2+} or ADP activated platelets from control and T2D subjects onto immobilized collagen and fibrinogen in the flow chambers. A qualitative examination of the raw data (Figure 7) revealed that

platelets from T2D subjects gave rise to more platelet adhesion irrespective of the activator used or the immobilized surface. These observations were elegantly substantiated upon kinetic treatment of the data (Fig 8 i to iv and Tables 1 and 2).

The rate constants extracted from first order kinetic treatment of the data (Table 2) revealed that the binding rate constants for platelets from normal subjects were in general independent of the activator used or the protein immobilized since the differences between the rates (0.014 ± 0.002 sec^{-1}) were not statistically significant. However, when the rate constants of the various activator/protein surface combinations from T2D were compared to normal, in all cases the T2D gave rise to 1.12-fold to 1.33-fold larger and statistically significant, platelet-binding rate constants (0.018 ± 0.002 sec^{-1}).

Conclusions

In conclusion, here we have introduced a simple and robust method for the construction of flow cells made out of PDMS as well as the chemistry for the covalent attachment of any platelet-reactive peptides or proteins onto the PDMS surface. We have also demonstrated that the flow cells can readily provide real time data on the kinetics of platelet binding and can detect subtle pathological changes in platelet function introduced as a result of pathologies such as type 2 diabetes.

References

Dittmar S, Polanowska-Grabowska R and Gear AR. Platelet adhesion to collagen under flow conditions in diabetes mellitus. Thrombosis Research 1994; 74: 273-83.

Glassman AB. Platelet abnormalities in diabetes mellitus. Ann Clin Lab Sci. 1993; 23: 47-50.

Goncalves I, Hughan SC, Schoenwaelder SM, Yap CL, Yuan Y and Jackson SP, Integrin alpha IIb beta 3-dependent calcium signals regulate platelet-fibrinogen interactions under flow. Involvement of phospholipase C gamma 2. J Biol Chem 2003; 278: 34812-34822.

Haouari M El and Rosado JA. Platelet signaling abnormalities in patients with type 2 diabetes mellitus: a review. Blood Cells Mol Dis. 2008; 41: 119-123.

Miersch S, Sliscovic I, Raturi A and Mutus B. Antioxidant and antiplatelet effects of rosuvastatin in a hamster model of prediabetes. Free Radical Biology & Medicine 2007; 42: 270–279.

Miyaki K, Zeng HL, Nakagama T and Uchiyama K. Steady surface modification of polydimethylsiloxane microchannel and its application in simultaneous analysis of homocysteine and glutathione in human serum. Journal of Chromatography.A. 2007; 1166: 201-206.

Remijn JA, Wu YP, Jeninga EH, Jsseldijk MJW, Willigen GV, Groot PG, Sixma JJ, Nurden AT and Nurden P. Role of ADP Receptor $P2Y_{12}$ in Platelet Adhesion and Thrombus Formation in Flowing Blood. Arteriosclerosis,Thrombosis, and Vascular Biology 2002; 22: 686-691.

Turner NA, Moake JL and McIntire LV Blockade of adenosine diphosphate receptors $P2Y_{12}$ and $P2Y_1$ is required to inhibit platelet aggregation in whole blood under flow. Blood 2001; 98: 3340-3345.

Vinik AI, Erbas T, Park TS, Nolan R, Pittenger GL. Platelet dysfunction in type 2 diabetes. Diabetes Care 2001; 24: 1476-1485.

CHAPTER 4

Whole blood, flow-chamber studies in real-time indicate a biphasic role for thymosin β-4 in platelet adhesion

Published as original research as Kaur *et al*. 2010

Introduction

Thymosin β4 (Tβ4) is a water-soluble, ubiquitous, highly conserved 43-amino acid acidic polypeptide (pI 5.1) with a molecular weight of 4.9 kDa (Low *et al* 1981, 1982; Yu *et al* 1994; Goodall *et al* 1983, 1983). It was originally isolated from the thymus but is present in different concentrations in different tissues, cell types and extracellular fluids (blood, plasma, saliva, tears). It is found at concentrations of ~5 nM to ~80 nM in plasma to ~500 μM in platelets (Hannappel *et al* 1982, 1985, 1987; Huff *et al* 2001). Tβ4 lacks a secretion signal and hence its presence in extracellular fluids could be due to cellular damage.

The major intracellular function of Tβ4 in mammalian cells is to form a 1:1 complex with G-actin, preventing its polymerization (Low *et al* 1981; Hannappel *et al* 1985; Safer *et al* 1991). Apart from its interactions with actin, Tβ4 is capable of modulating a wide array of biological functions including tissue (Goldstein *et al* 2005) and wound repair (Sosne *et al* 2002) as well as anti-inflammatory (Young *et al* 1999) antiapoptotic and neurotrophic (Sun *et al* 2007) properties. Tβ4 has been also shown to play a relevant role in angiogenesis (Smart *et al* 2009) and neural development (Lin *et al* 1990). It also protects the cells against oxidative damage and upregulates anti-oxidative enzymes catalase and SOD (Ho *et al* 2008). The role of Tβ4 in increasing hair growth and dermal repair has also been studied, where it promotes stem cell migration and their subsequent differentiation into keratinocytes and hair follicles (Philip *et al* 2004).

The ability of Tβ4 to affect these diverse biological functions has been ascribed to an array of short, bioactive, peptide sequences within the Tβ4-primary sequence (Sosne *et al* 2010) (Fig. 1).

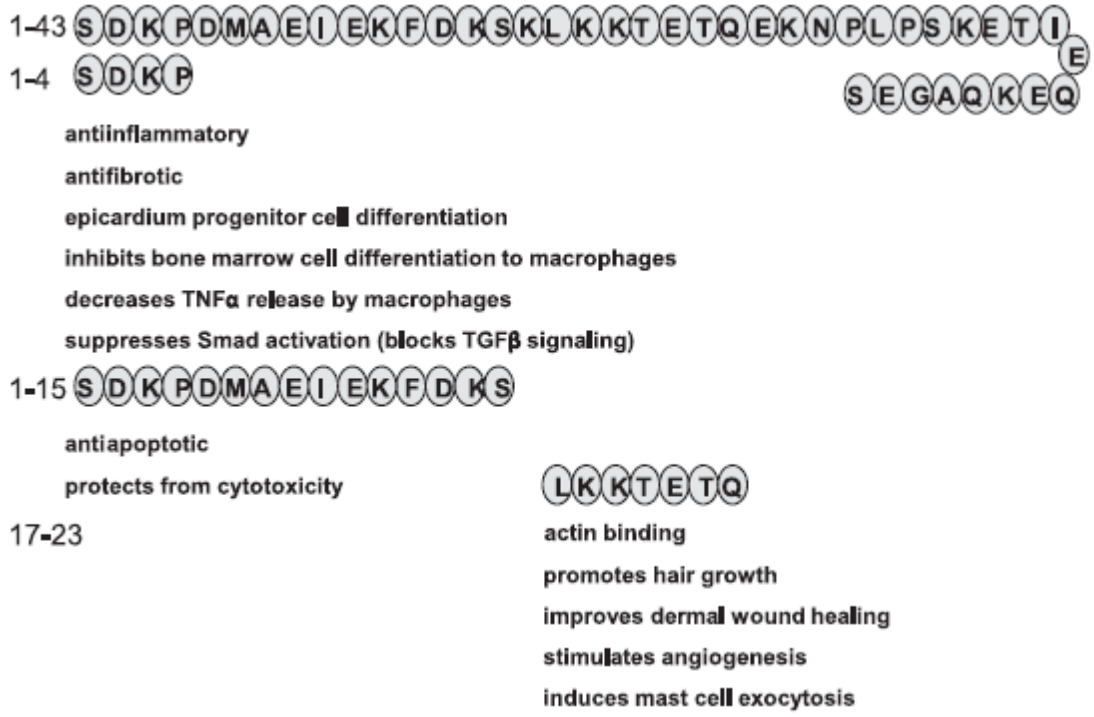

Figure 1 – Location and activity of different peptides derived from Tβ4 (Image taken from Sosne *et al* 2010).

The largest concentrations of Tβ4 are found in leukocytes and platelets (Low *et al* 1981; Yu *et al* 1994; Goodall *et al* 1983; Hannappel *et al* 1985, 1987). In resting platelets, it has been estimated that ~60% of the actin is prevented from polymerizing by complexing with Tβ4 (Fox 1993). Upon platelet activation, Tβ4 is secreted and cross-linked enzymatically by factor XIIIa (a transglutaminase) to fibrin in a time- and Ca^{2+}-dependent manner (Huff *et al* 2002; Makogoneko *et al* 2004) thus increasing the local concentration of Tβ4 near sites of clots and tissue damage, where it is postulated to contribute to wound healing, angiogenesis and inflammatory responses. Platelets carry and release large amounts of Tβ4. Yet the role of Tβ4 on platelet thrombus formation has yet to be fully investigated. The current study represents a small step towards this goal. Here, we have tested the effects of Tβ4 extraneously added to whole blood, on deposition of ADP activated platelets onto fibrinogen under conditions of continuous flow and shear.

Experimental methods

Subject selection

Healthy human subjects (n=5), ages 25–40 years were chosen to participate in the study only if they showed no overt symptoms of disease and were taking no medication. The experimental protocols were approved by the University of Windsor Research Ethics Board.

Construction of the flow chamber

The flow chamber consisted of a Teflon boundary with matching holes (1.75mm) drilled through sides a and b (Fig. 2A). The Teflon boundary was first attached onto 1.5 cm microscope coverslips by painting a small amount of Sylgard 184 (trade name of polydimethylsiloxane- PDMS), (Dow Corning) base plus curing agent (mixed in a 10:1 ratio). Teflon® tubing (2 cm) was then inserted through the holes and enough Sylgard 184, (Dow Corning) base plus curing agent was poured to fill the mold. After curing for 6 h at 60 °C the Teflon tubing was removed by pulling through the holes (sides a or b, Fig. 2A). The flow chamber was then placed into a plasma cleaner PDC-32G (Harrick Plasma, USA) in order to generate silanol groups (Miyaki *et al* 2007) on the otherwise inert PDMS-walls of the flow chamber (Fig. 2B).

Protein immobilization onto plasma activated PDMS surfaces in the flow chambers

After plasma oxidation, 5 μl of 2% aminopropyltrimethoxysilane (APTMES) (Sigma, Canada) was added to the geometric centre of each of the flow channel with the aid of a Hamilton syringe. After 10 min, a 0.5-μl portion of 0.5 mM disuccinimidyl suberate (DSS) (Pierce, USA) solution was added to the APTMES ring at the centre of the flow channels. Within 30 s of DSS addition, either 1 μl of either Type I fibrinogen (5 μM) from bovine plasma (Sigma-Aldrich, Canada) or of collagen type I (8 μM) from rat tail (BD Biosciences) was introduced into the reaction mixture. The reaction was stopped after 15 min by pumping 10 mL of Tris–HCl buffer (0.15 M, pH 8.0) at a rate of 2 ml/min through the flow chamber.

Blood collection and washing of platelets

Platelets were isolated as described previously (Miersch *et al* 2007) and were fluorescently labelled by reacting for 30 min, with 60 μM BODIPY® FL N-(2-aminoethyl) maleimide (Molecular Probes, Canada). The labelled platelets were harvested by 2 centrifugation-wash (HEPES-ACD buffer) steps to remove the excess dye and were reintroduced into the whole blood sample that they were originally isolated from.

Monitoring platelet deposition via flow cells

A flow cell with the coverslip face-down was placed in the turret of a Zeiss Axiovert 200 M inverted fluorescence microscope equipped FITC filter cube, and 5×objective. Fluorescence images were captured at 20-s intervals with the aid of a CCD camera (Hitachi KP-F140F). Two syringe pumps (New Era Pumps, NE-300) were utilized to mix the activating agent (ADP, 400 μM/ Ca^{2+}, 100mM; flow rate 0.05 mL/min) with the whole blood containing the fluorescently-labelled platelets (flow rate 0.95 mL/min) at a t-junction. This yields final Ca^{2+} and ADP concentrations in the flow cell of 5 mM and 20 μM, respectively. At the start of the experiment only the blood was pumped through the channel to adjust the focus and to optimize image capture parameters. At t=0 the activating agent pump was started and image capture initiated. A given blood sample was pushed separately though each flow channel thus generating 4 sets of binding data per sample. The estimated shear on the wall of the flow cells was 150 s^{-1} (5 dyne/cm^2), which represents shear rate in the descending aorta or veins. Image analysis was performed with the aid of Northern Exposure 6.0 (Empix, Mississauga, ON) and ImageJ
(NIH) imaging software packages.

Tβ4 binding assay

A 96-well plate was filled with 50 μL of PDMS at a ratio of 10:1, base: curing agent. Fibrinogen was immobilized on PDMS as described before. Tβ4 was labelled with eosin-isothiocyanate (EITC) at room temperature for 2 h in the presence of 1 M sodium bicarbonate buffer pH 9.0. The labelled Tβ4 was run over a G25 column in the dark to remove unbound EITC. Protein concentration was determined by bicinchoninic acid

(BCA) assay. Tβ4 was added to the wells at concentrations of 0.1 μM, 0.2 μM, 0.5 μM, 1 μM, 2 μM and 4 μM. In some wells, unlabelled 4 μM Tβ4 was also added. For control, labelled Tβ4 was added to the activated PDMS alone. The plate was incubated under gentle agitation for 2 h in the dark. Fluorescence was monitored in the solution before and after incubation by Cary Eclipse Fluorescence Spectrophotometer with excitation at 520 nm and emission at 540 nm. To study the thymosin beta 4 binding to fibrinogen under flow, fibrinogen was immobilized in the flow chamber (i.e. the yellow region Fig. 1A) and excess eosin-Tβ4 was introduced onto the fibrinogen. The flow chamber was then washed with PBS to remove excess eosin-Tβ4. Increasing concentrations of unlabelled Tβ4 (10 nM–1 μM) were pumped through the flow cells with a syringe pump (New Era Pumps, NE-300) at a rate of 1.0 mL/min and 0.2 mL fractions were collected using a fraction collector (Bio-Rad, Model 2110). Fluorescence was monitored in the fractions by Cary Eclipse Fluorescence Spectrophotometer with excitation at 520 nm and emission at 540 nm.

Statistical analysis

Data is expressed as an average of all trials and statistical analysis was performed by Student's t-test the error bars represent s.d. Chemical structures in Fig. 1 were drawn with ChemDraw 11.0.

Results

Flow chamber geometry and immobilization chemistry

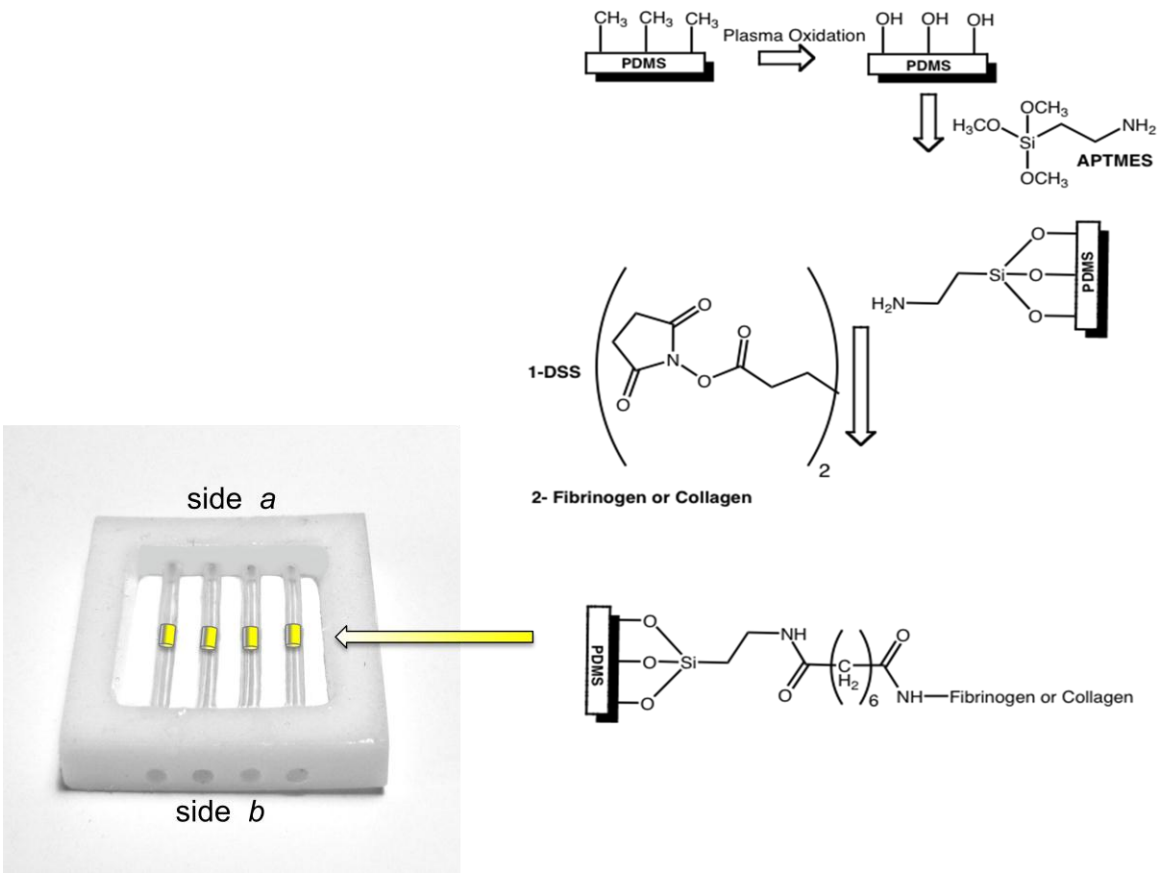

Figure 2 – Geometry of the flow chamber and chemistry used for immobilizing fibrinogen/collagen in the flow chamber.

Validation of the flow chambers

In these studies, the raw image files collected at 20 s intervals were converted to 8-bit gray scale images. We then used the ImageJ plugin, Multi Otsu Threshold introduced by Dos Santos et al. (Santos *et al* 2009) to ensure that we did not count the platelets that were transiently associated with the immobilized proteins (appear as streaks in the raw images: indicated with arrows in Fig. 3). Otsu multi-thresholding eliminated the streaks as well as the out of focus platelets deposited on the edges (see Fig. 2 a, b, c, d, e vs. a', b', c', d', e'). The processed-images were subsequently counted by using ImageJ: Step 1 menu>image>adjust>threshold; and Step 2—Menu>analyze>analyze particles.

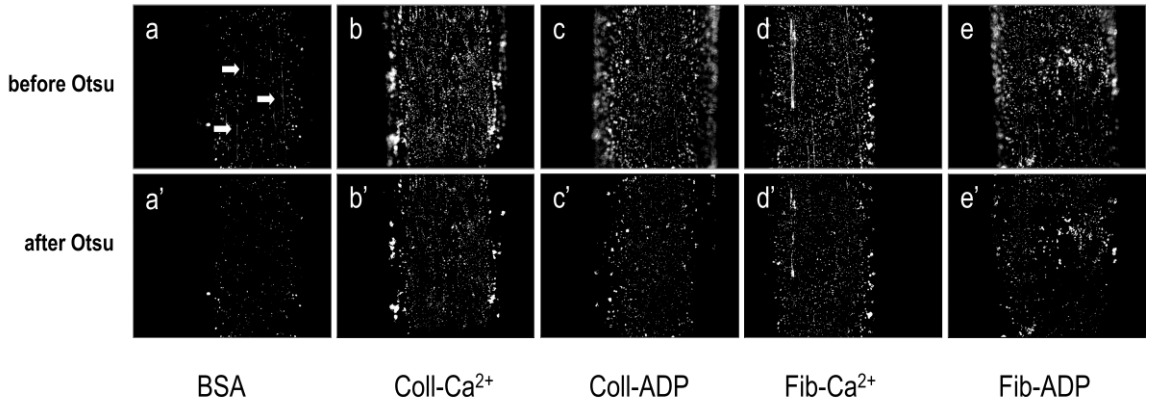

Figure 3 – Demonstration of the Otsu Multi-Thresholding ImageJ plugin to exclude non-deposited, transiently associated platelets from being counted in the deposition data. Representative raw images obtained at 120 s in flow cells with immobilized BSA, a; immobilized collagen with Ca^{2+} as activator, b; immobilized collagen with ADP as activator, c; immobilized fibrinogen with Ca^{2+} as activator, d; immobilized fibrinogen with ADP as activator, e. The same Images after Otsu Multi Thresholding with immobilized BSA, a'; immobilized collagen with Ca^{2+} as activator, b'; immobilized collagen with ADP as activator, c'; immobilized fibrinogen with Ca^{2+} as activator, d'; immobilized fibrinogen with ADP as activator, e'. Arrows point to non deposited platelets appearing as streaks.

Platelet deposition on collagen/fibrinogen in the presence of Ca^{2+}/ADP

A representative set of platelet deposition data from blood samples isolated from the same subject, exposed to the either Ca^{2+} or ADP as activator with either BSA or fibrinogen or collagen immobilized into the flow cell surfaces is presented in Fig. 4 A – F. The platelet deposition data for collagen and fibrinogen were well accommodated by a first order kinetic process [# of platelets deposited at a given time (t) =Maximum # of platelets deposited*(1- $e^{-k_{obs}*t}$)]. The rate constants estimated from first order kinetic treatment of the data revealed that the rate of platelet deposition was independent of both the activators used (Ca^{2+} or ADP) and the protein immobilized (collagen or fibrinogen) since the differences in the rates obtained under the various conditions were not statistically significant (Fig. 4G). This same trend was observed with all subjects tested (n=5).

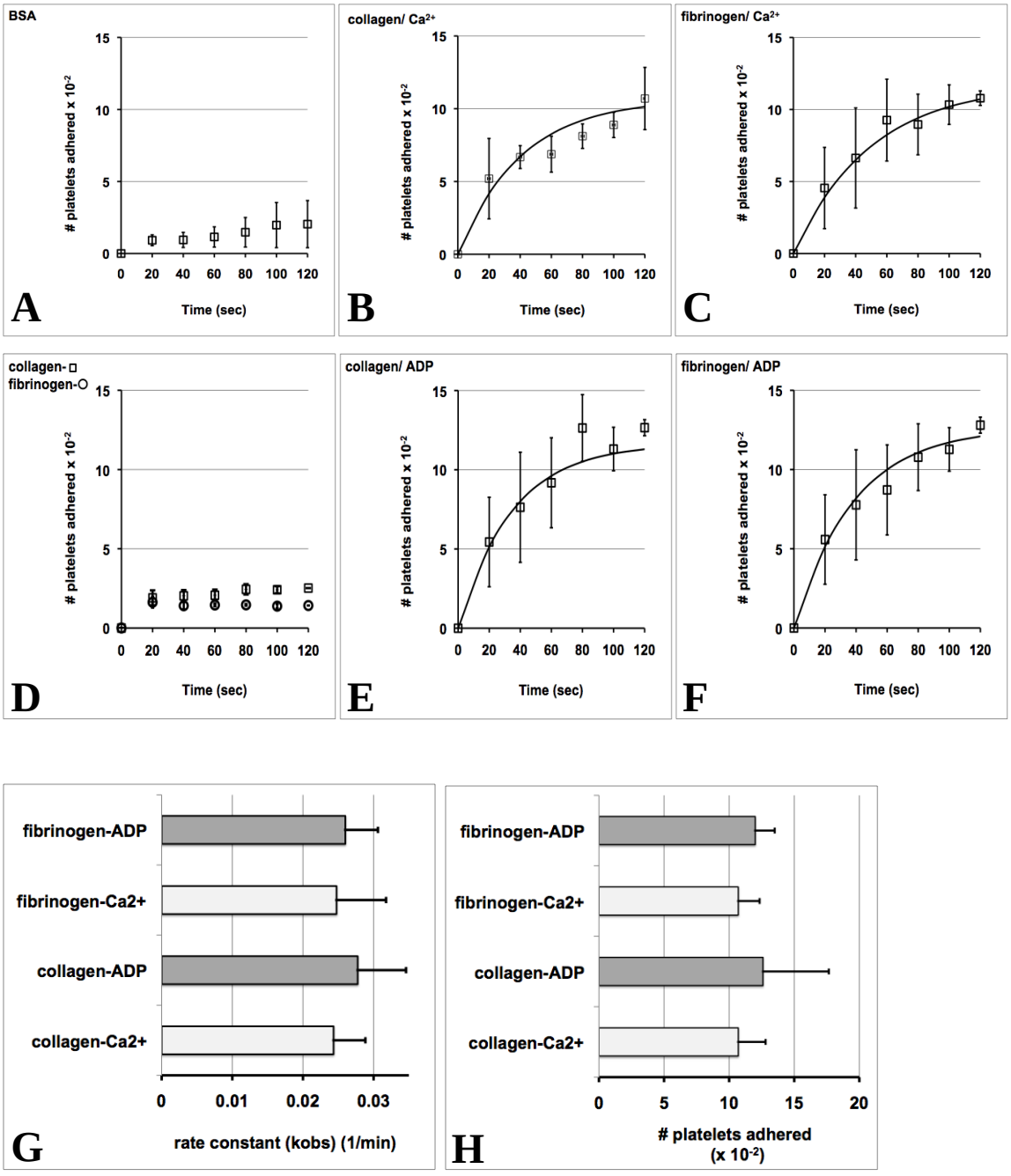
BSA
collagen/ Ca2+
fibrinogen/ Ca2+
collagen-□
fibrinogen-○
collagen/ ADP
fibrinogen/ ADP
platelets adhered x 10-2
Time (sec)
A
B
C
D
E
F
fibrinogen-ADP
fibrinogen-Ca2+
collagen-ADP
collagen-Ca2+
rate constant (kobs) (1/min)
platelets adhered (x 10-2)
G
H

Figure 4 – Kinetic plots obtained from particle counts of Otsu Multi Threshold images for platelets deposited onto immobilized BSA, A; immobilized collagen with Ca^{2+} as activator, B; immobilized fibrinogen with Ca^{2+} as activator, C; immobilized fibrinogen/collagen without any activator, D; immobilized collagen with ADP as activator, E; immobilized fibrinogen with ADP as activator, F; (n=4 from a single subject). Composite rate constants: an average rate constant from each subject was obtained by performing the deposition experiment under each condition (A to F) in quadruplicate. The average value for each condition was then averaged for all the subjects (n=4), G. Composite # of deposited platelets: an average # of deposited platelets from each subject were determined from the 120 s images by performing the deposition experiment under each condition (A to F) in quadruplicate. The average value for each condition was then averaged for all the subjects (n=4), H. The solid lines represent the best fit line for the first order treatment of the binding data: $Y = A (1- e^{-kt})$. Error bars represent s.d.

The effect of Tβ4 on platelet deposition under conditions of flow.

The flow system was then employed to test the effect of Tβ4-dose on the deposition of ADP-activated platelets to fibrinogen immobilized flow cells. In these studies, Tβ4, at the concentrations indicated (Fig. 5) was incubated for 15 min with the blood/fluorescently labelled platelet mixtures before the deposition experiments were carried out. As can be seen from the kinetic binding data (Fig. 5A) and a representative data set of the images captured at 120 s from the blood samples obtained from the different subjects (S1 to S4, Fig. 5B), Tβ4 had a biphasic effect on both the rates of deposition as well as the number of platelets deposited. Above a critical concentration of ~0.2 μM Tβ4 the platelet deposition is not uniform over the flow cell surface as observed in the control or the validation experiments (Fig. 3 and 4). Instead, large thrombi are evident indicative of platelet–platelet interactions. These are reflected in the ~4-fold increase in the estimated number of platelets deposited (Fig. 5D). The estimated rate constants of platelet deposition also increased ~1.5-fold during this process.

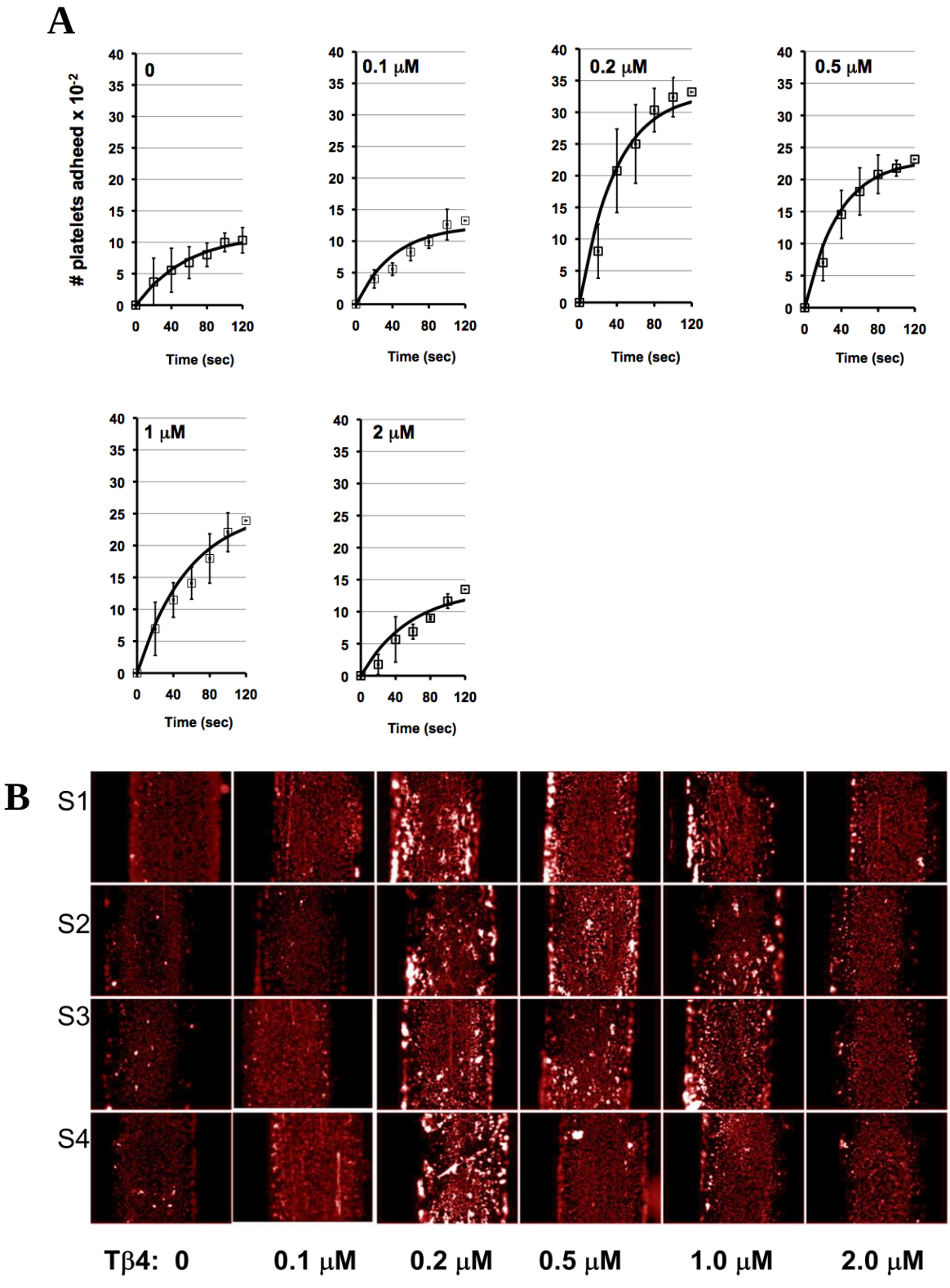
A
platelets adheed x 10-2
0
0.1 μM
0.2 μM
0.5 μM
1 μM
2 μM
Time (sec)
B
S1
S2
S3
S4
Tβ4: 0
0.1 μM
0.2 μM
0.5 μM
1.0 μM
2.0 μM

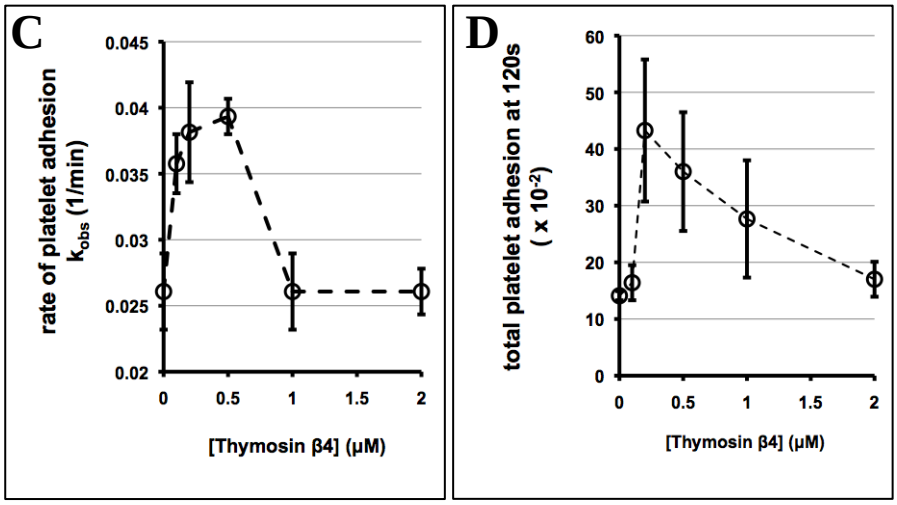

Figure 5 – The effect of Tβ4-dose on the rate and density of platelet deposition.

(A) Kinetic plots obtained from particle counts of Otsu Multi Thresholded images for platelets deposited on immobilized fibrinogen with ADP as activator, as a function of Tβ4-dose. The solid lines represent the best fit line for the first order treatment of the binding data: $Y = A\ (1- e^{-kt})$. Error bars represent s.d. (n=4). (B) Representative raw images from each subject (S1 to S4) at 120 s as a function of Tβ4-dose. (C) Composite rate constants: an average rate constant from each subject was obtained by performing the platelet deposition as a function of Tβ4-dose, in quadruplicate. The average value for each [Tβ4] was then averaged for all the subjects. Error bars represent s.d. (n=4). (D) Composite # of deposited platelets: an average # of platelets deposited from each subject was determined from the 120 s images as a function of Tβ4-dose, in quadruplicate. The average value for each [Tβ4] was then averaged for all the subjects. Error bars represent s.d. (n=4).

Tβ4 binding to immobilized fibrinogen

The decrease in platelet aggregation in the presence of high concentrations of Tβ4 suggests that Tβ4 might be binding with fibrinogen and hence inhibiting fibrinogen mediated platelet aggregation. This led us to propose this hypothesis that Tβ4 might have a binding site on fibrinogen. In order to test our fibrinogen binding hypothesis, we immobilized fibrinogen onto PDMS on the bottom of 96-well plates using the same chemistry as in the flow cells (Fig. 1). We then used a fluorescent Tβ4 derivative, eosin-Tβ4, to perform equilibrium binding studies. In these experiments increasing amounts of eosin-Tβ4 were added to either activated PDMS (Fig. 6A, diamonds) or PDMS-fibrinogen (Fig. 6A, triangles) or PDMS-fibrinogen containing a constant amount of unlabelled Tβ4 (Fig. 6A, circles). There was only significant Tβ4-binding to fibrinogen immobilized PDMS and not to PDMS alone or when labelled Tβ4 was added to PDMS-fibrinogen in the presence of a constant amount of unlabelled Tβ4. These experiments indicate that we are observing a specific interaction between fibrinogen and eosin-Tβ4. The K_D estimated for this interaction was ~126±18 nM (i.e. negative reciprocal of the slope of the Scatchard plot of the binding data, Fig. 6B).We also estimated the Tβ4-fibrinogen interaction under flow. To do this, excess eosin-Tβ4 was introduced onto the fibrinogen immobilized in the flow chambers (i.e. the yellow region Fig. 2). The excess eosin-Tβ4 was removed by pumping 2 mL of PBS over the flow cells. Next increasing amounts of unlabelled Tβ4 was pumped through the flow cells with a syringe pump at a rate of 1.0mL/min and 0.2 mL fractions were collected. The total fluorescence (eosin-Tβ4) summed over fractions 1 and 2 was plotted against unlabelled [Tβ4] (Fig. 6C). The data were fitted to the competitive binding equation Eq. (1)

100% (total fluorescence) - % fluorescence eluted f ([½Tβ4])) =

$$\frac{[\text{eosin}-\text{T}\beta4]}{K_{\text{D-eosin}-\text{T}\beta4}\,(1 + [\text{T}\beta4]/\,K_{\text{D-T}\beta4}\,) + (\text{eosin}-\text{T}\beta4)}$$

where $K_{D-\text{ eosin-T}\beta4}$ = the dissociation constant between fibrinogen and eosin-Tβ4; and K_D- Tβ4 = the dissociation constant between fibrinogen and unlabelled-Tβ4. The $K_{D-\ T\beta4}$ estimated under flow conditions was 66±20 nM.

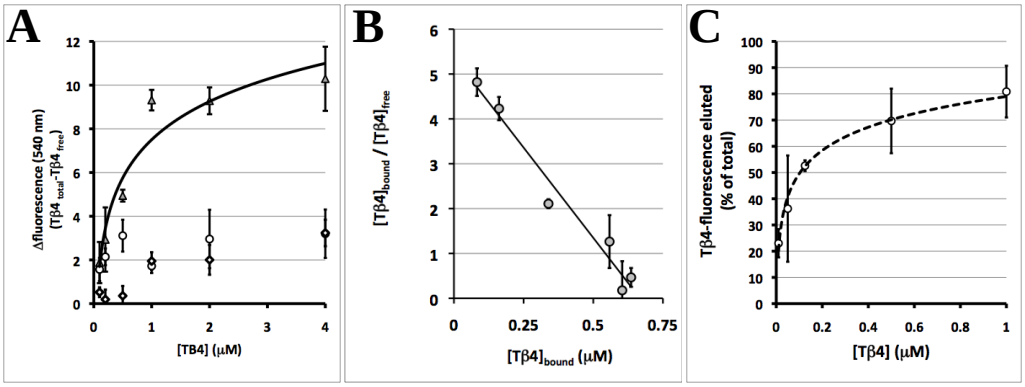

Figure 6 – Binding of eosin-Tβ4 to fibrinogen immobilized on PDMS.

(A) Equilibrium binding of eosin-Tβ4 to fibrinogen. Increasing amounts of eosin-Tβ4 were added to activated PDMS (diamonds) or PDMS-fibrinogen (triangles) or PDMS-fibrinogen containing a constant amount, 4 μM, of unlabelled Tβ4 (circles). Bound eosin-Tβ4 fluorescence = total eosin-Tβ4 fluorescence−free eosin-Tβ4 fluorescence (i.e. fluorescence of the supernatant after addition onto PDMS-wells) as a function of eosin-Tβ4-dose. Error bars represent s.d. (n=5). (B) Scatchard plot of the binding data. KD=−1/slope. Error bars represent s.d. (n=5). (C) Binding of eosin-Tβ4 to fibrinogen under flow. Increasing concentrations of unlabelled Tβ4 were pumped over the flow cell containing immobilized fibrinogen and eosin-Tβ4. The total fluorescence (eosin-Tβ4) was plotted against unlabelled [Tβ4]. Error bars represent s.d. (n=3).

Discussion

In the present study, a new perfusion chamber to study platelet adhesion *in vitro* was introduced. To validate the chamber, platelet deposition onto collagen and fibrinogen was determined using Ca^{2+} and ADP as activating agents.

The average rate constant of platelet accumulation obtained under the various conditions (immobilized collagen and fibrinogen with Ca^{2+} and ADP as agonists) was $0.026\pm0.0015\ s^{-1}$. This rate constant corresponds to a half-life of 27 s. This indicates that the deposition process in the flow system is complete by ~130 s (i.e. 5× half-life). This value corresponds well to 2 min to 6 min bleed times (i.e. the time it takes for a small skin wound to stop bleeding) in normal humans (Schafer *et al* 2003). There were also no statistically significant differences in the total number of platelets deposited to the flow cell surfaces covered with fibrinogen or collagen which is indicative of the reproducibility of the immobilization methodology employed here.

Platelets have high concentrations of Tβ4 and during blood clotting, Tβ4 concentration in the serum increases substantially. During blood coagulation, or by ADP induced aggregation of platelets, Tβ4 is liberated from platelets and partially cross-linked to fibrin by a transglutaminase, factor XIIIa. The covalent cross-linking of Tβ4 to the fibrin clot might represent a mechanism to guarantee a high local concentration of the peptide at the site of injury, probably supporting subsequent wound healing.

When Tβ4 was added to the blood, there was an increase in platelet deposition as compared to the controls. However, at high concentrations of Tβ4, the platelet deposition diminished. In terms of the half-life of deposition, this corresponds to a decrease from 27 s to 17 s (i.e. deposition is complete in ~85 s in the presence of Tβ4 as opposed to ~130 s in its absence). Interestingly, as the concentration of Tβ4 reaches ~2 μM the deposition rates and density return to near normal levels.

One possible explanation for Tβ4-mediated transient in platelet deposition could be that Tβ4 has multiple effects on platelet thrombus formation. At low concentrations Tβ4 could promote platelet activation by interacting with platelet receptors (ADP, fibrinogen, etc.) converting them to high affinity states. Tβ4 could also bind to fibrinogen

in such a manner to prevent its interaction with platelet receptors, thus as Tβ4 concentrations rise, platelet deposition would be attenuated.

The binding of Tβ4 to fibrinogen and fibrin in the presence and absence of transglutaminase was tested previously (Makogoneko *et al* 2004). In these studies, fibrinogen was attached onto plastic, blocked and the amount of Tβ4-bound was estimated by anti-Tβ4-antibodies conjugated to horse radish peroxidase. The concentration range of Tβ4 employed was 5 μM to 30 μM. Although these authors did observe the largest amounts of Tβ4 incorporation to fibrin in the presence of transglutaminase, they did report a small amount of Tβ4-binding to fibrinogen (Makogoneko *et al* 2004).

Our present result suggests that there is a high affinity Tβ4-binding domain on fibrinogen that was previously undetected possibly owing to differences in the Tβ4-dose or the binding assays employed. The fibrinogen binding ability of Tβ4 could explain the biphasic response of Tβ4 on platelet deposition under conditions of flow as observed here.

Furthermore, the results obtained in this study suggest a key modulatory role for Tβ4 in thrombus formation. At low doses Tβ4 promotes platelet deposition and aggregation by as yet unknown mechanism(s). But as platelets are activated and more Tβ4 is released from platelets, its serum levels rise and prevent excessive thrombus formation by binding to fibrinogen and preventing its interaction with platelets. It is also very tantalizing to postulate that platelets hyperactivity in pathologies like type 2 diabetes can result from deficiencies in intraplatelet Tβ4. The consequences of this would be that more actin would be polymerized in the resting platelet and less Tβ4 would be released into the blood during platelet activation to modulate the inhibitory phase by binding to fibrinogen thus resulting in platelet hyperactivity.

Conclusions

These results suggest that Tβ4 could potentially increase the affinity of platelet receptors for their ligands thus promoting platelet deposition. Tβ4 could also bind to fibrinogen and as its concentration increased would prevent platelet–fibrinogen interactions resulting in the attenuation of platelet deposition. This work suggests that Tβ4 might have a dual role in platelet function.

References

Fox JE. The platelet cytoskeleton, Thromb. Haemost. 1993; 70: 884–893.

Goldstein AL, Hannappel E and Kleinman HK. Thymosin beta4: actin-sequestering protein moonlights to repair injured tissues. Trends Mol. Med. 2005; 11: 421–429.

Goodall GJ, Hempstead JL and Morgan JI. Production and characterization of antibodies to thymosin beta 4. J. Immunol. 1983; 131: 821–825.

Goodall GJ, Morgan JI and Horecker BL. Thymosin beta 4 in cultured mammalian cell lines. Arch. Biochem. Biophys. 1983; 221: 598–601.

Hannappel E and Leibold W. Biosynthesis rates and content of thymosin beta 4 in cell lines. Arch. Biochem. Biophys. 1985; 240: 236–241.

Hannappel E and Van Kampen M. Determination of thymosin beta 4 in human blood cells and serum. J. Chromatogr. 1987; 397: 279–285.

Hannappel E, Davoust S and Horecker BL. Thymosins beta 8 and beta 9: two new peptides isolated from calf thymus homologous to thymosin beta 4. Proc. Natl. Acad. Sci. U. S. A. 1982; 79: 1708–1711.

Hannappel E, Xu GJ, Morgan J, Hempstead J and Horecker BL. Thymosin beta 4: a ubiquitous peptide in rat and mouse tissues. Proc. Natl. Acad. Sci. U. S. A. 1982; 79: 2172–2175.

Ho JH, Tseng KC, Ma WH, Chen KH, Lee OK, Su Y. Thymosin beta 4 upregulates anti oxidative enzymes and protects human corneal epithelial cells against oxidative damage. Br. J. Opthalmol. 2008; 92:992-997

Huff T, Muller CGS, Otto AM, Netzker R and Hannappel E. β-Thymosins, small acidic peptides with multiple functions. Int. J. Biochem. Cell Biol. 2001; 33 : 205–220.

Huff T, Otto AM, Muller CS, Meier M and Hannappel E. Thymosin beta4 is released from human blood platelets and attached by factor XIIIa (transglutaminase) to fibrin and collagen. FASEB J. 2002; 16: 691–696.

Lin SC and Morrison-Bogorad M. Developmental expression of mRNAs encoding thymosins beta 4 and beta 10 in rat brain and other tissues. J. Mol. Neurosci. 1990; 2: 35–44.

Low TL and Goldstein AL. Chemical characterization of thymosin beta 4. J. Biol. Chem. 1982; 257: 1000–1006.

Low TL, Hu SK and Goldstein AL. Complete amino acid sequence of bovine thymosin beta 4: a thymic hormone that induces terminal deoxynucleotidyl transferase activity in thymocyte populations. Proc. Natl. Acad. Sci. U. S. A. 1981; 78: 1162 1166.

Makogonenko E, Goldstein AL, Bishop PD and Medved L. Factor XIIIa incorporates thymosin beta4 preferentially into the fibrin(ogen) alphaC-domains. Biochemistry 2004; 43: 10748–10756.

Miersch S, Sliskovic I, Raturi A and Mutus B. Antioxidant and antiplatelet effects of rosuvastatin in a hamster model of prediabetes. Free Radic. Biol. Med. 2007; 42: 270–279.

Miyaki K, Zeng HL, Nakagama T and Uchiyama K. Steady surface modification of polydimethylsiloxane microchannel and its application in simultaneous analysis of homocysteine and glutathione in human serum. J. Chromatogr. A 2007; 1166: 201–206.

Safer D, Elzinga M and Nachmias VT. Thymosin beta 4 and Fx, an actin-sequestering peptide, are indistinguishable. J. Biol. Chem. 1991; 266: 4029–4032.

Santos SM, Klinkhardt U, Schneppenheim R and Harder S. Using ImageJ for the quantitative analysis of flow-based adhesion assays in real-time under physiologic flow conditions. Platelets 2010; 21 (1): 60-66.

Schafer AI and Loscalzo J. Thrombosis and hemorrhage. Lippincott Williams & Wilkins, Hagerstwon, MD. 2003: 397.

Smart N and Riley PR. Derivation of epicardium-derived progenitor cells (EPDCs) from adult epicardium. Curr. Protoc. Stem Cell Biol. 2009 Chapter 2 Unit2C 2.

Sosne G, Hafeez S, Greenberry AL II and Kurpakus-Wheater M. Thymosin beta4 promotes human conjunctival epithelial cell migration. Curr. Eye Res. 2002; 24: 268–273.

Sosne G, Qiu P, Goldstein AL and Wheater M. Biological activities of thymosin {beta} 4 defined by active sites in short peptide sequences. FASEB J. 2010; 24 (7): 2144 2151.

Sun W and Kim H. Neurotrophic roles of the beta-thymosins in the development and regeneration of the nervous system. Ann. N. Y. Acad. Sci. 2007; 1112: 210–218.

Young JD, Lawrence AJ, MacLean AG, Leung BP, McInnes IB, Canas B, Pappin DJ and Stevenson RD. Thymosin beta 4 sulfoxide is an anti-inflammatory agent generated by monocytes in the presence of glucocorticoids. Nat. Med. 1999; 5: 1424–1427.

Yu FX, Lin SC, Morrison-Bogorad M and Yin HL. Effects of thymosin beta 4 and thymosin beta 10 on actin structures in living cells. Cell Motil. Cytoskeleton 1994; 27: 13–25.

CHAPTER 5

Thymosin beta 4 alleviates endoplasmic reticulum stress in retinal pigment epithelial cells

Introduction

Endoplasmic reticulum (ER) stress is caused by the accumulation of unfolded proteins in the endoplasmic reticulum lumen. It has been implicated in the pathogenesis of many neurodegenerative diseases including Alzheimer's, Parkinson's and Huntington's disease (Li *et al* 2008). All of these diseases are similar to age related macular degeneration (AMD) in various pathological features. It has been recently proposed that ER stress might have an important role in the pathogenesis of AMD (Salminen *et al* 2010). It has also been shown to play a critical role in the early stages of diabetic retinopathy progression (Li *et al* 2009). ER stress has been triggered by chronic ocular hypertension in glaucoma mouse models, which leads to retinal ganglion cell death (Doh *et al* 2010).

The retinal pigment epithelium (RPE) is a monolayer of pigmented simple cuboidal cells, which performs many functions essential for vision. The basolateral membrane of the RPE faces the Bruch's membrane and the apical membrane faces the photoreceptor outer segments. RPE has many critical functions including transport of nutrients (Vitamin A and C) from blood to retina, phagocytosis of the shedded photoreceptor membranes, setting up the ion gradients within the interphotoreceptor matrix and building up the blood-retina barrier. RPE dysfunction is central to the development of AMD.

Age related macular degeneration (AMD) is the leading cause of loss of central vision in elderly individuals. AMD is characterized by morphological and functional abnormalities in RPE cells (Binder *et al* 2007). The pathogenesis of AMD involves the buildup of drusen between Bruch's membrane and RPE and accumulation of lipofuscin, a pigmented aggregate of proteins and lipids, in RPE. Subretinal neovascularization, which occurs due to VEGF overexpression in the RPE, is a major development of AMD. Recently, it has been shown that ER stress causes increased expression of VEGF (Roybal *et al* 2005).

Oxidative stress is a very important factor in the progression and onset of AMD and can initiate ER stress in RPE (Beatty *et al* 2000, He *et al* 2008). It has been recently proposed that ER stress might play an important role in the pathogenesis of AMD (Libby *et al* 2010).

Thymosin β 4 (Tβ4) is a water-soluble, 43 amino acid polypeptide with a

molecular weight of 4.9kDa (Low *et al* 1981; Yu *et al* 1994). It is a major G actin sequestering protein in mammalian cells. Tβ4 has diverse biological roles including angiogenesis, cell migration, tissue protection, and regeneration in skin, eyes and heart. It has been previously reported that Tβ4 decreases inflammation and promotes wound healing in corneal epithelial cells (Sosne *et al* 2002). Internalization of Tβ4 has been reported in human corneal epithelial cells, HUVEC, bovine corneal endothelial cells and human bone marrow-derived mesenchymal stem cells (Grant *et al* 1999; Ho *et al* 2007).

Herein we hypothesize that ER stress might play an important role in the RPE damage during AMD and that Tβ4 can mitigate those effects. In the present study, we report that Tβ4 can alleviate ER stress in retinal pigment epithelial cells.

Experimental methods

Cell Culture and treatment

Human retinal pigment epithelium cell line ARPE 19 was obtained from ATCC. Cells were grown in 1:1 mixture of Dulbecco's Modified Eagle's Medium with Ham's F-12 nutrient medium (DMEM F-12; ATCC, USA), 10% fetal bovine serum (FBS, Sigma, Canada) and penicillin – streptomycin (Gibco, Canada). The cells were either plated on coverslips in 35 mm plates or in 100 mm plates and were incubated at 37°C in 5% CO_2 to reach ~70% confluence before the experiments. The ARPE 19 cells were incubated with either 0.2μM or 2μM of Tβ4 for 1 hour before inducing ER stress by adding 500 μM palmitate (Sigma, Canada) in 0.5% BSA (Sigma, Canada). The cells were then incubated at 37°C in 5% CO_2 for 24 hours.

Cell viability

Cell viability was determined by annexin V and trypan blue staining. For Trypan Blue exclusion, cells were seeded in 6 well plates (100,000 cells/well) and grown overnight. The cells were treated with Tβ4 and palmitate as described before. After 24 hour incubation, the cells were trypsinized and 100μl of the cell suspension was incubated with an equal volume of 0.4% Trypan blue solution (Gibco, Canada) for 2 min. Cells were counted using a hemocytometer on a light microscope, where live cells excluded Trypan Blue staining. For annexin V staining, an annexin V staining kit (BD Biosciences) was used. ARPE 19 cells were grown on coverslips in 35mm cell culture plates. The adherent cells were incubated with annexin V and propidium iodide (PI) for 15 min. The cells were fixed with 3% paraformaldehyde, washed with PBS and viewed under fluorescence microscope with a dual filter set for FITC (Annexin V) and rhodamine (PI).

Intracellular ROS production

The dye H_2DCFDA dye is used to detect intracellular ROS. ARPE 19 cells grown on coverslips were incubated with H_2DCFDA for 30 min at 37°C. The cells were washed with PBS 3X and viewed under fluorescence microscope with excitation at 488nm and emission at 530nm.

Cholesterol detection

Cholesterol estimation was done by using filipin (Sigma, Canada). For filipin staining, the cells were fixed in 3% paraformaldehyde for 30 min and were then washed 3 times with PBS. The fixed cells were incubated with 0.05mg/mL filipin (Sigma, Canada) for 1 hr in dark. After incubation, the cells were washed 3X PBS and slides were mounted on slides with fluoromount G (Southern Biotech). The slides were viewed under a fluorescent microscope using a UV filter with excitation at 340-380 nm and emission at 385-470 nm. To detect cholesterol, ARPE 19 cells were also stained with 750 nM PFO-D4-GFP for 30 min at 37 °C and 5% CO_2. The cells were washed three times with HEPES buffer and images were taken on an Axiovert fluorescence microscope with 535 nm/550 nm excitation/emission.

Nitric oxide measurement

ARPE-19 cells were seeded at a density of $2X10^5$ cells in a 10cm plate and were used after they reached ~90% confluence. The cells were pretreated with Tβ4 for one hour and then incubated in the presence of palmitate for 24 h. After the termination of the treatment times, media was aspirated and fresh media was added. The cells were incubated again and after 1 hr, 200 uL of media was withdrawn with a Hamilton gastight syringe and directly injected into the purge vessel of a Sievers Nitric Oxide Analyzer (Model 280i) which contained acetic acid and sodium iodide. A portion of NO produced by ARPE 19, is oxidized by oxygen to form nitrite in the media. The acidified iodide in the purging chamber of the NOA then reduces nitrite to NO. To further determine changes in NO production, ARPE 19 cells were incubated with cell culture medium containing 5 μM , 4,5-diaminofluorescein diacetate (DAF-DA , Invitrogen) at 37°C in a 95% air/5% CO_2 incubator for 30 min. Cells were then washed 3X with phosphate buffered saline (PBS) and mounted on the stage of an Axiovert 200 inverted fluorescence microscope. DAF-DA fluorescence was monitored using excitation and emission wavelengths of 485 and 538 nm, respectively.

Immunofluorescence

ARPE-19 cells were grown on coverslips in 35mm cell culture dishes. For the study of nuclear translocation of NF-κB, cells were incubated with 500μM palmitate for 24 hours,

with or without Tβ4 pretreatment. After incubation, the cells were washed with PBS and fixed in ice cold ethanol for 10 min. Rabbit polyclonal antibody against the p65 subunit of NFκB (1:200 dilution; Abcam) was used as the primary antibody. Alexa Fluor 488 - labeled goat anti-rabbit IgG was used as a secondary antibody (1:500 dilution; Santa Cruz Biotechnology). Preparations were mounted in Fluoromount G and examined by fluorescence microscopy.

Nuclear and cytoplasmic fractions

After treatments, ARPE-19 cells were trypsinized, resuspended and homogenized in buffer A (10 mM HEPES pH 7.8, 10 mM KCl, 1.5 mM $MgCl_2$, 0.5% Nonidet P-40, 1 mM dithiothreitol (DTT) and protease inhibitor cocktail (Sigma)). Nuclei and cytosolic fractions were separated by centrifugation at 1000*g* for 20 minutes. The cytosolic fractions (supernatant) were stored at −80°C until further analysis. The nuclear fractions (pellets) were resuspended in buffer B (5mM HEPES pH 7.8, 1.5mM $MgCl_2$, 0.2mM EDTA, 1mM DTT, 26% glycerol, 300mM NaCl pH 7.8 and protease inhibitor cocktail). Nuclei were extracted for 30 min at 4°C. Soluble nuclear fractions were obtained by centrifuging at 12,000*g* for 10 min. Supernatants (nuclear extracts) were stored at −80°C until further NFκB analysis. Protein concentration was determined by the BCA method.

Western blots

Proteins were extracted from ARPE 19 cells with lysis buffer (10g/L sodium deoxycholate, 1% Triton X, 0.01% SDS, 150mM NaCl, 50mM Tris pH 7.5, 0.05 mM EDTA, 50mM NaF, 10mM sodium pyrophosphate, 0.5mM sodium peroxyvanadate and protease inhibitor cocktail). Protein concentration was determined by the BCA method. 10 μg of protein samples were resolved in 10% sodium dodecyl sulfate–polyacrylamide gel and transferred onto polyvinylidene fluoride (PVDF) membranes. Membranes were probed with primary antibodies against anti-rabbit eNOS (1:1000; Abcam), anti-rabbit phospho-eNOS (1:1000; Cell Signalling), anti-rabbit p65 subunit of NFκB (1:1000; Abcam), anti-rabbit Grp78 (1:1000; Abcam), anti-mouse PDI (1:1000, Abcam), anti-rabbit Topo II (1:500; Santa Cruz) and anti-mouse actin (1:5000; Abcam). Membranes were then incubated with HRP-conjugated anti-rabbit and anti-mouse secondary

antibodies (1:2000; Abcam) for 1 h and visualized using enhanced chemiluminescence reagent (Pierce, USA).

Statistical analysis and images

Data is expressed as an average of all trials and statistical analysis was performed by Student's t-test. The error bars represent standard deviation. The images were captured with a Zeiss Axiovert fluorescence microscope and analyzed using Northern Eclipse.

RESULTS

Cell viability

The cells under ER stress for prolonged periods eventually undergo apoptosis. Apoptosis is detected by the flipping of phosphatidylserine from the inner leaflet of the plasma membrane to the outer leaflet. We determined the viability of the cells using FITC-Annexin V, which binds to phosphatidylserine and detects apoptosis. PI was used to stain the nucleus of viable cells. As shown in Fig. 1A, no apoptotic signal is observed in controls and cells pretreated with 2 μM Tβ4. Very little annexin V binding is seen in cells which were under ER stress (no Tβ4 pretreatment) and those pretreated with 0.2μM Tβ4. The trypan blue exclusion assay showed that ~92% cells were viable in the controls; however the cell viability decreased to ~78% in palmitate treated cells. The ARPE 19 cells which were pretreated with 0.2 μM and 2 μM Tβ4 had 80% and 82% viable cells respectively (Fig. 1B). These results illustrated that after induction of ER stress for 24 hours, the cells are still viable and healthy and can be used for the subsequent studies.

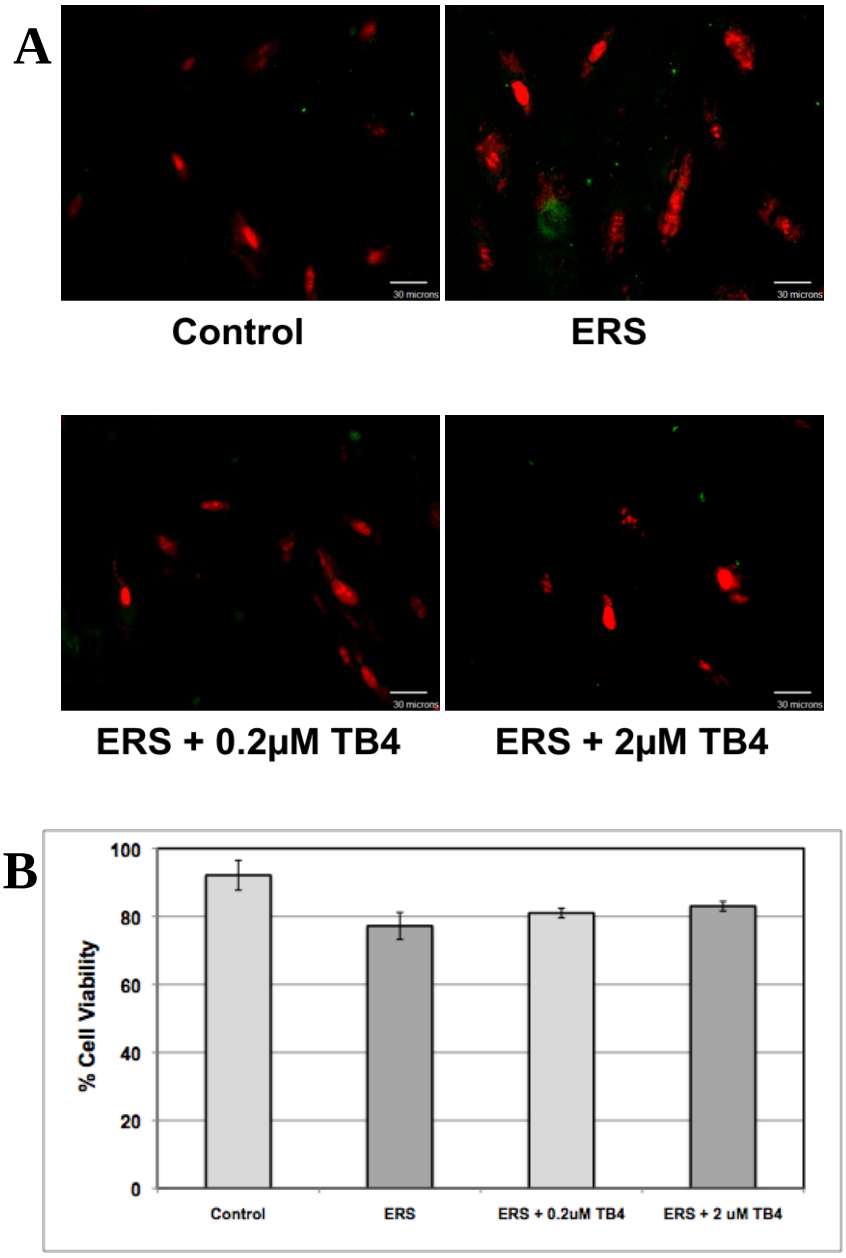

Figure 1 – Detection of apoptosis and cell viability in ARPE 19 cells treated with palmitate with or without Tβ4.

ARPE 19 cells were treated with 500 μM palmitate in the presence and absence of Tβ4 concentrations as indicated. (A) After 24 hours, cells were stained with PI (red) and apoptotic cells were detected by Annexin V staining (green). Images were taken of a minimum of five different fields in a slide using a 40X oil immersion objective. (B) ARPE 19 cells were treated with palmitate and Tβ4 as described before. Live and dead cells were determined using the trypan blue exclusion assay. The results are presented as percentage of cell viability. Data is shown as mean ± S.D (n=4).

Induction of ER stress markers by palmitate

Grp78 and PDI are very important markers for ER stress induction. These molecular chaperones are upregulated in response to ER stress. As shown in Figure 2, palmitate treatment upregulated expression of Grp78 and PDI proteins which indicates induction of ER stress. The Grp78 protein levels are brought down to normal (almost similar to controls) when ARPE 19 cells were pretreated with 0.2 μM Tβ4 before inducing ER stress.

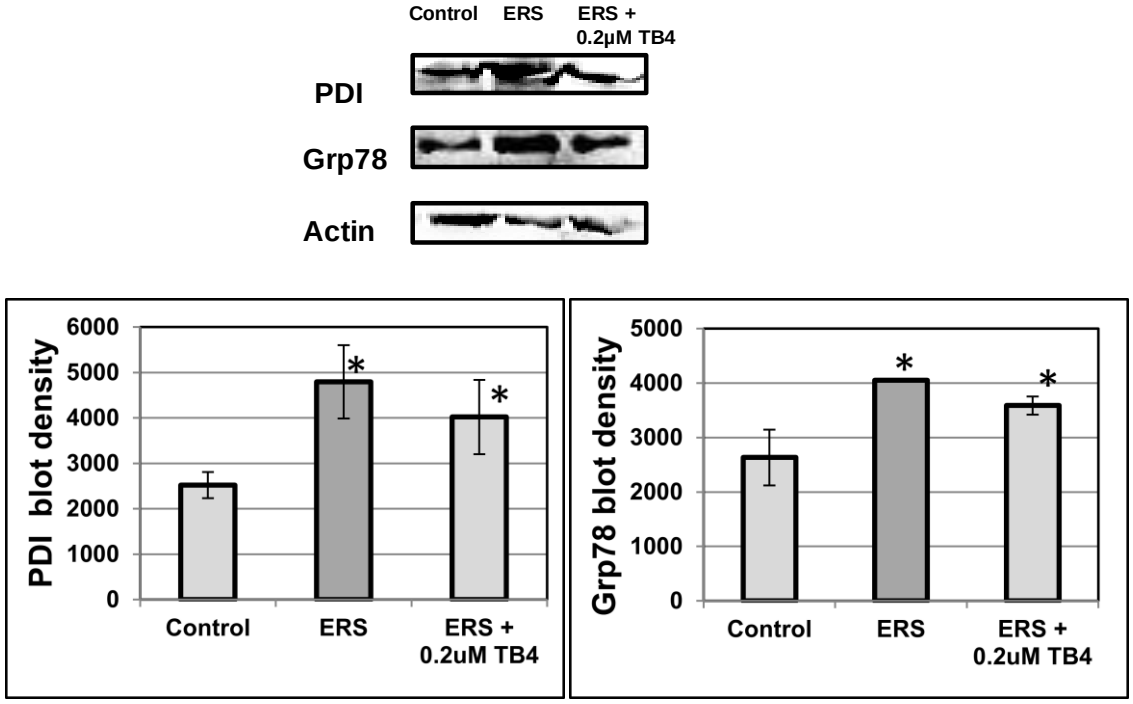

Figure 2 – Expression of ER stress markers, Grp78 and PDI, in ARPE 19 cells treated with palmitate in the presence or absence of Tβ4.

ARPE 19 cells were treated with 500 μM palimate with or without Tβ4 for 24 hours. Expression of Grp78 and PDI was determined from the cell lysates separated by SDS-PAGE. The blots were probed with anti-rabbit Grp78 antibody and anti-mouse PDI antibodies. Upper and middle panels show PDI and Grp78 expression in response to ER stress and Tβ4 pretreatment and the lower panel shows actin, which was used as a loading control. The graphs depict the blot densities determined by using Image J (n=3); * $P < 0.05$.

Tβ4 attenuates ER stress induced cholesterol production

ER stress is known to increase cholesterol levels in cells. Increased cholesterol accumulation in RPE has also been associated with the pathogenesis of AMD (Curcio *et al* 2005). The cholesterol determinations in ARPE-19 indicated that there was a ~4.5 fold increase in cholesterol in cells under ER stress as compared to controls, however, treating the cells with 0.2μM Tβ4 before ER stress induction significantly reduced cholesterol levels by ~20%. Pretreatment with 2μM Tβ4 further decreases the cholesterol levels by ~27% (Figure 3).

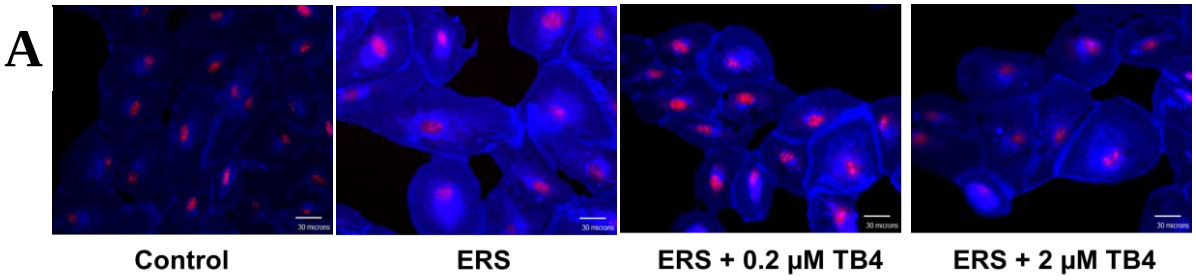
A
Control
ERS
ERS + 0.2 μM TB4
ERS + 2 μM TB4

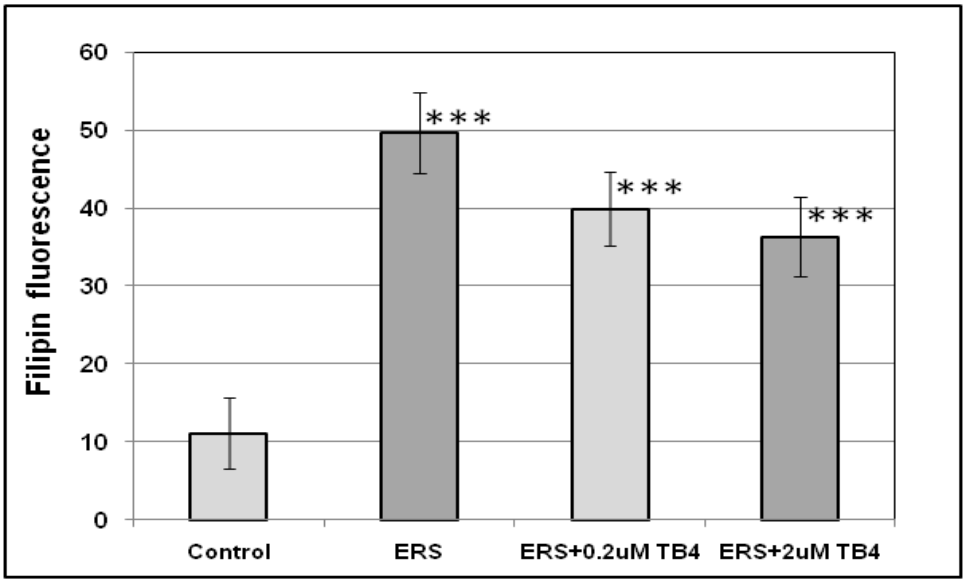
Filipin fluorescence
60
50
40
30
20
10
0
***
***
***
Control
ERS
ERS+0.2uM TB4
ERS+2uM TB4

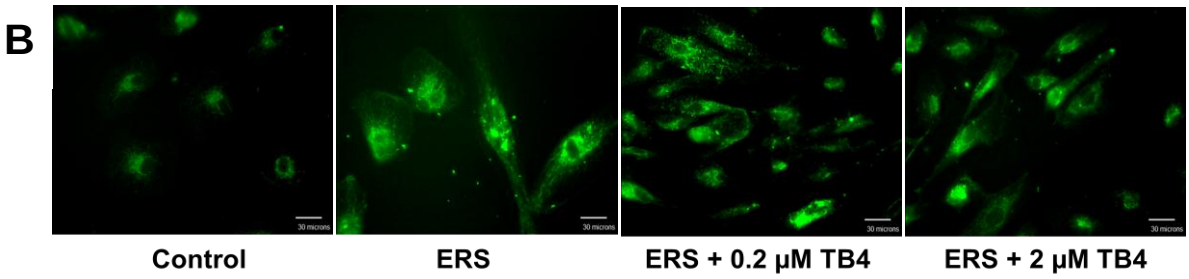
B
Control
ERS
ERS + 0.2 μM TB4
ERS + 2 μM TB4

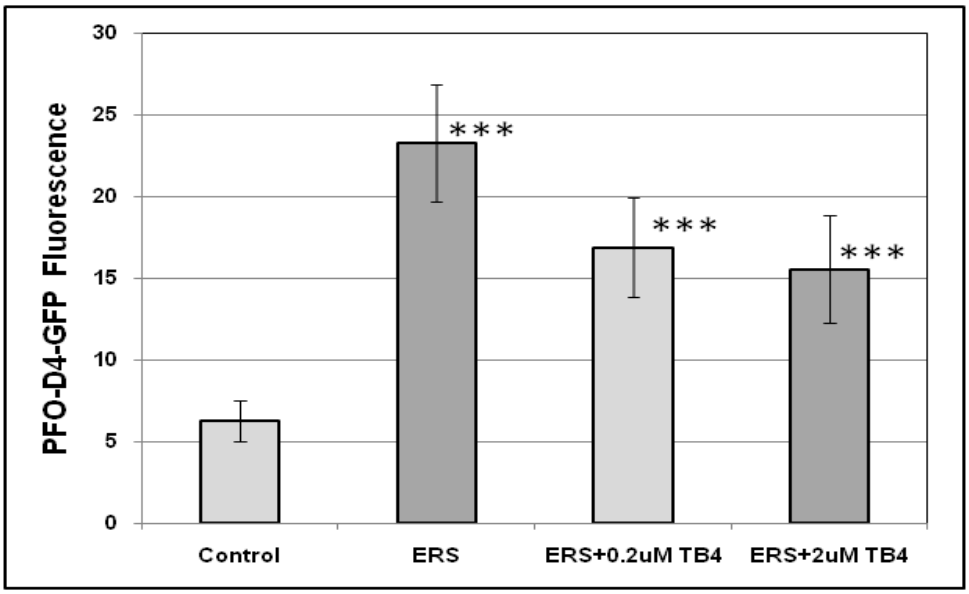

Figure 3 – Effect of Tβ4 pretreatment on cholesterol in retinal pigment epithelial cells under ER stress.

ARPE 19 cells were treated with palmitate for 24 hours, in the presence or absence of Tβ4. (A) The cells fixed with 3% paraformaldehye were stained with filipin (blue) and PI (red) and examined by fluorescence microscope. Filipin stains intracellular cholesterol and PI stains the nucleus. The pictures were captured using 40X oil immersion objective The graph depicts average fluorescence of filipin from four separate experiments (± SD); *** $P < 0.001$. (B) Cholesterol was also estimated by staining with PFO-D4-GFP. After treatment, the cells were incubated with PFO-D4-GFP at room temperature. After 30 min incubation, the cells were fixed with 3% paraformaldehyde and visualized under fluorescence microscope using 40 X oil immersion objective. The graph represents average fluorescence of PFO-D4-GFP ± SD (n=4); *** $P < 0.001$.

Tβ4 pretreatment decreases ER stress induced ROS production

Oxidative stress is associated with the onset of ER stress and is one of the most important factors associated with the progression of AMD. H_2DCFA, a cell permeable dye which incorporates into the hydrophobic regions of the cell, was used for this purpose. The cellular esterases cleave the acetate moiety leaving impermeant, non-fluorescent, 2′,7′-dichlorodihydrofluorescein (H_2DCF), which is oxidized by reactive oxygen species to fluorescent dichlorofluorescein (DCF**)**. To determine whether Tβ4 has the ability to reduce reactive oxygen species (ROS) formation after induction of ER stress, the levels of ROS were determined. It can be clearly seen in Figure 4 that ER stress increased ROS production by ~ 4 fold. Pretreatment with 0.2μM Tβ4 decreased ROS production by ~ 42%. Higher concentration of Tβ4 (2μM) was able to reduce ROS formation by ~ 57%.

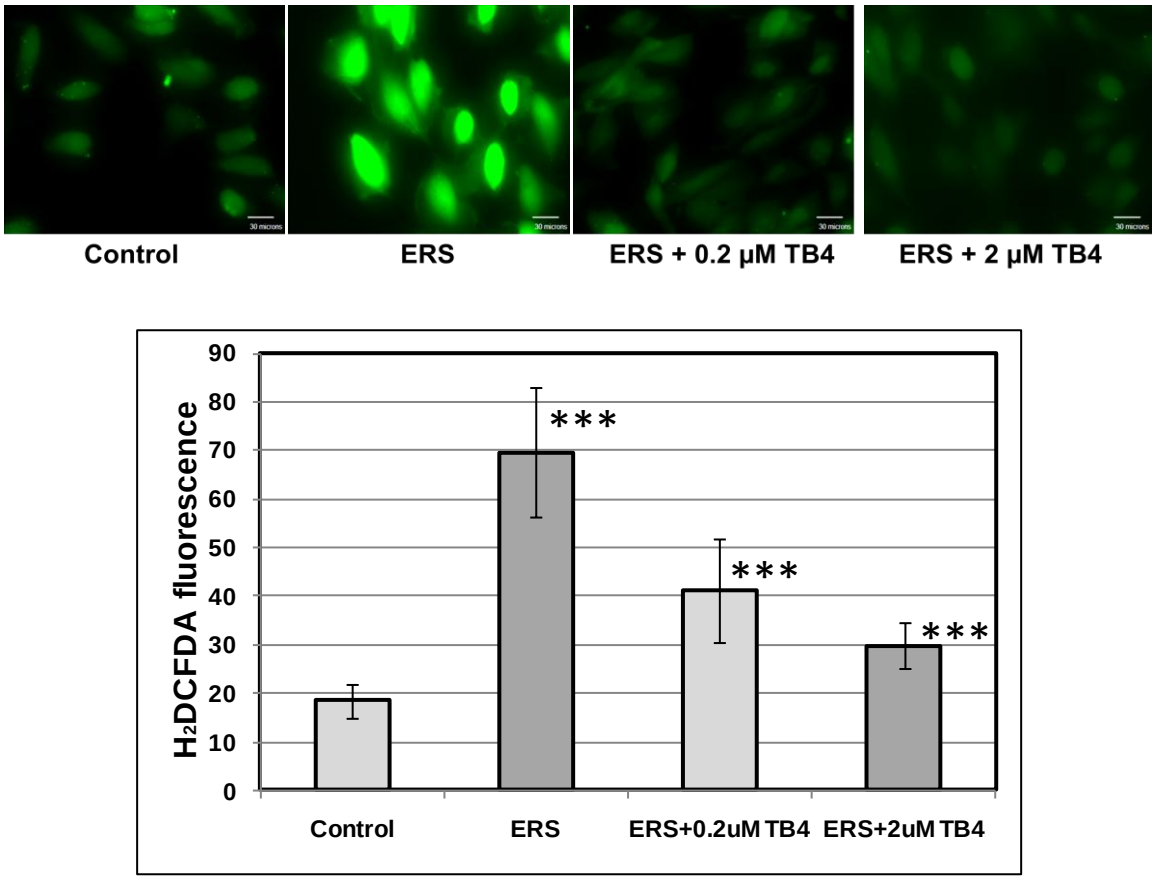

Figure 4 – Effect of Tβ4 pretreatment on intracellular ROS production in ER stress induced retinal pigment epithelial cells.

ARPE 19 cells were incubated with 500 µM ER stressor palmitate, with or without Tβ4 (0.2µM or 2 µM) for 24 hours. The cells were analyzed for intracellular ROS using H_2DCFDA. The fluorescence (green) is generated by the oxidized product of H_2DCFDA, which indicates ROS formation. The graph shows an average of H_2DCFDA fluorescence and the results are an average of five different set of experiments (n=4); *** $P < 0.001$. Pictures were taken using 63X objective.

Tβ4 promotes nitric oxide production and eNOS phosphorylation

The palmitate treated cells were compared with the controls and Tβ4 pre treated cells with respect to nitric oxide production. The nitric oxide was determined in the media, which is an indirect method to analyze changes in nitric oxide production by cells. ER stressor palmitate decreased nitric oxide production by ~ 55%, but NO production was upregulated by ~ 88% in the cells which were treated with Tβ4 before inducing ER stress as compared to cells under ER stress (Figure 5A). To further verify the role of Tβ4 in nitric oxide production, eNOS expression and phosphorylation was determined. The activity of eNOS is increased by its phosphorylation at Ser 1177. As illustrated in Figure 5C, there is no significant difference in the expression of eNOS in palmitate treated cells as compared to the control and Tβ4 pretreated cells. eNOS phosphorylation decreased after induction of ER stress by palmitate, whereas pretreatment with 0.2μM Tβ4 upregulated the phosphorylation of eNOS.

A

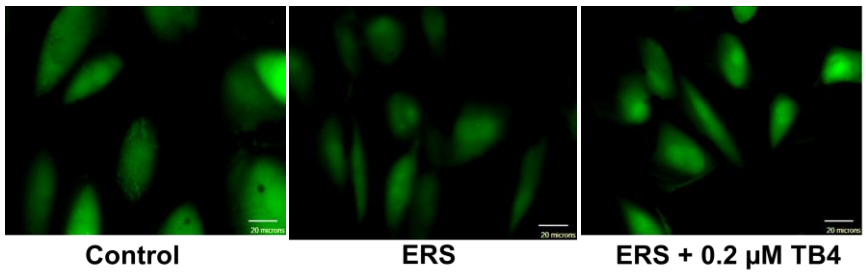
Control
ERS
ERS + 0.2 μM TB4

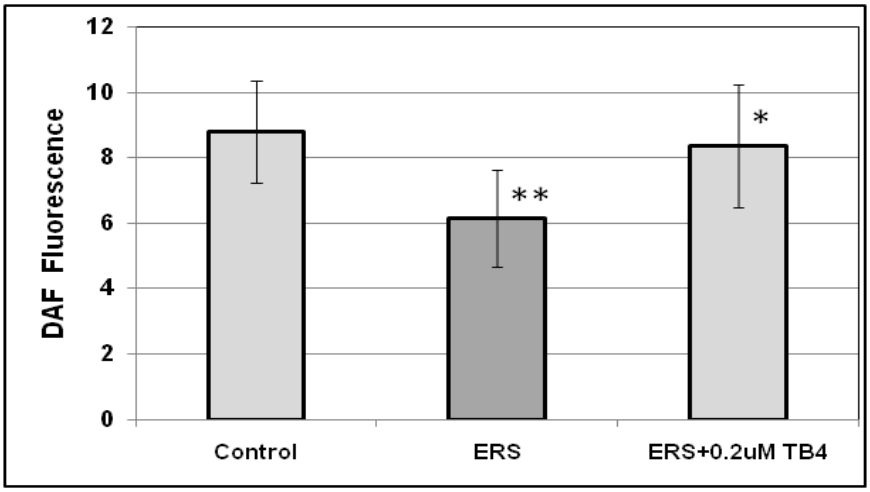
DAF Fluorescence
12
10
8
6
4
2
0
**
*
Control
ERS
ERS+0.2uM TB4

B

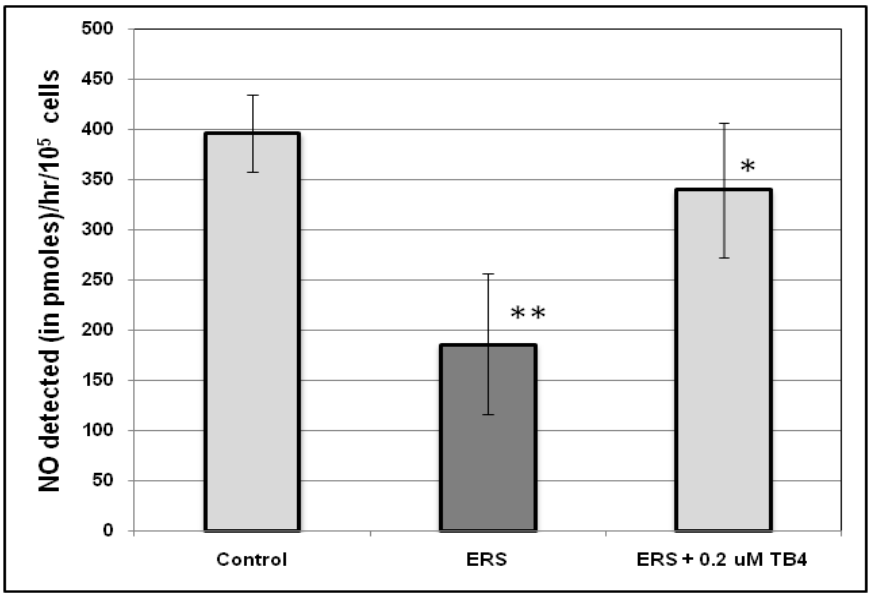
NO detected (in pmoles)/hr/10^5 cells
500
450
400
350
300
250
200
150
100
50
0
**
*
Control
ERS
ERS + 0.2 uM TB4

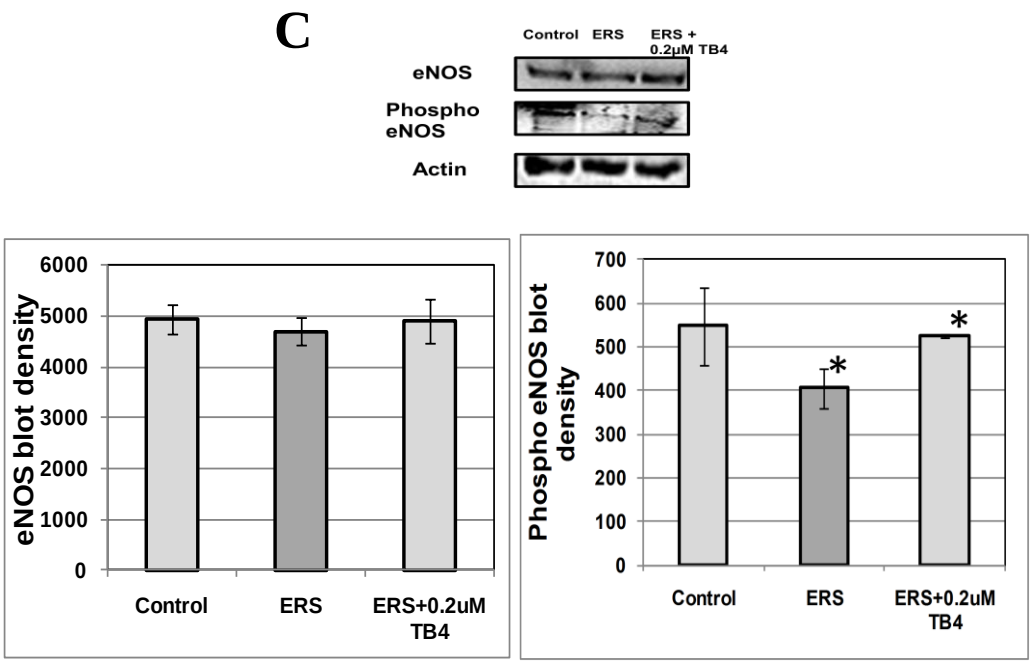

Figure 5 – Effect of Tβ4 on nitric oxide production, eNOS expression and phosphorylation in retinal pigment epithelial cells under ER stress.

The ARPE 19 cells were treated with palmitate in the presence or absence of Tβ4 as previously described. (A) After 24 hours, the cells were stained with 5μM DAF-DA for 30 min. The cells were washed with PBS and viewed under Zeiss Axiovert fluorescence microscope using a 20X objective. The graph shows average intensity of DAF-DA fluorescence from three independent experiments (± SD); * $P < 0.05$; ** $P < 0.01$. (B) Total nitrite was measured for retinal pigment epithelial cells treated with palmitate for 24 hours with or without Tβ4. After treatment, the cell culture media was replaced with fresh media and the cells were incubated again for 1 hour. The data shown is representative of three different experiments (± SD); * $P < 0.05$; ** $P < 0.01$. (C) The expression of eNOS and its phosphorylation at Ser 1177 was estimated from western blots using cell lysates of control, cells under ER stress and cells treated with 0.2 μM Tβ4 before inducing ER stress. The blots were probed with eNOS and Ser1177 phospho eNOS antibodies. Actin was used as a loading control. The graph represents blot densities of eNOS and phospho eNOS which were quantified using Image J software.

Tβ4 reduces nuclear localization of NFκB

ER stress activates and induces the nuclear translocation of the transcription factor NFκB (Pahl *et al* 1995; Kaneko *et al* 2003). As demostarted in Figure 6A, the immunofluorescence staining of the p65 subunit of NFκB in control cells shows cytoplasmic distribution. Incubation with ER stressor palmitate predominantly relocates NFκB to the nucleus; however when the ER stressed cells were pretreated with 0.2 μM and 2 μM Tβ4, this nuclear translocation was decreased, with large amounts of the p65 subunit being in the cytoplasm.

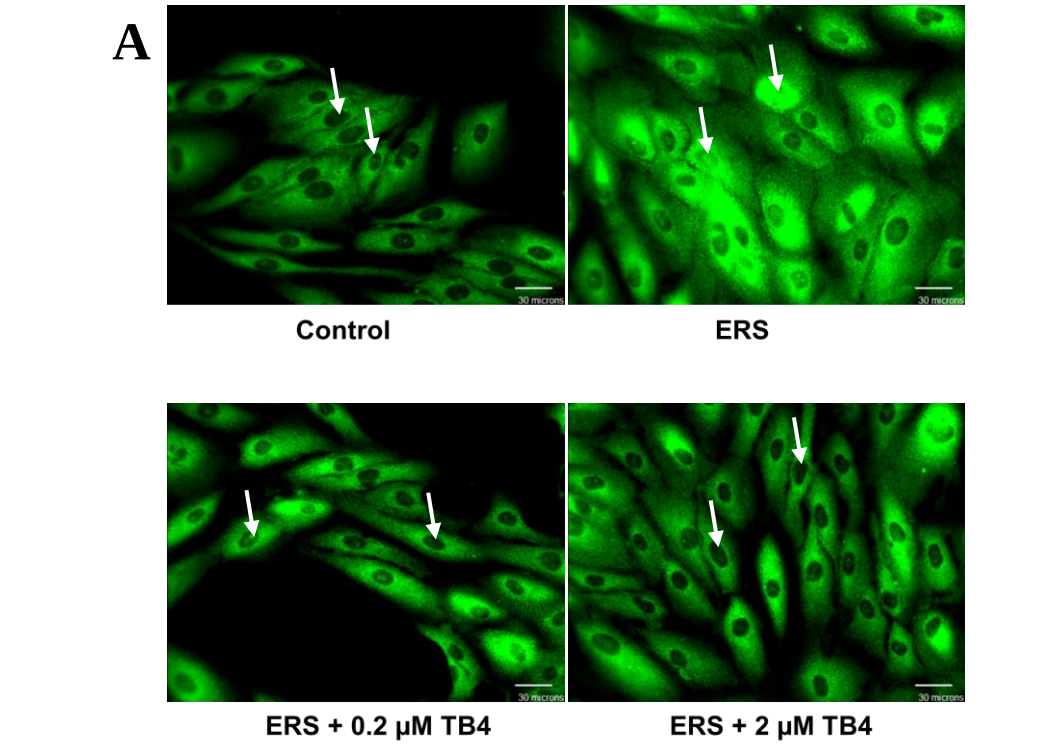
A
Control
ERS
ERS + 0.2 μM TB4
ERS + 2 μM TB4
B
ERS+ 2μM TB4
ERS+ 0.2μM TB4
ERS
Control
NFκB
Actin
Topo II
Nuclear fraction
Cytoplasmic fraction

Figure 6 – NFκB localization in response to ER stress and Tβ4 pretreatment.

(A) ARPE 19 cells were cultured on glass coverslips and treated with 500μM palmitate with or without 0.2μM Tβ4 and 2μM Tβ4. The cells were fixed with ethanol and FITC conjugated goat anti-rabbit secondary antibody was used to detect the p65 subunit of NFκB. Nuclear localization of NFκB is shown by arrows. Images were taken at 40X oil immersion objective. (B) Nuclear localization of NFκB was further detected by Western blots of nuclear and cytoplasmic fractions. Relative levels of NFκB in nuclear fractions were determined. There is a significant increase in nuclear NFκB protein in cells under ER stress. Pretreatment with Tβ4 decreases NFκB localization to the nucleus in a concentration dependent manner. Actin was used as a control for cytoplasmic fractions and Topo II was used as a control for nuclear fractions.

Discussion

RPE dysfunction is one of the key factors involved in the progression of AMD. Retina and RPE are under constant oxidative stress due to high metabolic activity, oxygen consumption and light absorption. The fluctuations in the redox environment and ROS production leads to disturbances in the ER hence causing ER stress (Lai E *et al* 2007). ER stress has been proposed to be an important parameter involved in the pathogenesis of AMD. A recent study has shown increased expression of tight junctions in retinal pigment epithelial cells *in vitro*. This has been shown to alter the function of RPE cells which might be involved in AMD (Yoshikawa *et al* 2011). However, not many studies have foccussed on the effects of ER stress on RPE cells so far.

Tβ4 is a major actin sequestering protein which plays an important role in various other physiological processes. It decreases cytochrome c release from the mitochondria and also increases the expression of anti-apoptotic gene, bcl-2 (Sosne *et al* 2005). Previous studies have illustrated the role of Tβ4 in decreasing inflammation (Sosne *et al* 2002) and preventing apoptosis (Ho *et al* 2010).

In the present study, we illustrated the effects of ER stress on retinal pigment epithelial cells and the ability of Tβ4 to alleviate ER stress in RPE. ER stress disrupts protein folding in the endoplasmic reticulum leading to accumulation of unfolded proteins. An unfolded protein response (UPR) is initiated in order to maintain cell homeostasis. UPR upregulates expression of chaperone proteins in order to augment the protein folding capacity of the ER. When UPR is not able to alleviate ER stress, it initiates an apoptotic signaling pathway, which involves JNK and caspases (Harding *et al* 2002; Kaufman *et al* 2002).

In this study, we evaluated the expression of molecular chaperones in retinal pigment epithelial cells, in response to ER stress. Grp78 and PDI protein expression were upregulated in the cells treated with palmitate, however, Tβ4 decreases the expression of these chaperones (Fig. 2). The ability of Tβ4 to decrease Grp78 and PDI levels indicates its potential role in protecting the cells against ER stress.

The role of oxidative stress in RPE dysfunction and AMD pathogenesis is very well known. Previous reports have also linked oxidative stress with ER stress and RPE dysfunction. The role of ER stress in RPE neovascularization in AMD has also been

implicated (He *et al* 2008; Libby *et al* 2010). It has been demonstrated in a previous study that there is accumulation of free and esterified cholesterol in the RPE of AMD patients (Lakkaraju *et al* 2007; Curcio *et al* 2005). The results of our study showed that Tβ4 pretreatment decreases cholesterol production, which accumulates as a result of ER stress (Fig. 3). Oxidative stress, which occurs due to excessive ROS formation, plays a very important role in RPE dysfunction. It is illustrated by our results that Tβ4 is able to reduce intracellular ROS in RPE and hence protect the cells from oxidative damage.

We next determined the effect of Tβ4 on NO formation. Previous reports have suggested that there is less production of nitric oxide in the eyes of AMD patients (Bhutto *et al* 2010). In the present study, we demonstrate that Tβ4 is capable of upregulating NO production in cells under ER stress, however, when levels of eNOS were determined, there was no significant difference in its expression in treated versus untreated cells. There was, however a significant difference in the phosphorylation of eNOS at Ser1177, in the cells which were pretreated with Tβ4 before induction of ER stress (Fig 5). It has been previously reported that Tβ4 can increase eNOS phosphorylation at Ser1177 in endothelial progenitor cells (Qiu *et al* 2009). These results strongly suggest that Tβ4 is capable of increasing eNOS phosphorylation and hence NO production in ARPE 19 cells.

The induction of ER stress is also associated with the activation of the transcription factor NFκB. It is found in the cytoplasm but upon activation it translocates to the nucleus, where it further promotes the transcription of various pro-inflammatory genes and hence inflammatory signaling pathways. We further show that Tβ4 can also decrease nuclear localization of NFκB (Fig. 6). Our observations agree with a previous study done in corneal epithelial cells which showed that Tβ4 can minimize nuclear localization of NFκB after TNF-α stimulation (Sosne *et al* 2007).

Conclusions

In summary, the present preliminary study demonstrates the protective effects of Tβ4 in retinal pigment epithelial cells under ER stress. More work is required to be done in this field to determine the protective effects of Tβ4 in AMD and other retinal diseases.

References

Beatty S, Koh H, Phil M, Henson D and Boulton M. The role of oxidative stress in the pathogenesis of age-related macular degeneration. Surv Ophthalmol 2000; 45(2): 115-134.

Bhutto IA, Baba T, Merges C, McLeod DS, Lutty GA. Low nitric oxide synthases (NOSs) in eyes with age-related macular degeneration (AMD). Exp Eye Res; 90(1): 155-167.Binder S, Stanzel BV, Krebs I and Glittenberg C. Transplantation of the RPE in AMD. Prog Retin Eye Res 2007; 26(5): 516-554.

Curcio CA, Presley JB, Malek G, Medeiros NE, Avery DV, Kruth HS. Esterified and unesterified cholesterol in drusen and basal deposits of eyes with age-related maculopathy. Exp Eye Res 2005; 81(6): 731-741.

Doh SH, Kim JH, Lee KM, Park HY and Park CK. Retinal ganglion cell death induced by endoplasmic reticulum stress in a chronic glaucoma model. Brain Res 2010; 1308: 158-166.

Grant DS, Rose W, Yaen C, Goldstein A, Martinez J, Kleinman H. Thymosin beta4 enhances endothelial cell differentiation and angiogenesis. Angiogenesis 1999; 3(2): 125-135.

Harding HP, Calfon M, Urano F, Novoa I, Ron D. Transcriptional and translational control in the Mammalian unfolded protein response. Annu Rev Cell Dev Biol 2002; 18: 575-599.

He S, Yaung J, Kim YH, Barron E, Ryan SJ and Hinton DR. Endoplasmic reticulum stress induced by oxidative stress in retinal pigment epithelial cells. Graefes Arch Clin Exp Ophthalmol 2008; 246(5): 677-683.

Ho JH, Chuang CH, Ho CY, Shih YR, Lee OK, Su Y. Internalization is essential for the antiapoptotic effects of exogenous thymosin beta-4 on human corneal epithelial cells. Invest Ophthalmol Vis Sci 2007; 48(1): 27-33.

Ho JH, Su Y, Chen KH and Lee OK. Protection of thymosin beta-4 on corneal endothelial cells from UVB-induced apoptosis. Chin J Physiol. 2010 Jun 30; 53(3):190-5.

Kaneko M, Niinuma Y, Nomura Y. Activation signal of nuclear factor-kappa B in response to endoplasmic reticulum stress is transduced via IRE1 and tumor necrosis factor receptor-associated factor 2. Biol Pharm Bull 2003; 26(7): 931 935.

Kaufman RJ, Scheuner D, Schroder M et al. The unfolded protein response in nutrient sensing and differentiation. Nat Rev Mol Cell Biol 2002; 3(6): 411-421.

Lakkaraju A, Finnemann SC, Rodriguez-Boulan E. The lipofuscin fluorophore A2E perturbs cholesterol metabolism in retinal pigment epithelial cells. Proc Natl Acad Sci U S A 2007; 104(26): 11026-11031.

Lai E, Teodoro T and Volchuk A. Endoplasmic reticulum stress: signalling the unfolded protein response. Physiology (Bethesda) 2007; 22: 193-201.

Li JH, Walter P and Yen TSB. Endoplasmic reticulum stress in disease pathogenesis. Annu Rev Pathol Mech Dis 2008; 3: 26.

Li J, Wang JJ, Yu Q, Wang M and Zhang SX. Endoplasmic reticulum stress is implicated in retinal inflammation and diabetic retinopathy. FEBS Lett 2009; 583(9): 1521-1527.

Libby RT, Gould DB. Endoplasmic reticulum stress as a primary pathogenic mechanism leading to age-related macular degeneration. Adv Exp Med Biol 2010; 664: 403-409.

Low TL, Hu SK, Goldstein AL. Complete amino acid sequence of bovine thymosin beta 4: a thymic hormone that induces terminal deoxynucleotidyl transferase activity in thymocyte populations. Proc Natl Acad Sci U S A 1981; 78(2): 1162-1166.

Pahl HL, Baeuerle PA. A novel signal transduction pathway from the endoplasmic reticulum to the nucleus is mediated by transcription factor NF-kappa B. EMBO J 1995; 14(11): 2580-2588.

Qiu FY, Song XX, Zheng H, Zhao YB, Fu GS. Thymosin beta4 induces endothelial progenitor cell migration via PI3K/Akt/eNOS signal transduction pathway. J Cardiovasc Pharmacol 2009; 53(3): 209-214.

Roybal CN, Marmorstein LY, Vander Jagt DL and Abcouwer SF. Aberrant accumulation of fibulin-3 in the endoplasmic reticulum leads to activation of the unfolded protein response and VEGF expression. Invest Ophthalmol Vis Sci 2005; 46(11): 3973-3979.

Salminen A, Kauppinen A, Hyttinen JM, Toropainen E and Kaarniranta K. Endoplasmic reticulum stress in age-related macular degeneration: trigger for neovascularization. Mol Med 2010; 16(11-12): 535-542.

Sosne G, Szliter EA, Barrett R, Kernacki KA, Kleinman H, Hazlett LD. Thymosin beta 4 promotes corneal wound healing and decreases inflammation in vivo following alkali injury. Exp Eye Res 2002; 74(2): 293-299.

Sosne G, Christopherson I, Barrett RP and Fridman R. Thymosin β4: modulates corneal matrix metalloproteinase levels and polymorphonuclear cell infiltration after alkali injury. Invest. Ophthalmol. Vis. Sci. 2005; 46: 2388– 2394.

Sosne G, Qiu P, Christopherson PL, Wheater MK. Thymosin beta 4 suppression of corneal NFkappaB: a potential anti-inflammatory pathway. Exp Eye Res 2007; 84(4): 663-669.

Yoshikawa T, Ogata N, Izuta H, Shimazawa M, Hara H and Takahashi K. Increased expression of tight junctions in ARPE-19 cells under endoplasmic reticulum stress. Curr. Eye Res. 2011 Oct 6 [Epub ahead of print].

Yu FX, Lin SC, Morrison-Bogorad M, Yin HL. Effects of thymosin beta 4 and thymosin beta 10 on actin structures in living cells. Cell Motil Cytoskeleton 1994; 27(1): 13-25.

CHAPTER 6

General Discussion

Laminar shear stress is very critical for maintaining proper vascular hemostasis functioning and hemostasis. From a clinical standpoint, shear stress is one of the most potent endothelial stimulators and it plays an important role in numerous processes including vasoregulation, chronic adaptive vessel remodeling (Helmke *et al* 2002), maintaining vascular homeostasis by inhibiting endothelial responses to cytokine stimulation (Chiu *et al* 2002) and in the development of atherosclerosis. Previous studies have shown that areas with low and oscillating shear stress are more prone to atherosclerosis (Moore *et al* 1994; Pedersen *et al* 1999).

Platelet adhesion and thrombus development also depends on the local hemodynamic environment to a large extent (Mustard *et al* 1966). Shear stress plays an important role in transporting platelets and mediating their adhesion at the site of injury. To understand the mechanisms responsible for platelet function under low and high shear rates, many studies have focused on the platelet adhesion to various matrices (fibrinogen, collagen) under flow conditions. In all of these studies, coating of glass slides with fibrinogen, collagen or vWF has been reported and these flow devices were then used to study platelet aggregation mechanisms (Neeves *et al* 2008; Fuchs *et al* 2010, Giesen *et al* 1999). This might result in heterogeneous coating and not all the surface might be coated.

To understand the role of physiological and pathological shear stress in various vascular diseases, many flow devices have been engineered (Andrews *et al* 2010; Man *et al* 2009; Shepherd *et al* 2009). These flow devices require a large population of endothelial cells which needs more chemicals and reagents. Recently, many studies have developed microfluidic flow chambers which are very costly. Out of the various flow devices available to study effects of shear stress, parallel plate flow chambers are the most common. Parallel plate flow chambers are used to mimic flow conditions occurring *in vivo* and study the dynamic response of vascular endothelial cells and platelets to controlled levels of fluid shear stress.

This thesis describes the development and validation of flow devices to study effects of shear stress on endothelial cells and platelet aggregation. The parallel plate flow chamber described in here can be used to study shear mediated effects on endothelial cells and platelets. These flow devices are very versatile and economical to make and allow real time study of the platelets and endothelial cells exposed to shear stress. In the present

study, I report the construction of another flow device for studying platelet function, in whole blood, in real time. In these flow chambers, the inert polydimethylsiloxane (PDMS) surface was plasma-activated and a homobifunctional cross-linker was used to immobilize platelet-binding proteins onto its surface. The current study introduces a new facile and robust method for the construction flow chambers which enable the kinetic monitoring of platelet adhesion in whole blood.

Type 2 diabetic patients are at a greater risk of developing vascular diseases like atherosclerosis. Increased levels of fibrinogen have been reported in diabetes, which might contribute to abnormal clot formation in diabetic patients (Banga *et al*, 1986). Plasmin activator inhibitor 1 (PAI 1) inhibits the formation of plasmin from plasminogen. Increased levels of this inhibitor have also been found in the diabetic blood (Juhan-Vague *et al*, 1989). Previous studies have also shown increased levels of vWF activity in diabetes (Van Zile J *et al* 1981). All of these factors contribute to the formation of a prothrombotic state in the diabetic patients.

The flow chamber developed in this thesis was used to study platelet aggregation in diabetic subjects *in vitro*. The flow chamber was able to discern differences between platelets from normal and diabetic subjects. These flow devices provide real time data on the kinetics of platelet binding and can detect subtle pathological changes in platelet function introduced as a result of pathologies such as type 2 diabetes.

Tβ4 is a 43 amino acid peptide found in various tissues and cells including platelets. It has been implicated in the sequestering of G actin in mammalian cells. Tβ4 plays an important role in preventing apoptosis, corneal wound healing, cell survival and angiogenesis (Sosne *et al* 2004; Hinkel *et al* 2008; Smart *et al* 2007).

The aim of this work was to evaluate the role of Tβ4 in various physiological processes. It has been shown previously that Tβ4 is secreted by platelets and is crosslinked by factor XIIIa (a transglutaminase) to fibrin in a time- and Ca^{2+}-dependent manner (Huff *et al* 2002; Makogoneko *et al* 2004). This increases the local concentration of Tβ4 near sites of clots and tissue damage, where it is postulated to contribute to wound healing, angiogenesis and inflammatory responses. Yet the role of Tβ4 on platelet thrombus formation has yet to be fully investigated.

The current study represents a preliminary effort towards this goal. Here, we have

tested the effects of Tβ4 extraneously added to whole blood, on deposition of ADP activated platelets onto fibrinogen under conditions of continuous flow and shear. There was an increase in platelet deposition when Tβ4 was added to the blood, as compared to the controls. However, at high concentrations of Tβ4, a decrease in the platelet deposition was observed. The results of the present study suggest that there could be a high affinity Tβ4-binding domain on fibrinogen. The fibrinogen binding ability of Tβ4 could explain the biphasic response of Tβ4 on platelet deposition under conditions of flow as observed here. Furthermore, the results obtained in this study suggest a key modulatory role for Tβ4 in thrombus formation. At low doses Tβ4 promotes platelet deposition and aggregation by as yet unknown mechanism(s). But as platelets are activated and more Tβ4 is released from platelets, its serum levels rises and prevent excessive thrombus formation by binding to fibrinogen and preventing its interaction with platelets.

Tβ4 has also been shown to decrease inflammation and promote corneal wound healing, and various studies have given evidence supporting the role of Tβ4 in cornea protection (Ho *et al* 2008; Sosne *et al* 2007; Dunn *et al* 2010). This thesis also investigates the effects of Tβ4 on endoplasmic reticulum stress in retinal pigment epithelial cells. In this study, we illustrated that Tβ4 is able to reduce ROS production, which is an important factor associated with the progression of various ophthalmologic diseases including AMD and DR (He *et al* 2008; Libby *et al* 2010). Tβ4 also promotes NO production and decreases NF-κB nuclear localization in RPE. Our observations agree with a previous study done in corneal epithelial cells which showed that Tβ4 can minimize nuclear localization of NFκB after TNF-α stimulation (Sosne *et al* 2007). The results reported in this thesis demonstrated that Tβ4 can mitigate the effects of ER stress in RPE cells.

Overall, the work done in this thesis has done significant contributions in understanding the role of Tβ4 in thrombosis. However, more work is needed in this field to fully understand the role of Tβ4 in thrombosis and evaluate the mechanisms and signalling pathways involved in this process. Very few studies have reported any role of ER stress in retinal diseases and this is one of those few studies. This thesis also presents preliminary data which demonstrates the protective effects of Tβ4 in retinal pigment epithelial cells under ER stress. More extensive study needs to be done in future in this

field to get better understanding of the mechanisms involved. In conclusion, the work presented in this thesis has made major contributions in development of flow devices to study thrombosis and endothelial cell function under flow. This work is also a very important step in studying the role of Tβ4 in various physiological processes.

References

Andrews AM, Jaron D, Buerk DG, Kirby PL, Barbee KA. Direct, real-time measurement of shear stress-induced nitric oxide produced from endothelial cells in vitro. Nitric Oxide 2010; 23(4):335-42.

Banga JD and Sixma JJ. Diabetes mellitus, vascular disease and thrombosis.Clin Haematol 1986; 15(2): 465-492.

Chiu JJ, Lee PL, Lee CI, Chen LJ, Chen CN, Ko YC, Lien SC. Shear stress attenuates tumor necrosis factor-alpha-induced monocyte chemotactic protein-1 expressions in endothelial cells. Clin J Physiol 2002; 45(4):169-76.

Dunn SP, Heidemann DG, Chow CY, Crockford D, Turjman N, Angel J, Allan CB, Sosne G. Treatment of chronic nonhealing neurotrophic corneal epithelial defects with thymosin beta 4. Arch Ophthalmol 2010; 128(5):636-8.

Fuchs B, Budde U, Schulz A, Kessler CM, Fisseau C and Kannicht C. Flow-based measurements of von Willebrand factor (VWF) function: Binding to collagen and platelet adhesion under physiological shear rate. Thrombosis Research 2010; 125 (3): 239-245.

Giesen PLA , Ursula Rauch U, Bohrmann B, Kling D, Roqué M, Fallon JT, Badimon JJ, Himber J, Riederer MA and Nemerson Y. Blood-borne tissue factor: Another view of thrombosis. Proc Natl Acad Sci U S A. 1999; 96(5): 2311–2315.

He S, Yaung J, Kim YH, Barron E, Ryan SJ and Hinton DR. Endoplasmic reticulum stress induced by oxidative stress in retinal pigment epithelial cells. Graefes Arch Clin Exp Ophthalmol 2008: 246(5); 677-683.

Helmke BP, Davies PF. The cytoskeleton under external fluid mechanical forces: hemodynamic forces acting on the endothelium. Ann Biomed Eng. 2002; 30(3):284-96.

Hinkel R, El-Aouni C, Olson T, Horstkotte J, Mayer S, Müller S, Willhauck M, Spitzweg C, Gildehaus FJ, Münzing W, Hannappel E, Bock-Marquette I, DiMaio JM, Hatzopoulos AK, Boekstegers P and Kupatt C. Thymosin beta 4 is an essential paracrine factor of embryonic endothelial progenitor cell-mediated cardioprotection. Circulation 2008; 117: 2232–2240.

Ho JH, Tseng KC, Ma WH, Chen KH, Lee OK, Su Y. Thymosin beta-4 upregulates anti oxidative enzymes and protects human cornea epithelial cells against oxidative damage. Br J Ophthalmol 2008; 92(7):992-7.

Huff T, Otto AM, Muller CS, Meier M and Hannappel E. Thymosin beta4 is released from human blood platelets and attached by factor XIIIa (transglutaminase) to fibrin and collagen. FASEB J 2002; 16: 691–696.

Juhan-Vague I, Roul C, Alessi MC, Ardissone JP, Heim M and Vague P. Increased plasminogen activator inhibitor activity in non-insulin-dependent diabetic patients: relationship with plasma insulin. Thromb Haemost 1989; 61:370–373.

Libby RT and Gould DB. Endoplasmic reticulum stress as a primary pathogenic mechanism leading to age-related macular degeneration. Adv Exp Med Biol 2010; 664: 403-409.

Makogonenko E, Goldstein AL, Bishop PD and Medved L. Factor XIIIa incorporates thymosin beta4 preferentially into the fibrin(ogen) alphaC-domains. Biochemistry 2004; 43: 10748–10756.

Man S, Tucky B, Bagheri N, Li X, Kochar R and Ransohoff RM. α4 Integrin/FN-CS1 mediated leukocyte adhesion to brain microvascular endothelial cells under flow conditions. J Neuroimmunol 2009; 210(1-2): 92–99.

Moore JE Jr, Xu C, Glagov S, Zarins CK, Ku DN. Fluid wall shear stress measurements in a model of the human abdominal aorta: oscillatory behavior and relationship to atherosclerosis. Atherosclerosis 1994; 110(2):225-40.

Mustard JF, Jorgensen L, Hovig T, Glynn MF and Rowsell HC. Role of platelets in thrombosis. Thromb Diath Haemorrh Suppl 1966; 21:131–58.

Neeves KB, Maloney SF, Fong KP, Schmaier AA, Kahn ML, Brass LF and Diamond SL. Microfluidic focal thrombosis model for measuring murine platelet deposition and stability: PAR4 signaling enhances shear-resistance of platelet aggregates. Journal of Thrombosis and Haemostasis 2008; 6: 2193–2201.

Pedersen EM, Oyre S, Agerbaek M, Kristensen IB, Ringgaard S, Boesiger P, Paaske WP. Distribution of early atherosclerotic lesions in the human abdominal aorta correlates with wall shear stresses measured in vivo. Eur J Vasc Endovasc Surg. 1999;18(4):328-33.

Shepherd RD, Kos SM, Rinker KD. Long term shear stress leads to increased phosphorylation of multiple MAPK species in cultured human aortic endothelial cells. Biorheology 2009; 46(6):529-38.

Smart N, Riseboro CA, Melville AA, Moses K, Schwartz RJ, Chien KR and Riley PR. Thymosin beta 4: induces adult epicardial progenitor mobilization and neovascularization. Nature 2007; 445: 177–182.

Sosne G, Qiu P, Christopherson PL and Wheater MK. Thymosin beta 4 suppression of corneal NFkappaB: a potential anti-inflammatory pathway. Exp Eye Res 2007; 84(4): 663-669.

Sosne G, Szliter EA, Barrett R, Kernacki KA, Kleinman KH and Hazlett LD. Thymosin beta 4 promotes corneal wound healing and decreases inflammation in vivo following alkali injury. Exp. Eye Res. 2002; 74 (2):293-299.

Van Zile J, Kilpatrick M, Laimins M, Sagel J, Colwell J and Virella G. Platelet aggregation and release of ATP after incubation with soluble immune complexes purified from the serum of diabetic patients. Diabetes 1981; 30:575–579.

APPENDIX

The results presented in this section of the thesis relate to the studies in Chapter 2 of this thesis.

Background

Earlier it was assumed that in parallel plate flow chambers, all cells are subjected to the same average shear stress. However recently it has been hypothesized that cells are subjected to variable shear stress depending on the area in the flow chamber (McCann *et al* 2005). The objective of this study is to develop a flow device to study effects of shear stress on endothelial cells and also to develop computational fluid dynamic (CFD) template with different shear rates. The templates are designed to match the geometry of a custom built *in vitro* flow cell device and define several regions of shear stress to which the cells are exposed during *in vitro* experiment. Since it has previously been reported that shear stress is correlated to NO production in endothelial cells, NO was measured in order to validate the proposed flow device and the shear stress template.

Experimental Methods

Cell Culture

Human dermal microvascular endothelial cells (HDMECs) were purchased from ScienCell. The cells were cultured in endothelial cell media (ECM, ScienCell) containing 10% fetal bovine serum (FBS, ScienCell), pencillin-streptomycin (ScienCell) and endothelial cell growth supplement (ECGS, ScienCell) at 37ºC in a 5% CO_2 incubator. The flow chambers were coated 0.1% fibronectin overnight and endothelial cells were grown until 95% confluent.

In vitro set-up

The flow cell circuit used for this investigation consists of a custom designed flow cell, sterile tubing, a medium reservoir, and a peristaltic pump. The entire set-up was kept at 37ºC in a 5% CO_2 incubator. The cells were exposed to shear stress for 12 hours.

Fluorescence Indicator (DAF-2)

To determine changes in NO production, endothelial cell monolayers were incubated with cell culture medium containing 5 μM, 4,5-diaminofluorescein diacetate (DAF-DA , Invitrogen) at 37°C in a 95% air/5% CO_2 incubator for 30 min. In the presence of oxygen, DAF-2 reacts with NO to yield the highly fluorescent triazolofluorescein (DAF-2T). The fluorescence was monitored using excitation and emission wavelengths of 485 and 538 nm, respectively.

Results

Geometry of the flow cell

The flow cell has the dimensions shown in Figure 2. The total area on the flow cell surface available for cell growth and attachment was 6.85 x $10^{-5}m^2$. The walls of the flow cell are made of PDMS (Dow Corning) and the cells are grown on a glass coverslip.

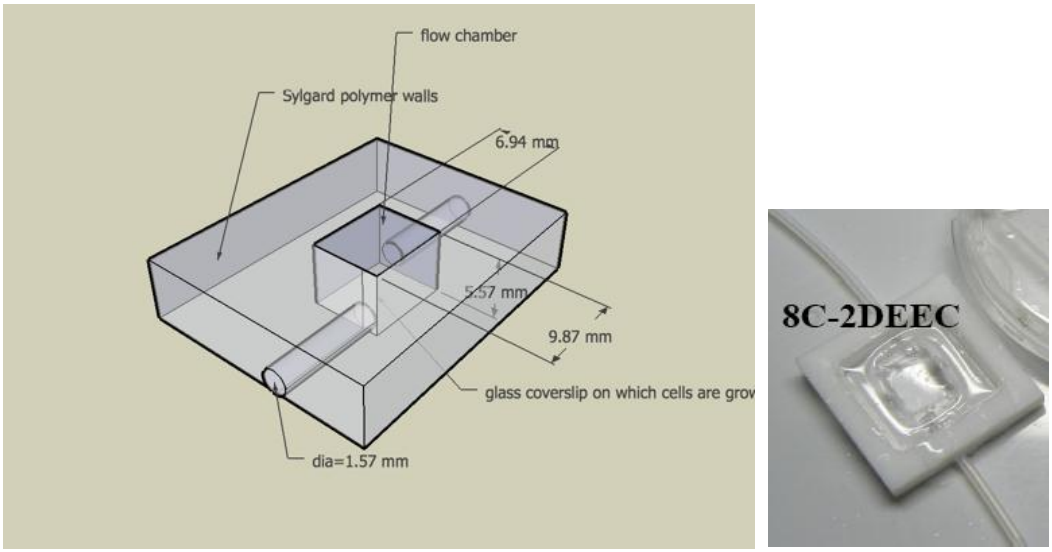

Figure 1 – Geometry of the custom flow cell.

Velocity gradient template

To simulate the flow in the chamber and estimate the shear stress for the testing program, a computational model of the flow channel was developed.

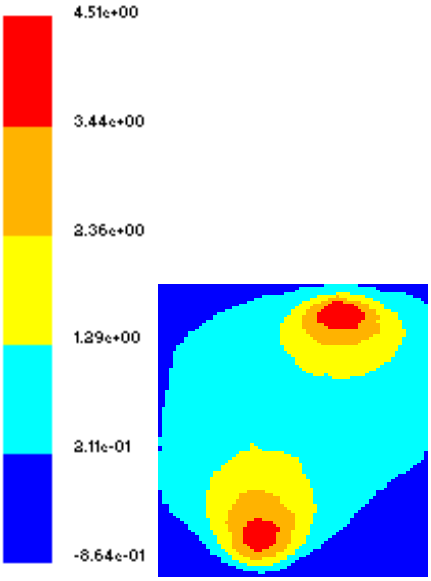

1mL/min

Figure 2 – Velocity gradient template.

Endothelial morphology in response to shear stress

The human dermal microvascular endothelial cells were exposed to laminar shear stress for 12 hours hours and morphological changes were observed using light microscope. The cells become elongated and aligned in the direction of flow; however no such change was observed in endothelial cells maintained under static conditions.

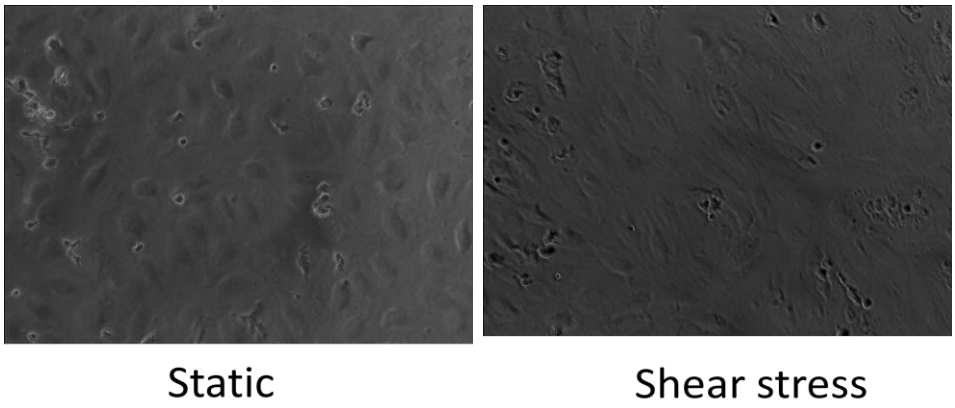

Figure 3 – Morphology of endothelial cells grown under static and laminar shear stress conditions.

Effect of shear stress on NOx production

In order to validate the flow chamber can be employed for studies in the areas of biomedical research; the effect of fluid shear stress on nitric oxide production in endothelial cells was examined. NOx formation was upregulated when cells were grown under shear as compared to static conditions. The increase in NOx production was more in endothelial cells which were exposed to high shear stress for 12 hours, compared with those under low shear (Fig. 3).

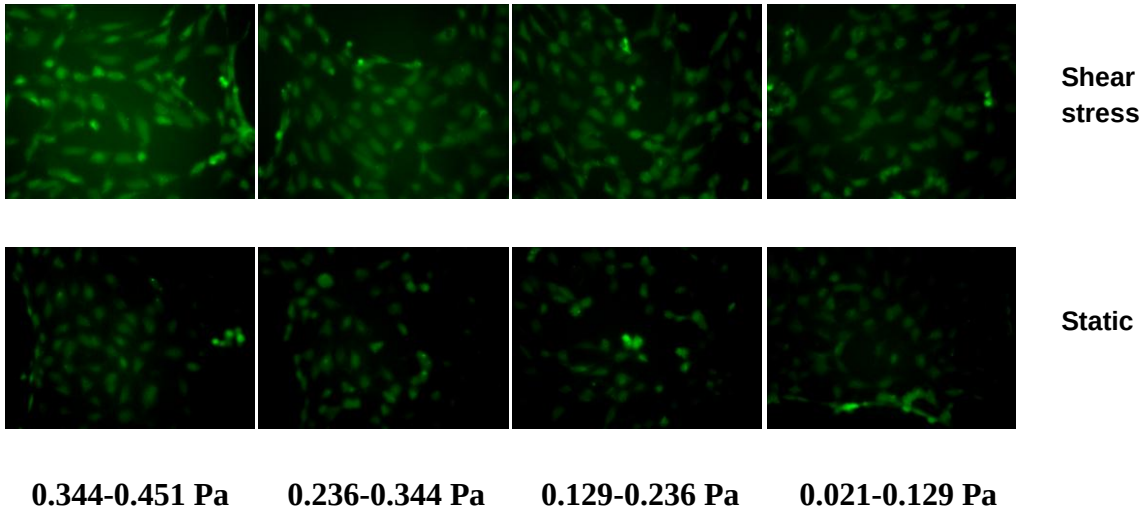

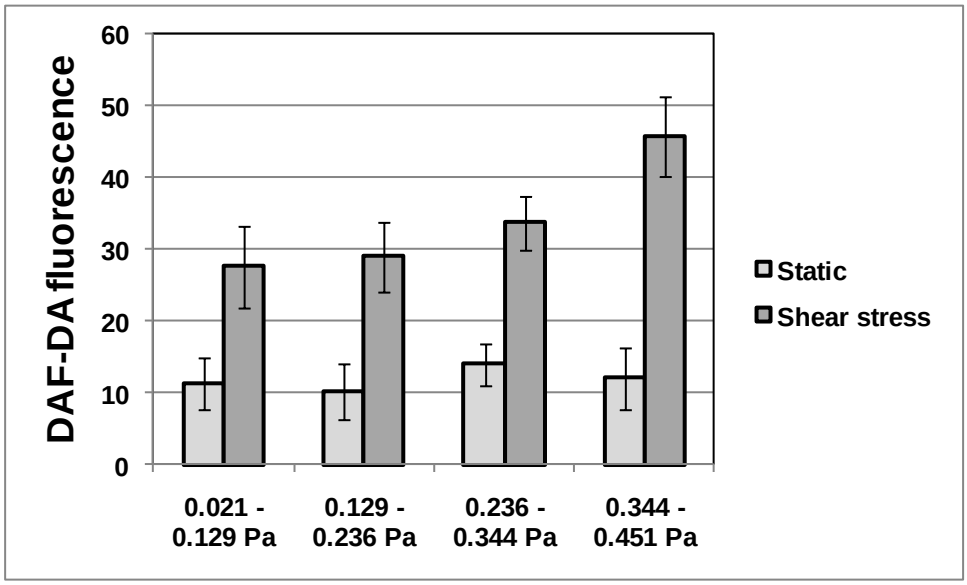

Figure 4 – NOx upregulation in response to shear stress.

HDMECs were exposed to shear stress for 12 hours and then stained with 5 μM DAF-DA. The regions exposed to high shear stress had increased NO production. The graph depicts the average fluorescence intensity of DAF-DA (± SD).

Discussion

Shear stress plays a critical role in maintaining vascular hemostasis and also in the pathogenesis of various diseases, particularly atherosclerosis. Numerous studies have focussed on investigating the effects of shear stress on endothelial cells. Parallel plate flow chambers are commonly used for this purpose.

In this study, we describe the development and validation of a flow chamber for shear stress studies. It has previously been shown that the endothelial cells align in the direction of the flow and that the alignment would be more pronounced at areas of higher shear. Our results also agree with these studies and show similar results.

There was an increase in NO production in regions of high shear. These findings are in agreement with the previous studies which reported NO upregulation in response to shear stress. These results suggest that this chamber can be used to study shear stress effects on endothelial cells. This chamber is very simple to make, convenient to use and inexpensive. It can be re used and requires very less number of cells. The shear stress template described in here, can be used to define different regions of known shear stress. This allows simultaneous exposure to different shear stress levels within one flow cell under the exact same experimental conditions.

References

McCann JA, Peterson SD, Plesniak MW, Webstre TJ and Haberstroh KM. Non-uniform flow behavior in a parallel plate flow chamber alters endothelial cell responses. Annals of Biomedical Engineering 2005; 33 (3): 2005328–2005336.

VITA AUCTORIS

Name:	Harmanpreet Kaur
Place of Birth:	Ludhiana, Punjab, India
Year of Birth:	1981
Education:	Panjab University Chandigarh, India 2000 – 2003, B.Sc
	Panjab University Chandigarh, India 2003 – 2005, M.Sc Honors
	University of Windsor Windsor, Ontario, Canada 2006 – 2011, PhD Biochemistry